Suppression of Stimulated Brillouin Scattering in Analog CATV Transmission Systems

By

David Robert Jez

B.Eng., McMaster University, 1994
M.Eng., McMaster University, 1996

A THESIS SUBMITTED IN PARTIAL FULFILLMENT OF THE REQUIREMENTS FOR THE DEGREE OF

Doctor of Philosophy

in

THE FACULTY OF GRADUATE STUDIES

DEPARTMENT OF ELECTRICAL AND COMPUTER ENGINEERING

THE UNIVERSITY OF BRITISH COLUMBIA

February, 2001

Abstract

This thesis presents a systematic investigation of stimulated Brillouin scattering (SBS) in analog fiber-optic cable-television (CATV) transmission systems. To this end, the author has designed and built a high-bandwidth time-resolved chirp measurement system used to characterize the CATV transmitter. The complex average electric field and corresponding optical spectrum can be obtained using this system. From this, the relationship between SBS suppression and CATV transmitter characteristics is examined. We show that conventional SBS suppression theory breaks down for the high levels commonly used in optical CATV systems. A more suitable approach based on transmitter power and chirp measurement and detailed spectral analysis is demonstrated for two 1550nm distributed feedback (DFB) lasers. This new measurement technique can determine the level of SBS suppression in optical fiber over a much wider measurement range compared to conventional techniques. This makes it ideal for the development and characterization of enhanced SBS suppression schemes.

Using this approach, we investigated a variety of two-tone suppression schemes using a combination of direct laser and external phase dithering. Two-tone dithering is shown to be more effective at suppressing SBS than single-tone dithering. The best suppression scheme presently feasible is pure two-tone phase dithering at a frequency ratio of 3:2, generating an SBS threshold of 21.4dBm and requiring an RF bandwidth of only 3.9GHz. This level of suppression is 3.4dB higher than what has been previously reported. Applying this suppression technique to an 80-channel CATV system we show that self-phase modulation (SPM) becomes the dominant nonlinearity. The interaction of SPM with fiber dispersion degrades the CSO distortion to unacceptable levels. We discuss ways of overcoming this.

Contents

List of Figures

List of Tables

Acknowledgements

First and foremost, I would like to thank my parents for their love and support. This degree would not have been possible without you. I would also like to thank my supervisor, Dr. Mike Jackson, for giving me the opportunity to work on this project and to help me prepare for my career in industry.

Thank-you Onita and Martin for being such great friends and keeping me sane during the rough parts of my thesis.

I am also grateful to all the institutions that provided financial support for this project: BC Science Council, National Science and Engineering Research Council (NSERC), Advanced Systems Institute (ASI), and Scientific Atlanta Canada Inc.

Chapter 1

Introduction

1.1 Introduction to Thesis

While digital transmission predominates in telecommunication systems, analog transmission is still widely used in the cable-television (CATV) industry because of the large installed base of consumer analog television sets. The first systems deployed operated in the 1300nm range, but more recently 1550nm systems have been used because of low fiber loss at this wavelength and the availability of high-powered erbium-doped fiber amplifiers (EDFAs). To meet the stringent industry performance standards, the distortion and noise of these systems must be kept extremely low. One factor that can influence the performance of these systems is chirp. Chirp is the transient shift in optical frequency that occurs in most optical sources when the output intensity is changed. It is important in 1550nm systems because in the presence of fiber dispersion, chirp generates distortion. For this reason, direct modulation of semiconductor lasers is impractical at 1550nm because transmission links are limited to a few kilometers before distortion becomes unacceptably high. For long-haul transmission systems, external modulation of a constant power (CW) laser source is used, as chirp is virtually absent in these systems. While alleviating distortion due to dispersion, the narrow spectrum associated with chirp-free modulation enhances some nonlinearities in the fiber, particularly stimulated Brillouin scattering (SBS).

Starting at low levels and increasing launched optical power, SBS is the first nonlinearity encountered in long-distance fiber transmission systems using a narrow linewidth source and

has a CW threshold that ranges from 6 to 8dBm[1] in conventional single-mode fiber (SMF). For launch powers that exceed this threshold, SBS converts a significant portion of the transmitted signal to a backward scattered lightwave. In addition, SBS generates intensity noise at the CATV sub-carrier frequencies, degrading the carrier-to-noise ratio (CNR) of the signal to unacceptable levels. The most common approach for suppressing SBS is intentional chirping of the transmitter output by directly dithering the laser or phase dithering a CW laser source using an external phase modulator. With the appropriate choice of dithering frequency there is negligible distortion of the CATV signal. Using this technique, the SBS threshold for commercial transmitters can be increased to 18dBm.

The reason for suppressing SBS is to permit high launch powers into the optical fiber. For long-haul transmission systems, this increases the distance between repeaters and significantly reduces the cost of the system. Commercially available high-powered EDFAs are capable of generating output powers in excess of 23dBm, but current suppression techniques still limit the injection power to 18dBm. To accommodate higher launch powers more effective suppression techniques must be developed. While a considerable amount of work has been devoted to this subject, most of the work has been empirical as little quantitative information exists about the relationship between chirp and SBS. The purpose of this thesis is to develop a more quantitative approach to understanding this relationship, with the intent of developing enhanced suppression schemes.

1.1.1 Summary of Results

A high-bandwidth chirp measurement system has been designed to characterize the power and chirp output from optical CATV transmitters. The complex average electric field and corresponding optical spectrum can be obtained using this system. From this, the relationship between SBS suppression and CATV transmitter characteristics is examined. Conventional SBS suppression theory, using a single-peak analysis of the optical spectrum, is shown to break down for the high levels of suppression commonly used in optical CATV systems. A more suitable approach based on transmitter power and chirp measurement and detailed spectral analysis is introduced and demonstrated for two 1550nm distributed feedback (DFB) lasers.

[1]dBm defines power relative to 1mW, i.e. 0dBm=1mW, +3dBm=2mW, -3dBm=0.5mW, etc.

This new measurement technique can determine the level of SBS suppression in optical fiber over a much wider range compared to conventional measurement techniques, which makes it ideal for the development and characterization of enhanced SBS suppression schemes. With this approach, a variety of two-tone suppression schemes are investigated using a combination of direct laser dithering and external phase dithering. Two-tone dithering is shown to be more effective at suppressing SBS than single-tone dithering. The best suppression scheme presently feasible is pure two-tone phase dithering at a frequency ratio of 3:2, generating an SBS threshold of 21.4dBm and requiring an RF bandwidth of only 3.9GHz: this is 3.4dB higher than what has been previously reported. Applying this suppression scheme to an 80-channel CATV system it is shown that self-phase modulation (SPM) becomes the dominant optical nonlinearity. The interaction of SPM with fiber dispersion degrades the CSO distortion to unacceptable levels.

1.1.2 Outline of Chapter

The remainder of Chapter 1 deals with background material relevant to SBS suppression in analog optical CATV transmission systems. In Section 1.2, the differences between directly modulated and externally modulated CATV transmitters are discussed along with the CATV performance issues related to these two schemes in the presence of fiber dispersion. Section 1.3 gives a detailed explanation of why SBS occurs in optical fiber and how it can be suppressed with appropriate dithering of the CATV transmitter. Section 1.4 outlines the different techniques used in the past to characterize transient chirp generated by optical transmitters. The limitations of these techniques are analyzed and the motivation behind the new measurement approach used in the present work is given. In Section 1.5, the author presents other techniques in the literature that have been developed to try and suppress SBS in optical fiber. Finally, in Section 1.6 a brief introduction is given to the theory behind self-phase modulation (SPM) and how it may affect the performance of the CATV system in the absence of SBS.

1.2 Introduction to CATV Systems

Analog CATV systems transmit 80 to 110 channels of video and audio information with a system bandwidth up to 750MHz using vestigial sideband amplitude modulation (AM-VSB)

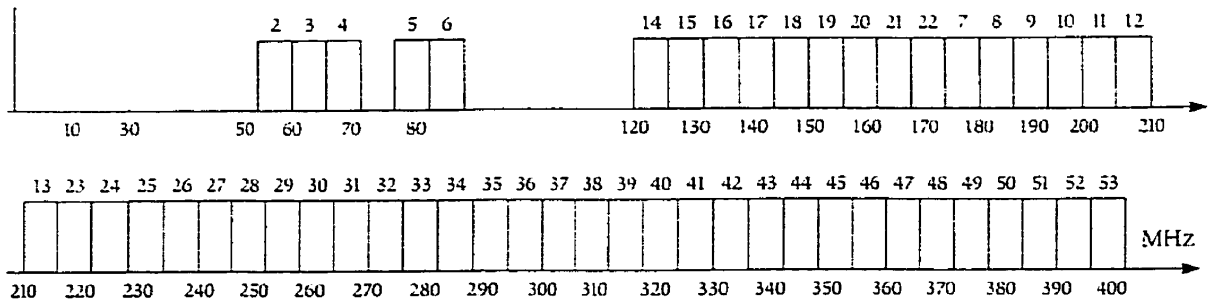

Figure 1-1: North American standard channel plan for frequencies up to 400MHz. (From [1]). Most analog television picture carriers are 6 MHz apart and offset 1.25MHz upwards from harmonics of 6MHz

Channel	Carrier (MHz)
2	55.25
13	211.25
42	311.25
62	451.25
79	553.25

Table 1.1: Specific frequencies in the North American standard channel plan.

[1]. The North American standard channel plan, as shown in Figure 1-1, places most analog television picture carriers 6 MHz apart and offset 1.25MHz upwards from harmonics of 6MHz. Each channel extends 1.25MHz below the picture carrier to 4.75MHz above it. Table 1.1 gives some specific channel frequencies associated with this plan. A high-quality broadband tuner and output circuitry in the consumer's television set allows tuning to a specific channel.

Intensity modulation is used to encode the electrical version of the CATV signal on the optical output. Transmitters use semiconductor lasers as their optical source; the intensity modulation is accomplished either by directly modulating the laser injection current or externally modulating the laser output using a Mach-Zehnder type device. A schematic of a typical CATV transmitter is shown in Figure 1-2, illustrating both direct and external modulation schemes. In the latter case, the laser operates at constant power in continuous wave (CW) mode.

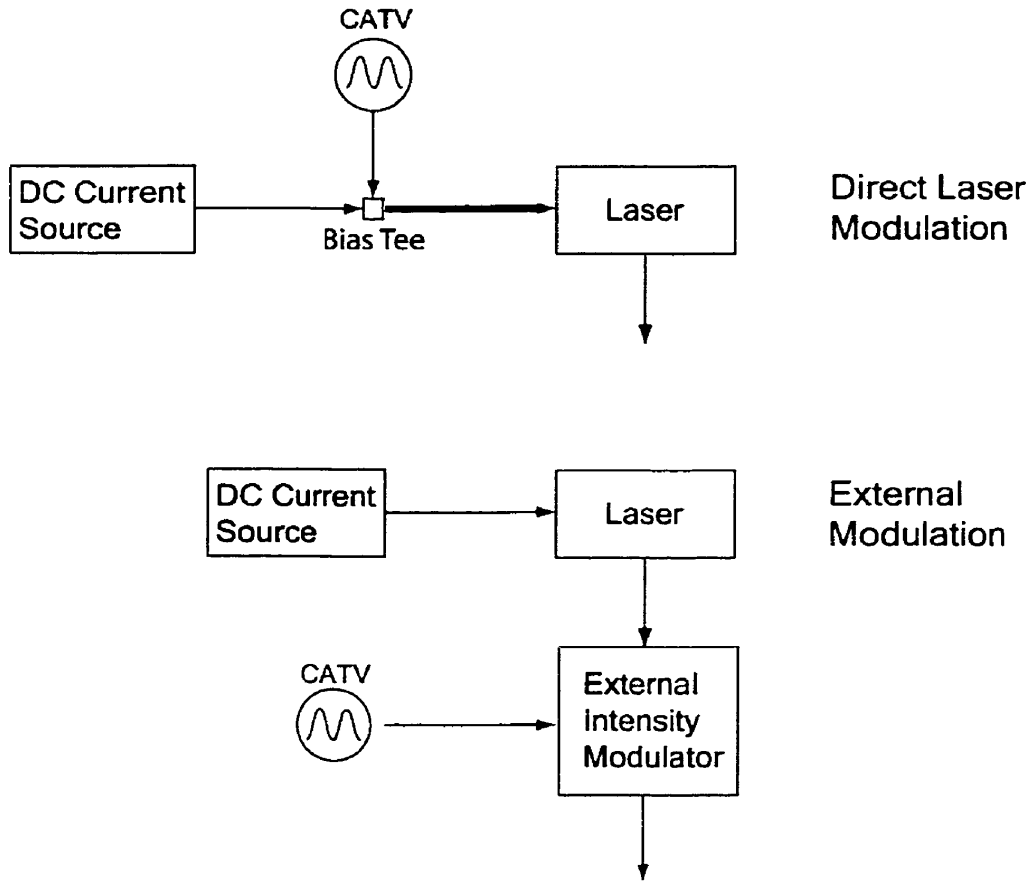

Figure 1-2: Schematic of an analog CATV transmitter. Both direct and external modulation schemes are shown. In the latter case, the laser operates at constant power (CW).

1.2.1 Direct Laser Modulation

For a directly modulated CATV system, intensity modulation of the optical output of a semiconductor laser is obtained by direct modulation of the injection current. When the current through the laser diode changes, however, there is a small effect on the instantaneous wavelength of the laser output; this incidental frequency shift is known as chirp. In typical laser diodes at large modulation depths, the frequency shift can be as large as ±20GHz. To understand how this chirp is generated, consider the modulation process in a simple Fabry-Perot laser diode, as shown in Figure 1-3. Modulation of the injection current leads to a corresponding variation of the carrier density, and consequently, of the refractive index in the active region of the device. The emission frequency is given by the standing wave equation

$$\nu_m = m \cdot \frac{c}{2nL} \tag{1.1}$$

where ν_m is the frequency of the m^{th} longitudinal mode, c is the speed of light, n is the refractive index, and L is the length of the laser cavity. From Equation 1.1, one can see that variations in the refractive index lead to corresponding variations in the laser emission frequency. For modulation depths below about 90%, the emission frequency will shift in an approximately linear manner with current modulation. This simple explanation for chirp in Fabry-Perot laser diodes captures the key physical process which occurs in the more sophisticated single-mode DFB lasers used in telecommunication applications. Figure 1-4[1] illustrates typical power and chirp waveforms generated by a directly modulated 1550nm DFB laser, using sinusoidal current modulation at a frequency of 1GHz and modulation depth[2] of 69%. Under sinusoidal current modulation, sinusoidal modulation of the power and emission frequency results. This transient shift in the optical emission frequency interacts with chromatic dispersion in optical fiber introducing significant distortion to a CATV signal. The data was acquired using the measurement system that will be described in Chapter 2.

[1] a.u. stands for arbitrary units and is used throughout the thesis.

[2] Modulation depth is defined as the peak power divided by the average power. This is limited to the case of sinusoidal modulation.

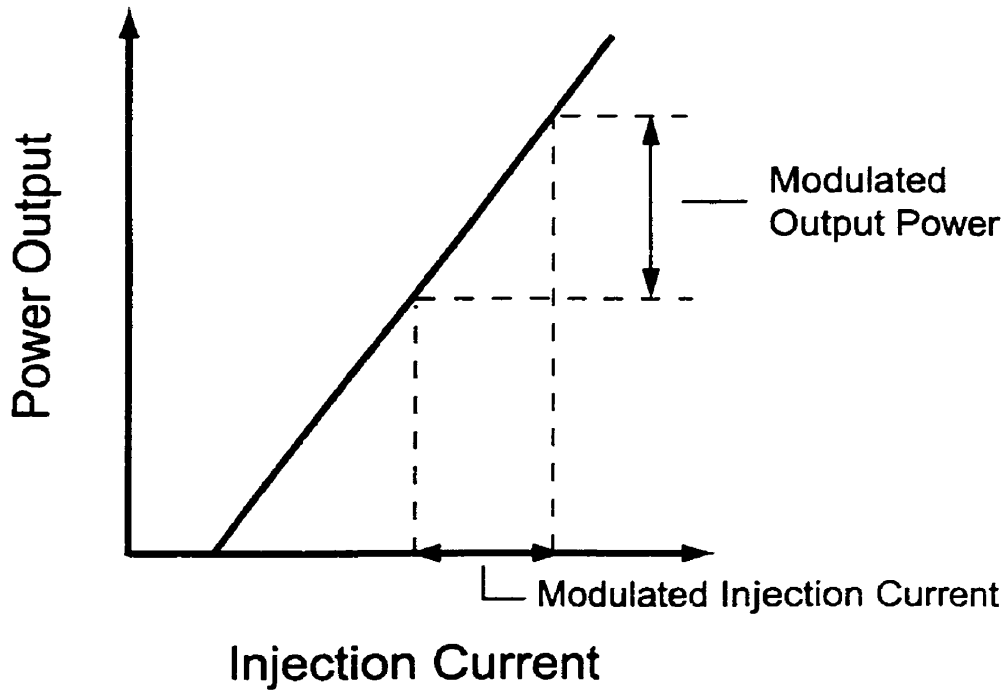

Figure 1-3: Power output versus injection current for a typical semiconductor laser. (From [1])

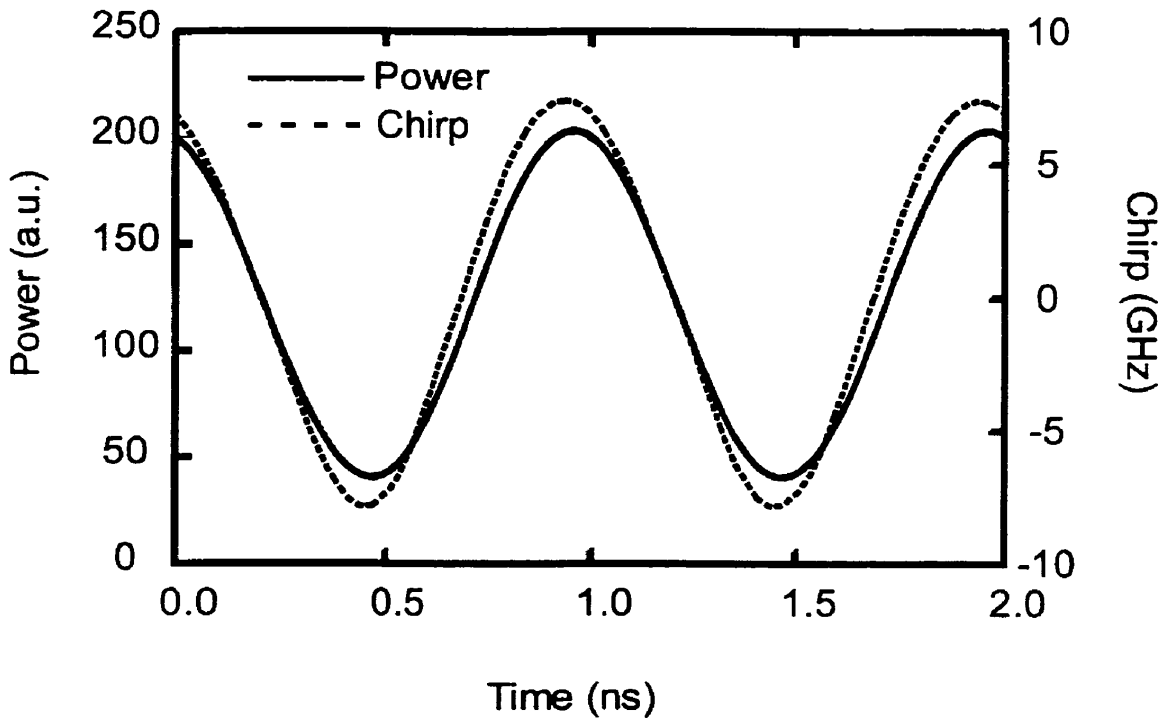

Figure 1-4: Power and chirp from a 1550nm DFB laser modulated at 1GHz and a modulation depth of 69%. Under sinusoidal current modulation, sinusoidal modulation of the power and emission frequency results.

1.2.2 Fiber Dispersion

Optical fiber has significant chromatic dispersion at a wavelength of 1550nm, which means that different frequencies travel at different speeds, or more precisely, at different group velocities. The dispersion parameter D quantifies the derivative of the group velocity with respect to wavelength, and describes how the group velocity of an optical signal will be affected by propagation inside the fiber; it has units of ps/(km-nm) [2]. Given an unchirped pulse with a wavelength spread $\Delta\lambda$, the time delay between the leading and trailing edge of the pulse will be approximately

$$\Delta T = DL\Delta\lambda \tag{1.2}$$

where L is the propagation distance. More precise calculation of the effects of dispersion are often calculated numerically, as described in [2]. Figure 1-5 illustrates the variation of dispersion with wavelength for a single-mode fiber. At 1310nm, the dispersion is zero; this wavelength is designated as the zero-dispersion wavelength, λ_D. For $\lambda > \lambda_D$, high frequency (blue-shifted) components of the optical signal travel faster than lower frequency (red-shifted) components; the opposite occurs for $\lambda < \lambda_D$. Over the relatively small wavelength shifts associated with chirp, the group index of refraction will vary in a manner which is approximately linear. Thus, as the instantaneous modulating signal swings in one direction the light will shift to a wavelength that travels slightly faster, whereas at the other polarity the generated light will travel slower. This causes even-order distortion products in the propagating signal, the dominant of which is composite second-order (CSO) distortion.

In an optical fiber, the dominant source of 'nonlinearity' is actually fiber dispersion. Although fiber propagation is linear in the electric field, it is nonlinear from the point of view of the optical power or intensity waveform, and these are the relevant quantities at the transmitter and receiver in the intensity modulated systems considered in this thesis. Therefore, a fiber behaves as a nonlinear element, even when the optical powers are low. The degree of nonlinearity depends on the amount of dispersion, and is generally quite weak for practical fiber lengths. We can expect 2^{nd}, 3^{rd} and perhaps 4^{th} order nonlinear terms to dominate the system. Dispersion is a symmetrical process that generates only even-order products, so we can justify ignoring the third-order term. If we assume the nonlinearity in the fiber is weak,

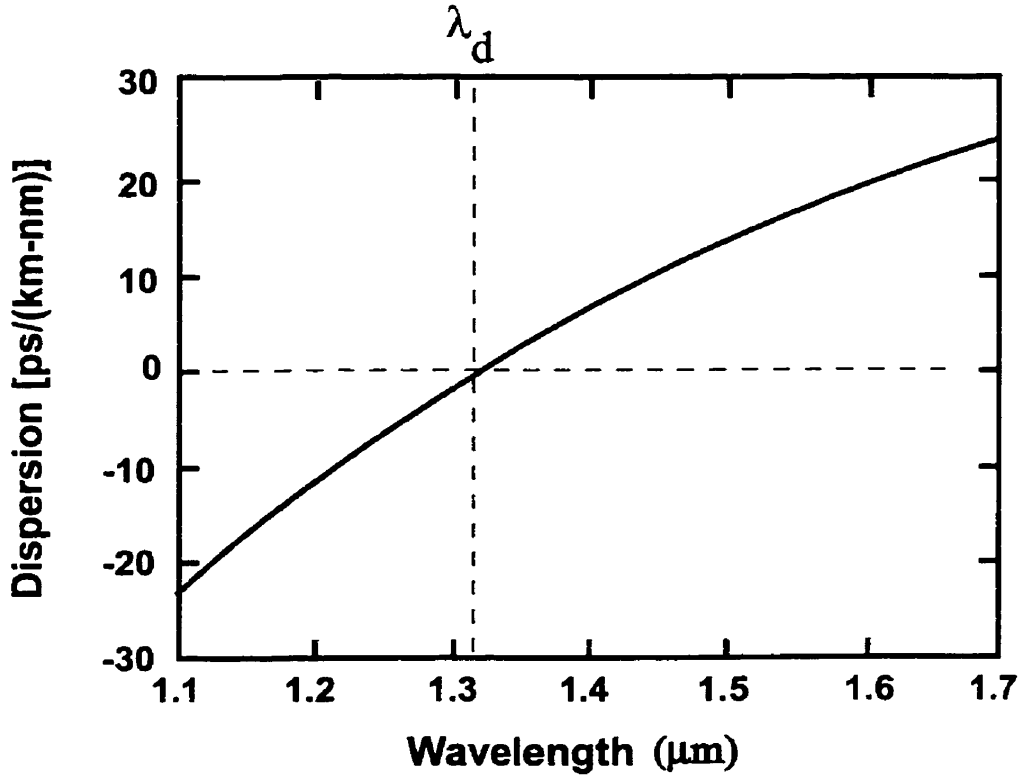

Figure 1-5: Dispersion versus wavelength for a conventional single-mode fiber. The zero dispersion wavelength is 1310nm, designated by λ_D. (From [1])

we can also justify ignoring the fourth-order term, as the second-order term will dominate. Weakly 'nonlinear' in this case refers to fiber with only a moderate product of dispersion and length. To understand the effects of this distortion on an analog CATV system, consider the propagation of an N-channel CATV signal through a nonlinear element. The input power, e_i, entering the fiber is

$$e_i = \sum_{k=1}^{N} c_k e^{i\omega_k t} + \text{complex conjugate} \tag{1.3}$$

$$= \sum_{k=1}^{N} c_k e^{i\omega_k t} + \sum_{k=1}^{N} c_k^* e^{-i\omega_k t} \tag{1.4}$$

where c_k is the power including phase, and ω_k is the frequency of the kth CATV channel. When this signal propagates through a nonlinear element with second order distortion, the signal detected at the receiver, e_0, is given by

$$e_0 = ae_i + be_i^2 \tag{1.5}$$

which can be written explicitly as

$$e_0 = a\left(\sum_{k=1}^{N} c_k e^{i\omega_k t} + \sum_{k=1}^{N} c_k^* e^{-i\omega_k t}\right) + b\left(\sum_{k=1}^{N} c_k e^{i\omega_k t} + \sum_{k=1}^{N} c_k^* e^{-i\omega_k t}\right)\left(\sum_{k'=1}^{N} c_k e^{i\omega_{k'} t} + \sum_{k'=1}^{N} c_k^* e^{-i\omega_{k'} t}\right) \tag{1.6}$$

The first term is linearly proportional to the input signal. The second terms generates new intermodulation frequencies. Many combinations of different CATV channels lead to the same intermodulation frequency. For example, consider channel 79, whose visual carrier frequency is at 553.25 MHz. If Channel 17 (139.25MHz) and Channel 56 (415.25 MHz) undergo second-order distortion, an intermodulation frequency is produced at the sum of these two frequencies which is 554.5MHz and is located 1.25MHz above the visual carrier for Channel 79. However, other combinations also lead to this frequency, so second-order distortion at Channel 79 is composed of many combinations of frequencies, hence the name composite in composite second-order (CSO) distortion. Figure 1-6 shows the number of CSO beats for the particular case of an 80-channel CATV system. The CSO tone 1.25MHz above the carrier at Channel 79 is actually formed by over 30 different intermodulation frequencies. Most optical CATV systems must maintain a

CSO below -65dBc[1] to ensure adequate signal quality at the receiver. For directly modulated transmitters, however, CSO is significantly degraded in the presence of fiber dispersion. An alternative approach to direct laser modulation is external intensity modulation.

1.2.3 External Modulation

Externally modulated transmitters consist of a continuous wave light source whose intensity is varied by an external device. The most common external modulator is a Mach-Zehnder (M-Z) constructed on a lithium niobate ($LiNbO_3$) substrate; the transfer function of this device is sinusoidal, as shown in Figure 1-7. One of the advantages of external modulation is that with proper device design it can be operated with little or no chirp [3][4]. Furthermore, by operating at the point of quadrature the distortion is nominally symmetrical about the inflection point of the transfer function, offering significantly reduced CSO distortion. The lower limit to CSO is then determined by the nonlinearity of the amplifier driving the external modulator, and deviations from the point of quadrature. Typical values of CSO in this case are usually less than -70dBc. The symmetric curvature of the transfer function will still cause large odd-order composite triple-beat (CTB) distortion. This can be compensated for by pre-distorting the driver circuit [5][6] or using a linearized version of the external modulator [7]. While externally modulated transmitters minimize distortion due to dispersion, the narrow spectrum associated with chirp-free modulation enhances nonlinearities in the fiber such as stimulated Brillouin scattering (SBS).

1.3 Stimulated Brillouin Scattering

1.3.1 Overview

When an optical signal propagates through the fiber in the forward direction, some energy is lost to an acoustic wave propagating in the forward direction and a backward going optical signal is formed. This process is called Brillouin scattering. The acoustic wave stresses the material, altering its local index of refraction and acts like a moving index grating with frequency ω_A and velocity v_A. Incident laser light of frequency ω_L, called the pump, spontaneously scatters

[1] dBc indicates the power of the composite CSO beat relative to the peak power of the visual carrier.

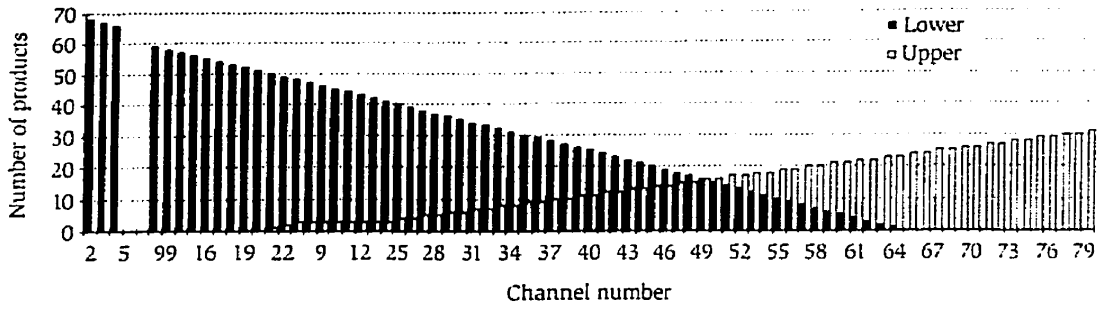

Figure 1-6: Number of CSO beats: 550MHz Standard channel plan. When equally spaced carriers are subjected to CSO, combinations of the individual carriers result in products 1.25MHz above and below the original carriers. (From [1])

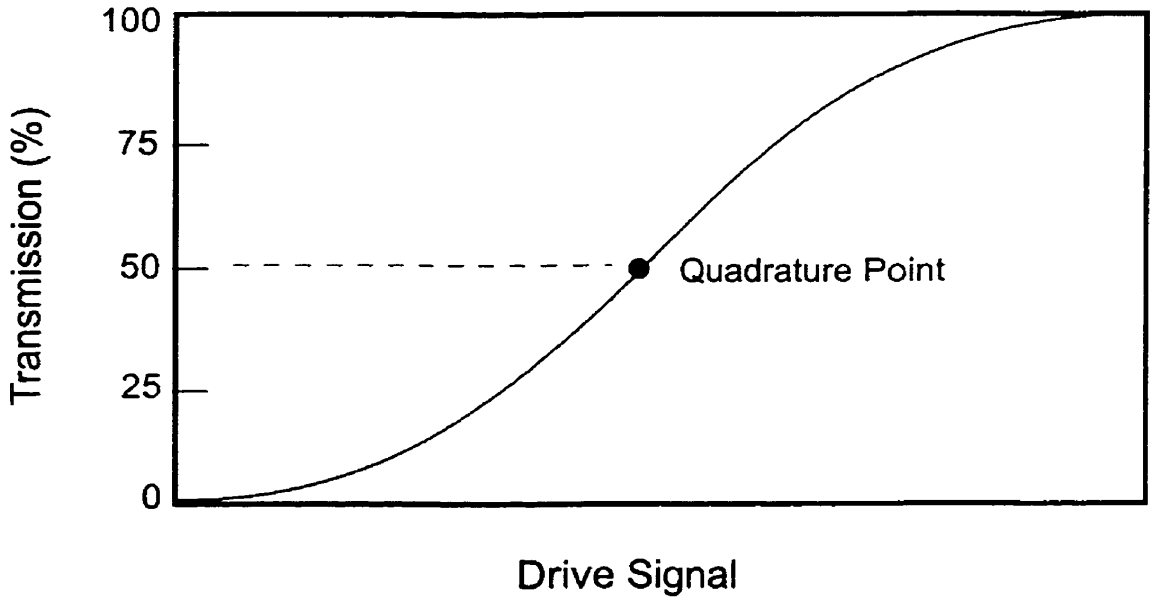

Figure 1-7: Transfer function for a standard Mach-Zehnder optical modulator. By operating at the point of quadrature, the distortion is nominally symmetrical about the inflection point of the transfer function, offering significantly reduced CSO distortion.

from this refractive index variation. The scattered light propagating back to the input is called the Stokes wave, and has frequency ω_S. The Stokes wave is downshifted in frequency because of the Doppler effect, thus $\omega_S = \omega_L$-ω_A. The interference of the pump and Stokes wave creates a time-varying intensity that can drive the acoustic wave. In other words, the beating of the pump wave with the sound wave tends to reinforce the Stokes wave, whereas the beating of the pump wave and Stokes wave tends to reinforce the sound wave. The positive feedback described by these two interactions can lead to exponential growth in the amplitude of the Stokes wave and is the origin of the term 'stimulated' as distinct from spontaneous Brillouin scattering which is a very weak process. The resulting backscattering is illustrated in Figure 1-8 for a 1550nm DFB laser operating at constant power (CW). The backscattering data was obtained using an erbium-doped fiber amplifier (EDFA), variable optical attenuator, and two optical splitters that are configured to measure the injected and reflected powers; further details of the experimental setup are discussed in Chapter 3.

For input powers below the SBS threshold, Rayleigh scattering is the dominant contribution to backscattering in the fiber. Rayleigh scattering is caused by density fluctuations in silica that lead to random fluctuations of the refractive index on a scale smaller than the optical wavelength λ. The intrinsic loss of silica fiber from Rayleigh scattering can be written as

$$\alpha_R = \frac{C}{\lambda^4} \tag{1.7}$$

where C is a constant in the range of 0.7-0.9 (dB/km)-μm^4 [2]. These values for C correspond to $\alpha_R = 0.12$ to 0.16 dB/km at 1550nm. While the term loss is used, the light is actually scattered in random direction with a fraction of the light scattered on-axis. It is this on-axis component, known as Rayleigh backscattering, that is the origin of the -33dB backscattering seen in Figure 1-8 at low input power. Above the SBS threshold, which occurs at approximately 8dBm, SBS becomes the dominant source of backscattering. It increases rapidly with input power, and by the time the injection power reaches 16dBm half the power is reflected back to the transmitter.

A portion of the reflected light is re-reflected at acoustic wavefronts due to the change in the index of refraction. The random phase relationship between the original and double-reflected signal, as received at the detector, causes increased noise [1]. Figure 1-9 and 1-10 illustrate the

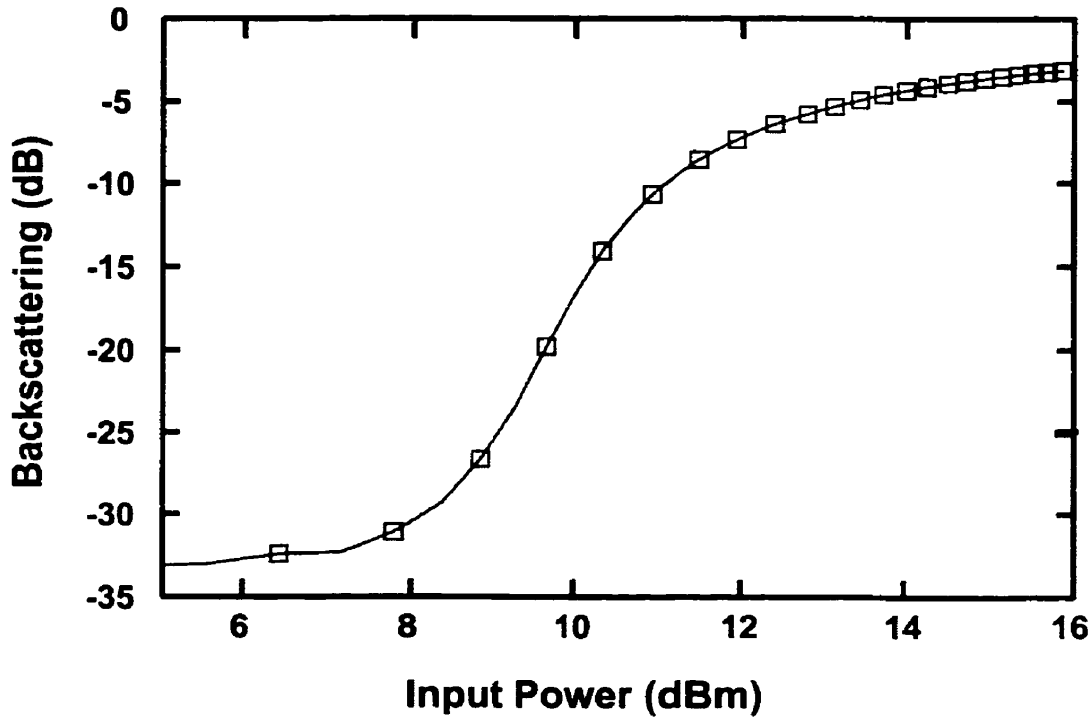

Figure 1-8: Brillouin-scattered power versus fiber injected power for a 1550nm DFB laser into 30km of single-mode fiber. For input powers below the SBS threshold, Rayleigh scattering is the dominant contribution to backscattering in the fiber. Above the SBS threshold, which occurs at approximately 8dBm, SBS becomes the dominant source of backscattering.

transmitted noise power and resulting carrier-to-noise ratio (CNR)[1] for a single CATV channel launched into 13km of single-mode fiber (SMF) [8]. The upper plot shows the noise spectral power density output of the receiver for a single CATV channel at 67.25MHz, versus power injected to the fiber; the laser is unmodulated in this case. When the test fiber is replaced by a short jumper that is too short for SBS or other nonlinearities to occur, with attenuation to match the loss of the test fiber, results show the noise performance of the receiver. Thermal noise sets a constant noise floor. As power is increased, shot noise from the received optical signal becomes the limiting noise source. The solid line is a theoretical prediction of the combination of shot noise and thermal noise. When the 13-km test fiber is present, a sharp increase in the noise is seen when the SBS threshold is exceeded. The lower plot shows the measured CNR as a function of power injected to the test fiber. At low power levels the CNR grows proportionally with injected power, but beyond the SBS threshold the CNR degrades rapidly.

In a typical long-haul CATV system, the total optical power budget is small because a high carrier-to-noise ratio (CNR > 55dB) must be maintained across 80 to 110 channels, where the modulation index for each channel is only a few percent; the power budget defines the maximum acceptable optical power loss in the system in order to ensure adequate performance at the receiver. Since these systems are primarily shot-noise limited, one should operate at the highest possible launched optical power. SBS limits this power. Fortunately there are techniques for suppressing SBS in optical fiber; this is discussed in the next section.

1.3.2 SBS Suppression

While it is possible to reduce SBS by fiber or link design [9] [10], this is not considered commercially practical in many situations because of the large installed base of conventional single-mode fiber. Therefore, there is an interest in modifying the optical source to reduce the impact of SBS. The most common approach is to broaden the optical spectrum of the signal launched into the fiber by intentionally chirping the source.

In digital transmission systems, the transmitter is chirped by direct current modulation of

[1]CNR is defined as the ratio of the visual carrier to total noise power in the 4MHz bandwidth of the video information.

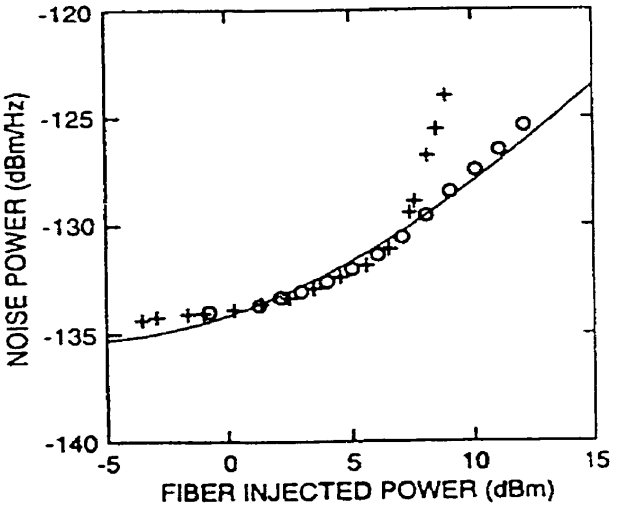

Figure 1-9: Transmitted noise power versus injected power. The solid line is a theoretical prediction of the combination of shot noise and thermal noise. The circles are experimental results without fiber propagation. The (+) symbols represent noise power after 13km of SMF. indicating the increase in noise for injection powers beyond the SBS threshold. (From [8])

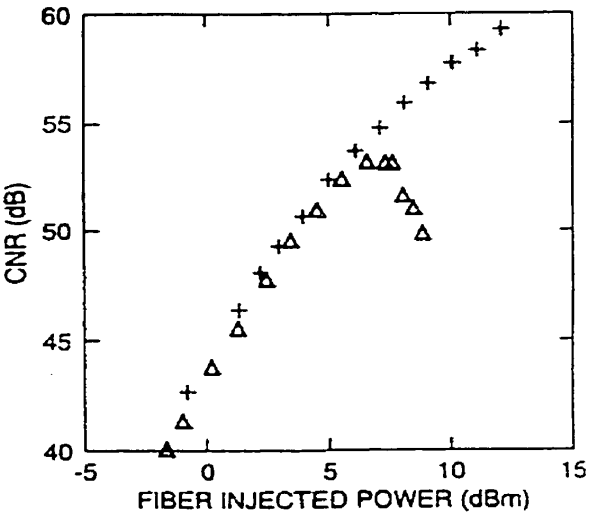

Figure 1-10: CNR versus fiber injected power. The (+) symbols represent CNR for no fiber propagation, the triangles are CNR after 13km of SMF indicating the degradation in CNR for injection powers beyond the SBS threshold. (From [8])

the laser at a very low frequency, usually in the kHz range. In this case, the optical spectrum can be viewed as quasi-continuous, and a detailed examination of the Brillouin gain profile is required. The Brillouin gain has a Lorentzian spectral profile given by [2]

$$g_B(\nu) = \frac{1}{1 + [(\nu - \nu_B) / (\Delta\nu_B/2)]^2} g_{SBS} \tag{1.8}$$

where g_{SBS} is the peak value of the Brillouin gain, ν is the frequency shift of the pump frequency, ν_B is the Brillouin frequency shift of the Stokes wave which is typically around 10GHz, and $\Delta\nu_B$ is the full width at half maximum (FWHM) of the gain curve which ranges from 30-200MHz in conventional single-mode fiber. SBS is reduced when the optical spectrum becomes wider than the SBS linewidth. Unfortunately, the low-frequency dither approach cannot be used in analog systems because it leads to unacceptable generation of distortion products. As described in Section 1.2.2, fiber propagation leads to second-order intermodulation products between frequencies present at the fiber input. In the case, for example, of a 40kHz dither tone, intermodulation sidebands are formed 40kHz above and below all the visual carriers: the distortion levels encountered are unacceptable for CATV transmission.

Extending this reasoning, we can determine the range of acceptable frequencies that will not result in second-order distortion products. To simplify the analysis, first consider a case where both the CATV signal *and* dithering tone are created using pure amplitude modulation (AM). At the output of the CATV transmitter, the power spectrum of the signal will have a band of frequencies between f_L and f_U, which are the lower and upper frequencies of the CATV signal, respectively, along with a single spectral component at the dithering frequency f_D. The power spectrum of this signal is given in Figure 1-11 (a). If this signal propagates through a nonlinear element, 2^{nd}, 3^{rd} and higher order beats are generated. Provided the nonlinearity is weak, however, one can justify only looking at the first few nonlinear terms and discarding the higher order terms. The 2^{nd} order nonlinear term will dominate, and so beat frequencies are produced which form a band of intermodulation frequencies on either side of the dithering frequency f_D. Provided the dithering frequency $f_D > 2f_U$, the low end of the intermodulation band does not enter the CATV band and distort the signal.

For externally modulated systems, where the spectrum is narrow because of chirp-free mod-

ulation, SBS suppression is accomplished by distributing the optical power over a number of subcarriers using direct dithering of the transmitter laser or phase dithering of a constant laser output, using an external phase modulator. This will generate a large number of optical carriers, equally spaced in frequency and each reduced in power compared to the unmodulated case. In most cases, single-tone dithering is used because it is easy to implement [11][12][13] [14]. Figure 1-12 illustrates the difference between an optical source operating at constant power and one that is intentionally broadened. When the dithering frequency, f_D, is much larger than the Brillouin linewidth, each spectral component many be treated as an independent carrier. This idea is discussed in Chapter 3.

To characterize SBS suppression in optical fiber, one needs a way of measuring the SBS threshold. There are a number of techniques outlined in the literature for measuring the SBS threshold. In one approach, it is defined as the point when the system relative intensity noise (RIN) is increased by more than 0.2dB [13]. The system RIN, in this case, is determined by EDFA noise, interferometric noise sources, and the laser intrinsic RIN. The threshold values obtained therefore depend on parameters of the specific transmitter and receiver that can vary from one setup to the next. Another technique measures the SBS threshold based on the point when the CNR begins to degrade [12]. The technique suffers from the same problem as the RIN measurements. A third approach analyzes SBS backscattering data from the optical fiber [12]. The advantage of the backscattering approach is that it only requires two inexpensive optical couplers and photodiodes configured to measure the injected and backscattered powers. and it is an unambiguous measure of SBS. The backscattering approach is the one used in this thesis.

Figure 1-13 presents three experimental backscattering curves for a directly dithered 1550nm DFB laser. The dithering frequency is 1GHz, the fiber link is 30km long, and the laser is operated in three conditions, without modulation, and modulation depths of 12% and 69%. When using experimental backscattering data, the SBS threshold is determined from the intercept of the tangent with the Rayleigh baseline. While somewhat arbitrary in the choice of the Rayleigh backscattering as a reference level to define the SBS threshold, this method is conventionally accepted. The increase in the SBS threshold relative to CW operation gives the SBS suppression, measured in dB. It is common to use the terms threshold and suppression

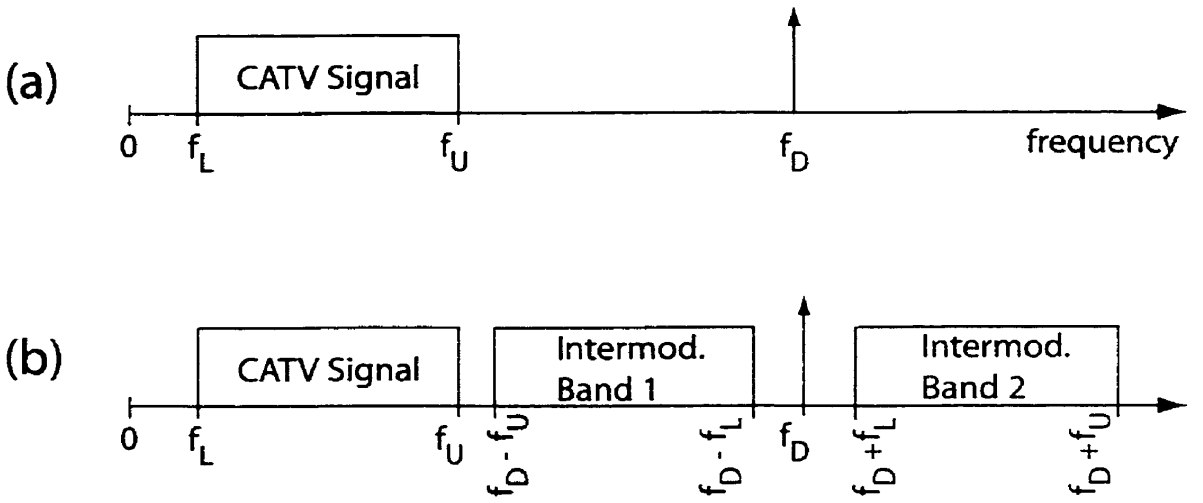

Figure 1-11: Power spectrum of an AM generated CATV signal and suppression tone before (a) and after (b) propagation through a second-order nonlinear element. The 2^{nd} order nonlinear term will dominate in a weakly dispersive fiber, and so beat frequencies are produced which form a band of intermodulation frequencies on either side of the dithering frequency f_D. Provided the dithering frequency $f_D > 2f_U$, the low end of the intermodulation band does not enter the CATV band and distort the signal.

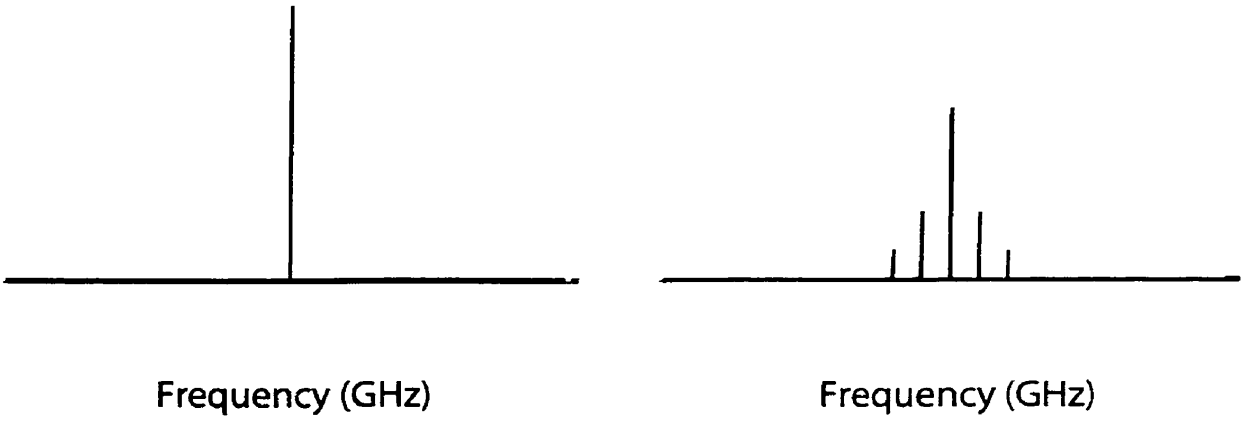

Figure 1-12: Illustrative optical power spectra when the laser is operating at constant power (left) and intentionally dithered using an external phase modulator (right), distributing the optical power over a number of subcarriers.

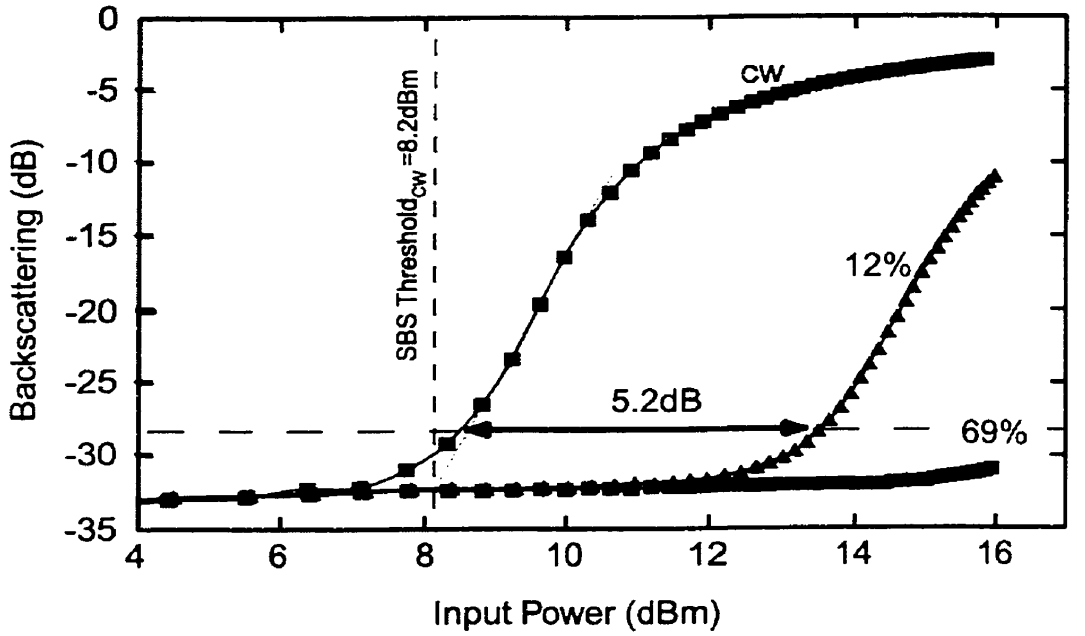

Figure 1-13: Experimental backscattering data for a directly dithered 1550nm DFB laser. The modulation frequency is 1GHz and the fiber is 30km of SMF. The laser is operated at CW and modulation depths of 12% and 69%.

interchangeably, where the units differentiate the two. SBS suppression is a more accurate measure of the effectiveness of transmitter dithering at reducing the impact of SBS, as the CW threshold of a semiconductor laser can vary from one laser to the next. This measure also eliminates the abitrariness mentioned earlier from choosing the Rayleigh backscattering baseline as the reference level. The lateral shift in the backscattering curve relative to CW determines the amount of SBS suppression. For the particular case illustrated in Figure 1-13, when the laser is directly dithered at 12% modulation depth, the SBS suppression is 5.2dB. The suppression at 69% modulation depth cannot be measured because the output of the EDFA used in these experiments cannot reach the necessary injection power. The maximum output power of the optical amplifier limits the overall measurement range. This limitation is common to all the techniques outlined above. An alternative to the backscattering approach is spectral analysis of the transmitter output. With a proper understanding of the relationship between SBS and transmitter characteristics, one can measure SBS suppression over a much wider measurement range.

Conventional SBS theory determines the level of suppression based on analysis of the peak power in the optical spectrum [13]. For example, consider a 1550nm DFB laser operated both at constant power (CW) and externally phase dithered at some arbitrary phase modulation index m[1]. Typical optical power spectra for these two cases are shown in Figure 1-14. When the laser is at a constant power, the spectrum consists of one peak. When the laser is dithered, the spectrum broadens and distributes the optical power over a number of subcarriers separated by the dithering frequency. Conventional theory estimates the SBS suppression from the difference between the original CW power of the laser and the peak power in the broadened spectrum. To assess the accuracy of this approach, we compare the suppression results using conventional theory with experimental backscattering measurements over a range of modulation depths of the 1550nm DFB laser. This comparison is illustrated in Figure 1-15. Conventional theory underestimates the level of suppression beyond the first local maximum of the suppression curve. The reason for this is the breakdown of single-peak analysis when two or more spectral components have similar powers. To improve the accuracy of this approach, a new technique for spectral analysis has been developed that encompasses the characteristics of the entire optical

[1]The phase modulation index m is the peak phase change in units of radians

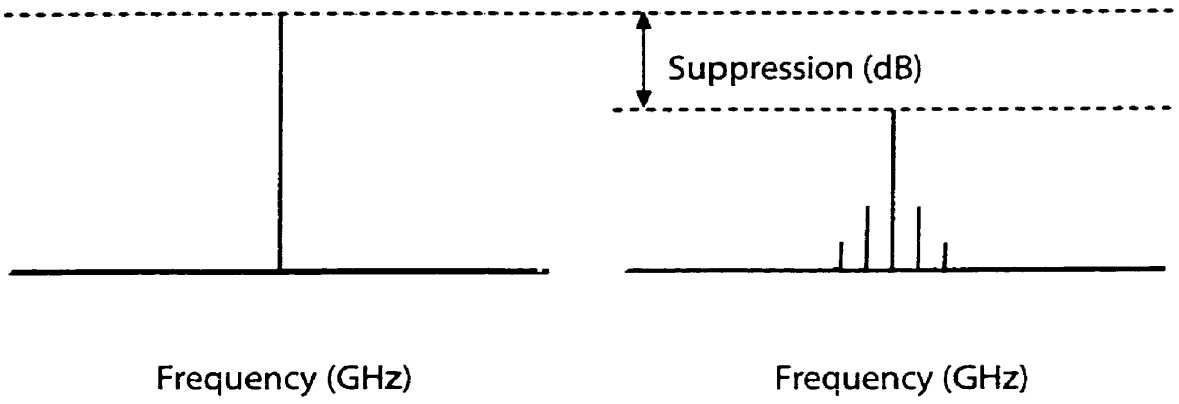

Figure 1-14: The optical spectrum of a 1550nm DFB laser operating at constant power and externally phase dithered. SBS suppression is determined by conventional suppression theory.

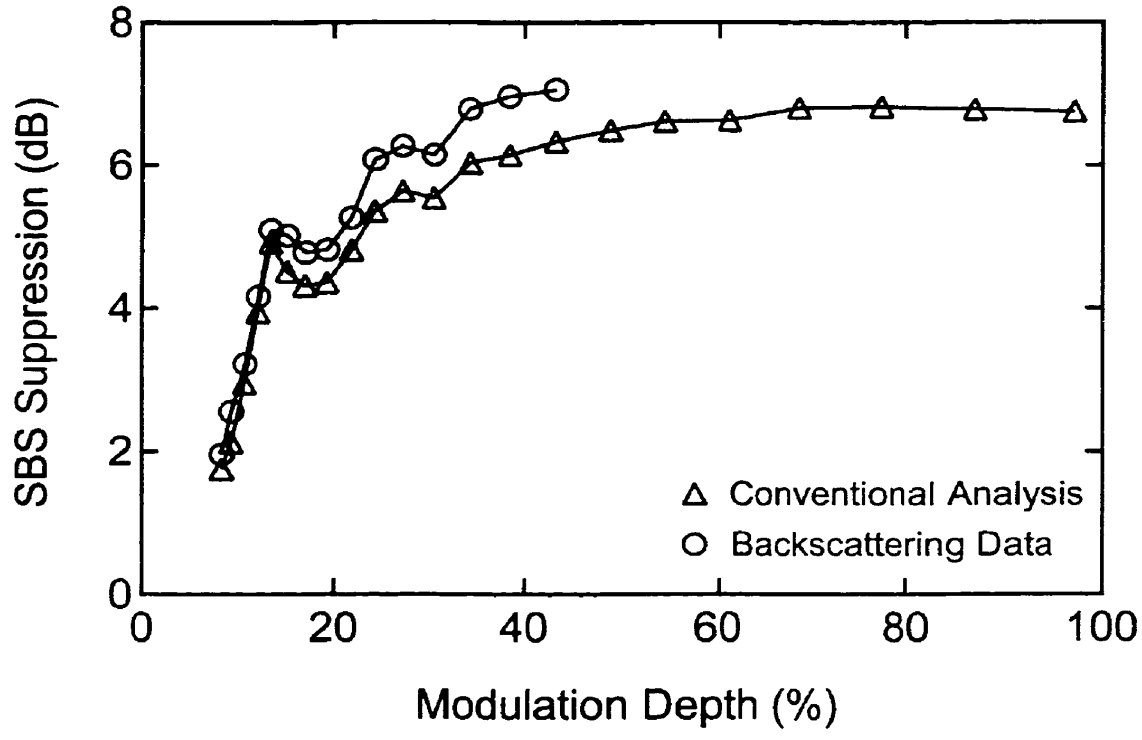

Figure 1-15: Comparison of SBS suppression results using both conventional theory and experimental backscattering data for a directly dithered 1550nm DFB laser. The dithering frequency is 1GHz and the optical fiber link is 30km of SMF.

spectrum. Results using this new technique are illustrated in Figure 1-16, showing much better agreement. The details of this approach are presented in Chapter 3.

1.4 Chirp Measurement System

The major premise upon which this thesis is based is that the key to developing better SBS suppression schemes is to gain a quantitative understanding of the relationship between transmitter characteristics and suppression. To this end, a high-bandwidth chirp measurement system has been designed to characterize the output from optical CATV transmitters. Both the time-resolved power and chirp waveforms are obtained using this system, allowing determination of the full complex average electric field and corresponding power spectrum of the outgoing optical signal. This information can be used to investigate the relationship between suppression and transmitter characteristics, with the goal of understanding why certain dithering techniques are more effective than others at suppressing SBS and designing improved schemes.

Chirp is extremely difficult to measure because typical values are less than $\pm$ 20GHz, which is one part in 10,000 compared to optical frequencies; furthermore, it is desirable to make measurements of chirp that are below $\pm$1GHz. A number of techniques in the literature have been used to measure chirp. For time-averaged spectra, Fourier transform spectroscopy [15][16] is capable of reasonably high resolution measurements over wide optical bandwidths. This method is based on measuring the interferogram output as a function of path-difference using a spectrometer such as a Michelson interferometer. The spectral irradiance distribution I(k) as a function of wavenumber can then be found by numerical Fourier-Transformation. Unfortunately, conventional Fourier transform instruments are only barely able to resolve the optical spectra involved in this work, limited by the path length difference in the instrument. Another approach is to use a scanning Fabry-Perot interferometer. Other lower resolution spectral techniques have also been used; for example, measurements are sometimes made in the presence of source modulation and are typically performed with a grating-based optical spectrum analyzer. These methods, however, cannot adequately characterize the source chirp because of the lack of time-resolved information; equivalently, these methods yield no information about the relative phases of the spectral components.

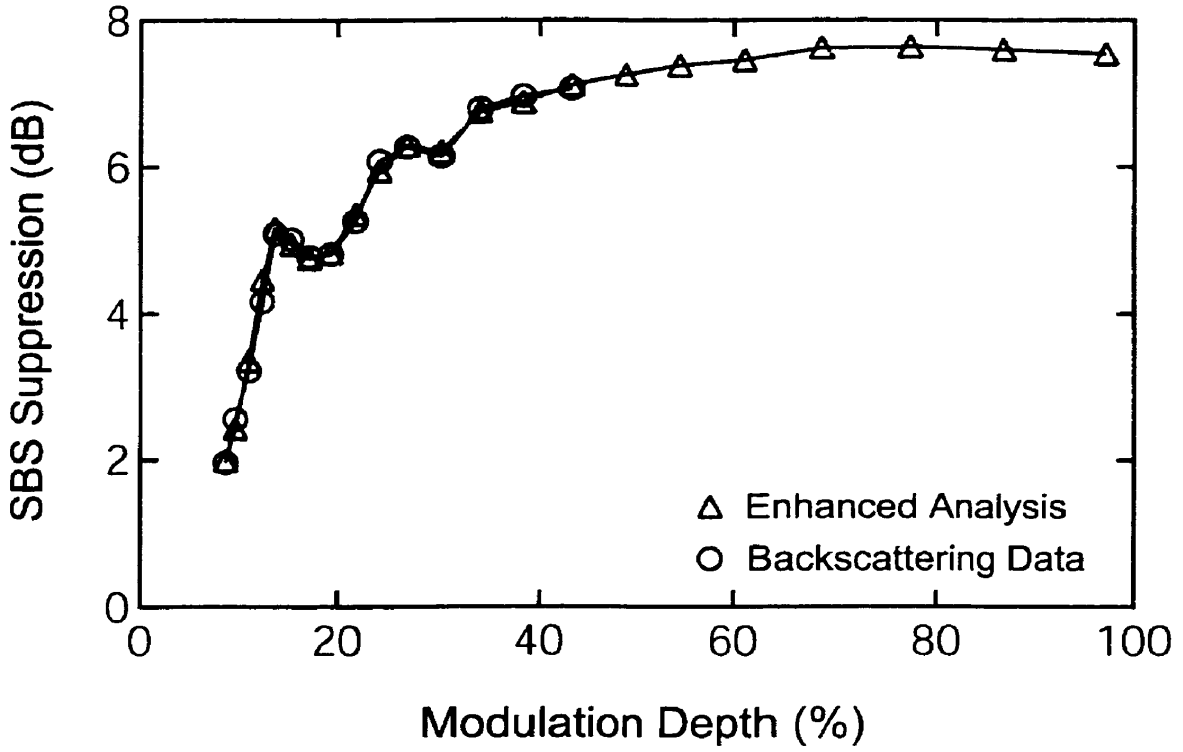

Figure 1-16: Comparison of SBS suppression results using both enhanced analysis and experimental backscattering data for a directly dithered 1550nm DFB laser. The dithering frequency is 1GHz and the optical fiber link is 30km of SMF.

Devaux [17] designed a simple and fast method to measure a quantity known as the chirp parameter. Unfortunately, this technique is only appropriate for small-signal modulation at constant sinusoidal chirp and is not time-resolved. In addition, it requires modulation of the source over a wide range of frequencies, which has limited general application. Linke [18] was one of the first to make time-resolved measurements of chirp on pulsed laser diodes. Figure 1-17 shows a block diagram of the experimental setup and a sample of the results. The spectrometer is scanned slowly while a sampling unit repeatedly samples at fixed times with respect to the start of the pulse. This pulse is generated repetitively, and so negative time on the figure indicates the trailing edge of the previous pulse. The experimental results give intensity versus wavelength for a number of times during the pulse evolution. While this technique is successful in measuring transient chirp, the spectra are hard to interpret quantitatively because the frequency chirp is accompanied by intensity modulation. This problem was addressed by a group of researchers at the University of Korea [19]. These researchers extract the transient chirp from the mean wavelength of the resulting spectra allowing interpretation of the measurements in the presence of intensity modulation. There are a number of disadvantages of this technique. First, the scanning optical spectrometer is not easily transportable and has a limited optical throughput. More fundamentally, scanning spectrometers are unable to reach resolutions appropriate to resolve chirp on the GHz scale - the data in Figure 1-17 correspond to a shift of around 25GHz.

In 1988, Vodhanel introduced a technique for measuring the AM and FM response of DFB lasers [20]. While not originally designed for time-resolved chirp measurement, this technique was used by Saunders in 1994 for that purpose [21]. Figure 1-18 shows a schematic of the necessary components for this approach. The general principle is to record the signal detected by a high-speed photodetector placed after an adjustable optical frequency discriminator, which converts optical frequency changes to intensity changes. In addition to detecting frequency modulation, the photodetector is also affected by intensity modulation of the source. The signal recorded on the sampling oscilloscope therefore has contributions from both chirp and amplitude modulation. Saunders showed that by making measurements with the optical frequency discriminator set to two points which give equal and opposite frequency to intensity conversion, but equal amplitude modulation to intensity conversion, the chirp can be related to

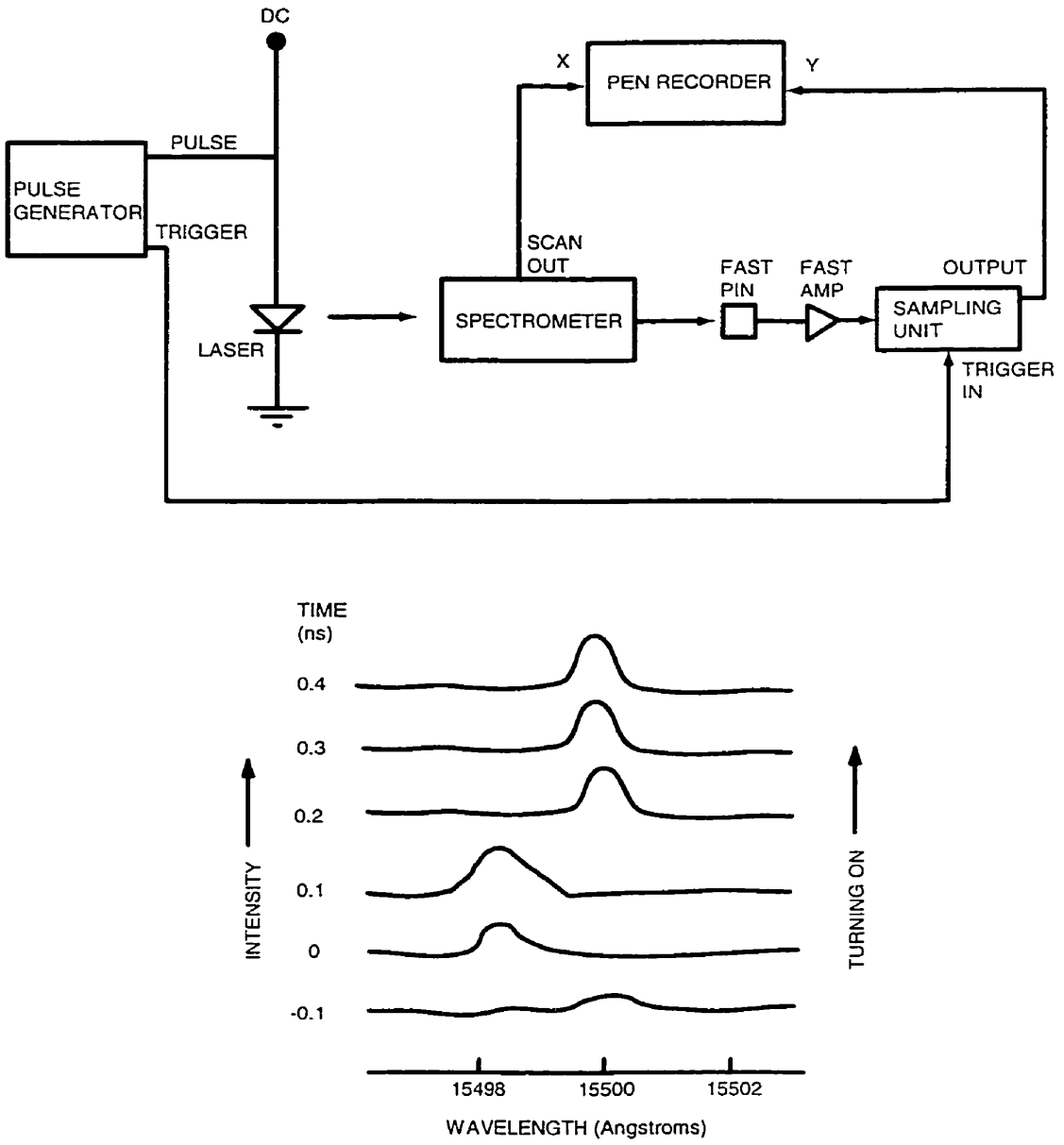

Figure 1-17: A block diagram of Linke's chirp measurement apparatus and results. The spectrometer is scanned slowly while a sampling unit repeatedly samples at fixed times with respect to the start of the pulse. The experimental results give intensity versus wavelength for a number of times during the pulse evolution.

the difference of the two measurements. Figure 1-19 illustrates this experimental technique in more detail, showing the transmission of the discriminator for two measurement points labeled A and B; the center frequency of the optical source is indicated by ν_0. The discriminator's transmission curve is tuned to these two points and the waveforms recorded with a digital sampling oscilloscope. The waveform recorded at setting A of the discriminator is given by

$$V_A(t) = V_{AM}(t) + V_{FM}(t) \tag{1.9}$$

where $V_{AM}(t)$ is due to the intensity modulation and $V_{FM}(t)$ is due to the source chirp. Similarly, the waveform recorded at setting B is given by

$$V_B(t) = V_{AM}(t) - V_{FM}(t) \tag{1.10}$$

where the sign of the components related to the chirp is opposite to that at point A. Using these two waveforms, the chirp is

$$\Delta\nu = \frac{FSR}{2\pi}\sin^{-1}\left(\frac{V_A(t) - V_B(t)}{V_A(t) + V_B(t)}\right) \tag{1.11}$$

where FSR is the free spectral range, defined as the frequency period of the transmission curve. Adding the two waveforms together cancels the chirp and the resulting intensity modulation is obtained

$$P(t) = 0.5 * (V_A(t) + V_B(t)) \tag{1.12}$$

Derivation of these equations is given in Appendix B. This chirp measurement technique is the one used in this thesis.

Equations 1.11 and 1.12 allow us to reconstruct the full complex average electric field, given by

$$E(t) = \sqrt{P(t)}e^{i\theta(t)} \tag{1.13}$$

where E(t) is the electric field envelope function [2] and the phase is directly related to the chirp by the expression

$$\theta(t) = -2\pi\int_{-\infty}^{t}\Delta f(t')\,dt' \tag{1.14}$$

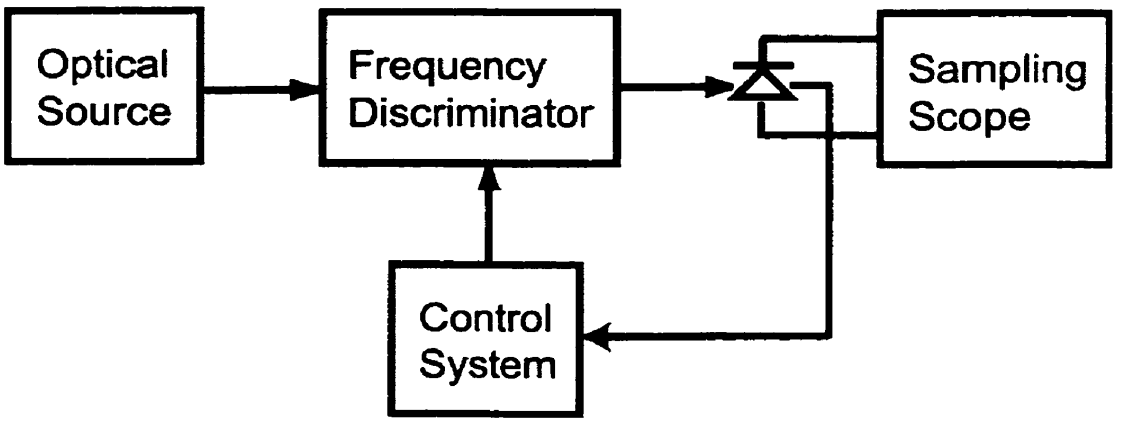

Figure 1-18: Schematic of Saunders' time-resolved chirp measurement system. The signal is detected by a high-speed photodetector placed after an adjustable optical frequency discriminator, which converts optical frequency changes to intensity changes.

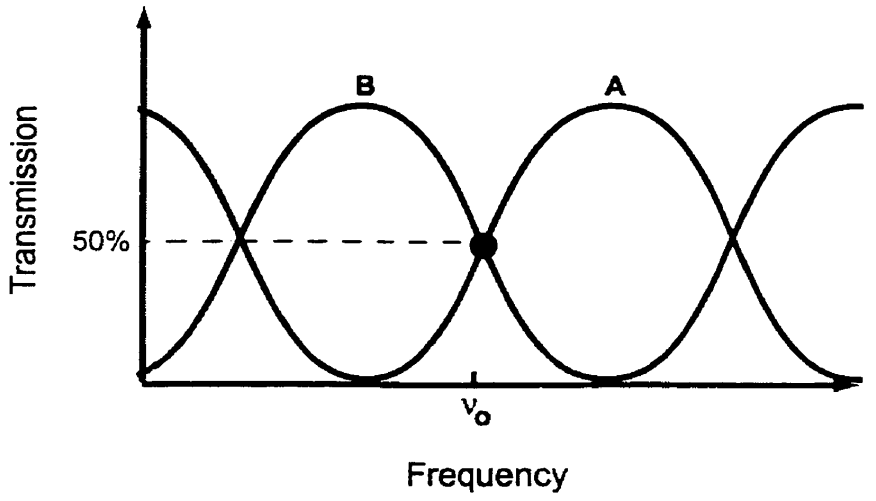

Figure 1-19: Operation of the frequency discriminator at the two 50% transmission points. The measurement points are labeled A and B.

The full complex electric field yields all the information about the averaged transmitted characteristics. It does not, of course, contain information related to the amplitude or phase fluctuations, as it was obtained from time-averaged measurements. With the complex electric field waveform, it is straightforward to evaluate the optical power spectrum by Fourier transform, given by

$$E(\omega) = \Im\{E(t)\} \tag{1.15}$$

The optical spectrum of the full electric field is centered at ω_0. However, in this thesis the electric field envelope function is sometimes used, which has the optical carrier suppressed. This envelope function is useful in describing optical signals with spectral width around the carrier, $\Delta\omega$, much less than the carrier frequency. A full derivation of the envelope function approach is given by Agrawal [2].

1.5 SBS Suppression Techniques

Single-tone dithering is the simplest and most commonly used approach for suppressing SBS, but can only generate suppression thresholds up to 18dBm. This is due to the limited spectral broadening capability of DFB lasers and external phase modulators when using just a single dithering tone at practically-achievable modulation levels. While modifications in device design to allow greater chirp could improve the suppression capabilities of these devices, this thesis examines new SBS suppression schemes using commercially available CATV components and *multi-tone* dithering techniques for enhanced spectral broadening.

A number of multi-tone suppression schemes have been developed and published in the literature to try and exceed the performance of single-tone dithering. In 1996, Korotky [22] developed an approach using external phase modulation of the laser output with one or more dithering frequencies, each at a phase modulation index of 0.45π and a frequency 1/3 the former. To understand how this technique works, consider pure single-tone phase modulation. When pure phase modulation is applied to the optical signal, assuming a normalized electric field, the amplitude of each k^{th} order sideband is given by $J_k(m)$ where J_k is the k^{th} order Bessel function and m is the phase modulation index. The evolution of the Bessel functions as a function of m is shown in Figure 1-20. The modulation index of 0.45π is chosen to achieve an equalization of

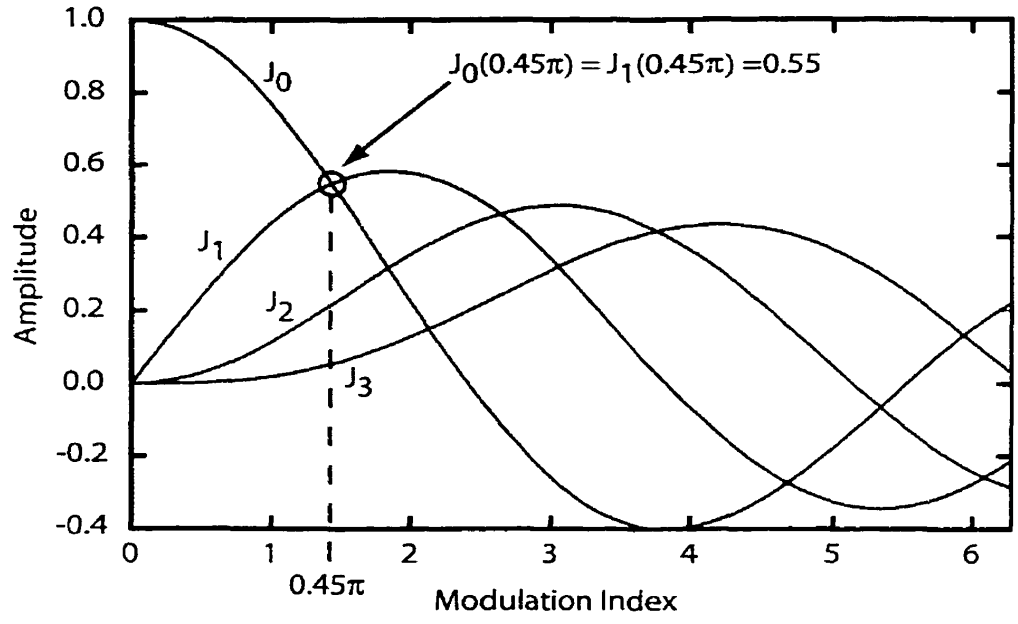

Figure 1-20: Evolution of Bessel functions for increasing phase modulation index.

power in the original and first order sidebands. The optical spectrum after single-tone dithering at frequency f_1 is shown in Figure 1-21(b), neglecting higher order harmonics. This generates three spectral components with equal amplitude and an SBS suppression of 5dB. Applying a second tone will generate nine components with an SBS suppression of approximately 10dB. as shown in Figure 1-21(c); this is the same level of suppression possible using single-tone dithering. Applying a third tone will generate 27 tones and an SBS suppression of 15dB. The lowest dithering frequency must be at least twice the upper CATV frequency, which means that applying more than two tones with this approach requires RF bandwidths above 10GHz. This goes beyond the bandwidth capabilities of currently available phase modulators.

In 1998, Nillson [11] developed a dual-tone suppression scheme where high-frequency modulation of the laser drive current is combined with lower frequency phase modulation. The frequency of the phase modulation is itself varied over a range of frequencies. The experimental layout for this approach is shown in Fig 1-22. A voltage-controlled oscillator (VCO_1) is kept at a constant frequency of f_1 for direct laser dithering. VCO_2 is applied to an external phase modulator and has a center frequency of f_2 with 25MHz excursions applied at a 10kHz

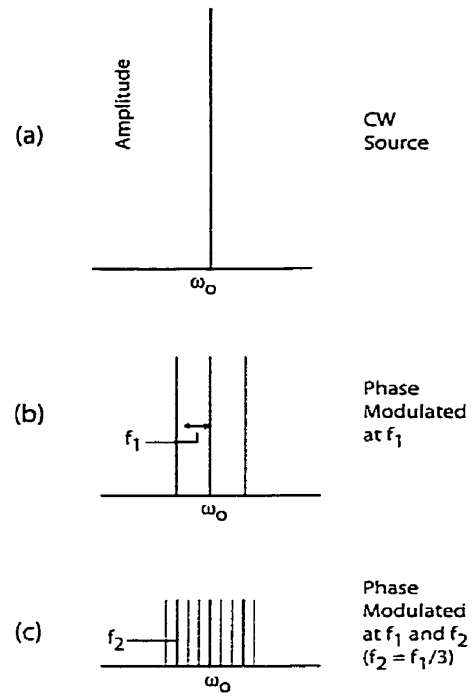

Figure 1-21: Spectral evolution of an optical signal using Korotky's suppression technique. Each dithering tone is 1/3 the previous tone and at a phase modulation index of 0.45π in order to equalize the power in the original and first-order sidebands. This creates a comb-like spectrum over a total of nine components.

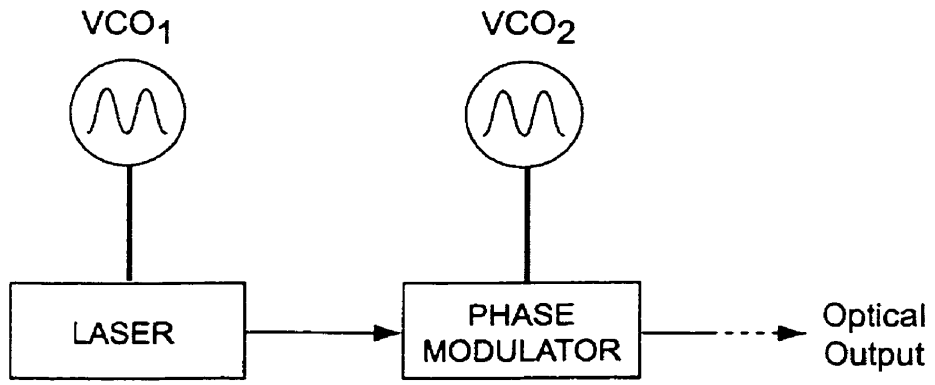

Figure 1-22: Nillson's dual-tone suppression scheme using two VCOs. VCO_1 is kept at a constant frequency f_1 for direct laser dithering. VCO_2 is applied to an external phase modulator and has a center frequency of f_2 with 25MHz excursions applied at a 10kHz dither rate. Both modulators are set to a modulation index of 2.4 and the two frequencies are non-commensurate.

dither rate. Both modulators are set to a phase modulation index m of 2.4, which is easily achievable using commercially available devices. The two frequencies are non-commensurate, which means that there are no solutions to the equation $Nf_1 = Nf_2$, where N and M are each integers. The enhanced spectral broadening of this dual-tone suppression scheme can generate SBS thresholds up to 17dBm. The suppression results using this technique are no better than single-tone dithering results.

In 1999, Atlas [23] suggested using two sinusoidal RF signals to dither the optical source. These signals can be applied to the laser, the external phase modulator, or a combination of the two. The difference between this technique and Korotky's is there is no required frequency ratio or pre-determined amplitude setting for each tone, allowing a large number of possible two-tone suppression schemes. While Atlas claims that two-tone dithering is more effective at broadening the spectrum than single-tone suppression, no specific technique is presented in this work.

In this thesis, a systematic investigation of two-tone SBS suppression is undertaken. A numerical model was used to investigate different combinations of direct laser and external phase dithering, frequency ratio, and modulation index to examine their effects on SBS. The final results show that pure two-tone phase dithering at a frequency ratio of 3:2 is the most effective technique presently feasible for suppressing SBS. Accurate setting of the amplitude and phase of each tone is necessary for optimal results. This new suppression scheme is demonstrated experimentally in an 80-channel CATV system. The SBS threshold is shown to be 21.4dBm, which is 3.4dB higher than what has been previously reported.

1.6 Self-Phase Modulation

SPM occurs when high intensities are launched into the transmission fiber, causing the index of refraction, n, to be slightly modified as a function of the optical intensity. Thus, at the peak swings of instantaneous intensity, the index varies from the unmodulated average value. This causes a different propagation velocity as the instantaneous power varies, resulting in phase modulation. SPM will generate new frequencies components in the optical spectrum as the signal propagates down the fiber. Desem showed that the effect of SPM will be an increase

in the level of CSO distortion [24]. Specifically, for high injection powers on the order of 16dBm, which can be readily obtained using commercially available EDFAs, SPM will result in significant CSO distortion over distances above 60km. With the development of enhanced SBS suppression techniques, we have the opportunity to analyze the effects of SPM on the CATV signal with SBS suppressed in the fiber. This topic will be discussed in Chapter 4.

1.7 Outline of Thesis

Chapter 2 describes the chirp measurement system in detail. The system layout, hardware components, performance issues, and measurement theory are discussed, emphasizing the original aspects of the design. Typical chirp and power results acquired with this new measurement system are outlined at the end of the Chapter.

In Chapter 3, the relationship between SBS suppression and transmitter characteristics is investigated. The limitations of conventional analysis of SBS suppression are discussed, and a new method for spectral analysis is presented. The improved accuracy of this approach is validated by comparison with actual SBS backscattering data for two different 1550nm DFB lasers.

Chapter 4 focuses on two-tone SBS suppression techniques. A numerical model is used to examine different combinations of laser and external phase dithering; the best suppression technique is demonstrated experimentally. Applying this suppression scheme to an 80-channel CATV system, we examine the effect that SPM has on CSO distortion.

Chapter 5 summarizes the conclusions from this work.

Chapter 2

Chirp Measurement System

2.1 Introduction to Chapter

The author designed, built, and tested a computer automated time-resolved chirp measurement system. While the approach closely follows that described by Saunders [21], substantial challenges were encountered in constructing a reliable, simple and accurate measurement system which would yield repeatable results. Section 2.2 presents the overall layout and design of the chirp measurement system. The key components are examined, including the frequency discriminator, control system, sampling oscilloscope, and high-speed photodetector. Section 2.3 presents typical chirp and power results acquired using this approach.

2.2 Layout and Design

The design approach for the chirp measurement system is original, although the underlying concept is based on work first introduced by Saunders in 1994 [21]. Figure 2-1 shows a block diagram of the system. It consists of an optical source, frequency discriminator, photodetector, sampling oscilloscope, and control system. These components were selected only after a significant amount of modeling was done to ensure that bandwidth, noise, and stability issues were addressed. Unlike previous measurement systems based on free-space optics [18][19] [25][26], the present system is completely modularized and interconnected with standard single-mode fiber (SMF) and angle-facet fiber connectors (FC-APC style) to eliminate the need for free-

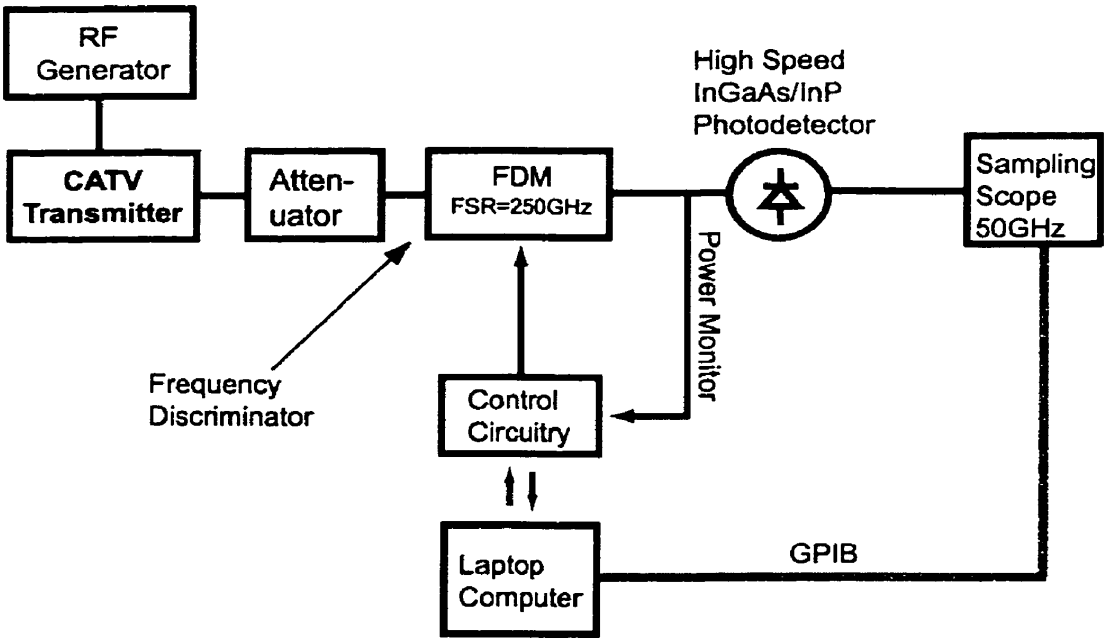

Figure 2-1: The overall layout of the chirp measurement system. It consists of an optical source, frequency discriminator, photodetector, sampling oscilloscope, and control system.

space optical alignment and associated mechanical instabilities. The system is controlled using a laptop computer with GPIB capability and has achieved the original design goal of being portable, allowing research at off-campus facilities.

2.2.1 Transmitter

The flow of the design starts at the optical transmitter, which is a 1550nm DFB laser contained in an analog CATV transmitter module provided by Scientific-Atlanta Canada Inc. It emits a wavelength of 1550nm and has a typical output power of 20mW. A control loop in the transmitter module maintains a constant DC output power level and an optical isolator after the laser prevents any destabilizing influence of back reflections into the transmitter. Modulation of the laser is accomplished by sending the RF output from a signal generator through a power amplifier and into the transmitter circuitry which modulates the laser current. This allows the frequency and modulation depth of the dithered source to be varied. At the high power levels and drive currents involved, it is not effective to predict the effects of dithering from the dither electrical drive levels and frequencies. Instead, the transmitter optical output is characterized with the chirp measurement system, and drive levels adjusted as required. Dithering of the laser is performed with an HP8648B 2GHz signal generator. The output from the transmitter goes through an optical attenuator that sets an appropriate power level to the photodetector. After the attenuator the optical signal passes through a frequency discriminator.

2.2.2 Frequency Discriminator

A PIRI FDM-2n-1.5-M frequency division multiplexer (FDM) was used, based on $LiNbO_3$ Mach-Zehnder technology, because of its insensitivity to polarization, large free spectral range (FSR) and tuning capabilities. Various types of optical frequency discriminators have been used to make time-resolved chirp measurements. Tammela et al. [25] used a thin silicon wafer as a low-finesse etalon. This free-space method is polarization insensitive, which is convenient. The disadvantage of this approach is the need for free-space alignment and the corresponding requirements for mechanical stability. Another technique uses a Mach-Zehnder fiber interferometer where a piezo-electric transducer is used to tune the transmission curve [21]. The two independent optical paths, however, makes stability a problem in the presence

of external fluctuations such as mechanical bending and air flow disturbances. A birefringent fiber interferometer allows for increased stability compared to the Mach-Zehnder interferometer [20][27]. In this thesis work, a frequency division multiplexer (FDM) is used whose circuit geometry is shown in Figure 2-2. This device is a Mach-Zehnder interferometer with unequal path lengths. Tunability of this device is achieved with a thin-film heater integrated on one of the two arms, as illustrated in Figure 2-3. It acts as a phase shifter because the path length of the heated waveguide arm varies due to changes in the refractive index. This allows the transmission function of the FDM to be tuned precisely by controlling the current through the thin-film heater. The advantage of this particular FDM over some of the others mentioned is that it is simple and compact, measuring 3" x 1". it does not require any alignment or mechanical components, and it is completely fiber connectorized so there are no free space optics.

Halfwave plates are integrated into the two arms of the FDM to ensure the device in insensitive to polarization. The half-wave plates are placed at mid-length of each arm of the Mach-Zehnder and rotated 45° to the directions of TE and TM polarization. If the light enters the device in TE mode, it will travel half the optical path length as a TE wave and then half the optical path length as a TM wave. This ensures that the total optical path length of each arm is independent of the incoming state of polarization. Initially, we used an FDM with no half-wave plates. After a detailed study, we found that the maximum and minimum transmission values change as a function of the polarization. This is important because at the beginning of each measurement we scan this transmission curve to find the two 50% transmission points. If the polarization drifts during acquisition of the two waveforms, the control system no longer maintains the 50% transmission points but rather ones that can be significantly higher or lower. The result is a DC offset error in the acquired waveforms and error in the corresponding chirp and power results. It was only after a detailed study of the system that we were able to isolate the problem. With the addition of half-wave plates integrated in the two arms of the FDM, the device was found to be insensitive to the polarization of the incoming signal.

The transmission curve and FSR of the device was characterized by launching broadband light from an unsaturated EDFA into the FDM and measuring the output spectrum using an optical spectrum analyzer. The resulting transmission curve is shown by the open circles in

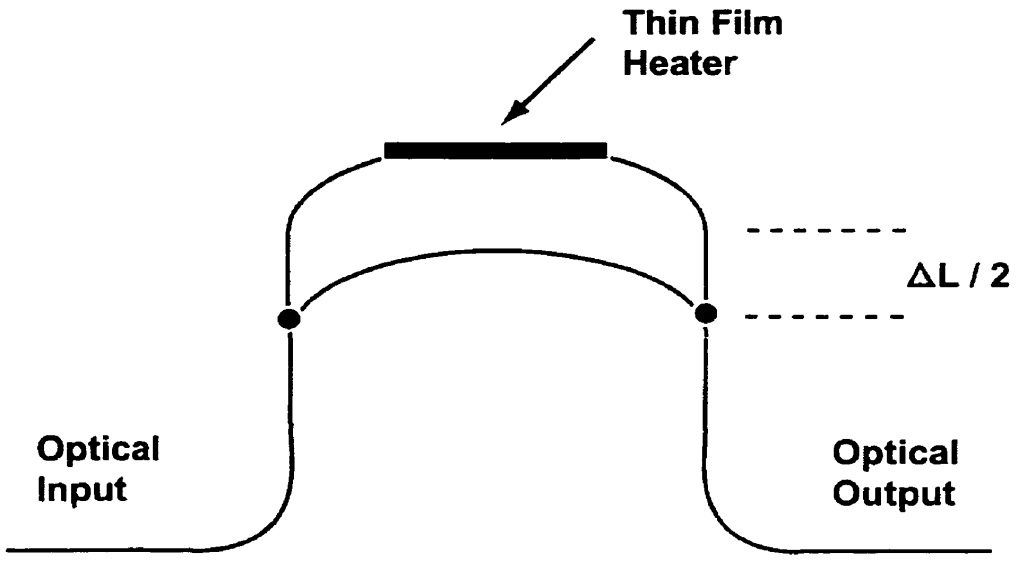

Figure 2-2: Geometry of the frequency division multiplexer (FDM). This device is a Mach-Zehnder interferometer with unequal path lengths. Tunability of this device is achieved with a thin-film heater integrated on one of the two arms.

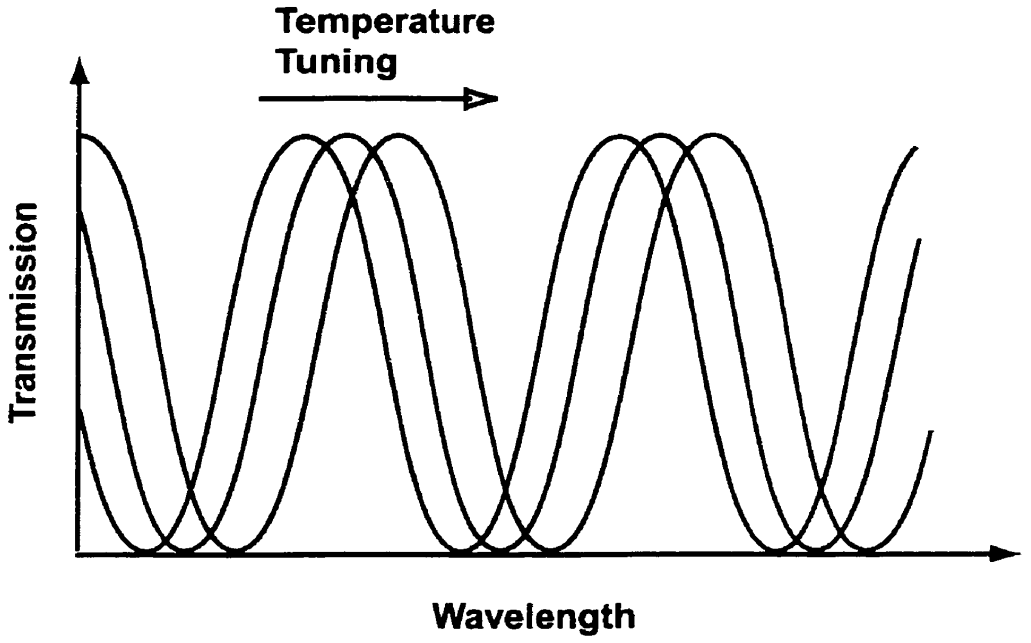

Figure 2-3: Temperature tuning of the transmission curve of the FDM by passing current through a thin-film heater imbedded in one of the two arms of the Mach-Zehnder.

Figure 2-4. A similar measurement without the FDM is used for calibration. Mach-Zehnder theory tells us that the transmission curve should follow a cosine-squared relationship with wavelength; by fitting the measured data to this function, given by the solid line, we extract a FSR of 245GHz at a wavelength of 1550nm. The variation in FSR with wavelength is +0.6GHz/nm for a 5nm range in either direction of the center wavelength of 1550nm.

2.2.3 Control System

The two control points of the FDM are determined using a control algorithm implemented in Labview, a software package for data acquisition programming. The control system is the heart of the experimental setup and is used to coordinate the steps necessary for making chirp and power measurements. These steps include tuning the frequency discriminator to the 50% transmission points, maintaining these control points while averaging incoming waveform data at the sampling oscilloscope, and transferring the averaged waveforms to the computer for analysis. Figure 2-5 shows the control system in detail. The overall control of the system is maintained by a laptop computer running Labview and communicating information with GPIB commands and data acquisition input/output. The system is completely automated and takes about 3 to 5 minutes to complete a measurement.

The key components in the control system are the variable current source and optical power monitor. The variable current source linearly translates voltage output from the computer DAQ card to current that is used to drive the thin-film heater on the FDM. This is a custom circuit designed by the author. Both a coarse and fine adjustment are implemented to ensure precise tuning; this minimizes relative offset errors between the two acquired waveforms that can introduce significant error into the measurement. Using the power monitor, the computer can scan the entire range of the FDM transmission curve and determine the location of the two 50% transmission points. Once the 50% transmission points have been found, a control algorithm takes over to maintain the desired control points while the incoming waveforms are averaged and recorded by the computer. The control algorithm, as shown in Figure 2-6, is a simple integrator with a multiplication factor that accounts for the response of the thin-film heater. The time constant of this integrator is approximately 250ms.

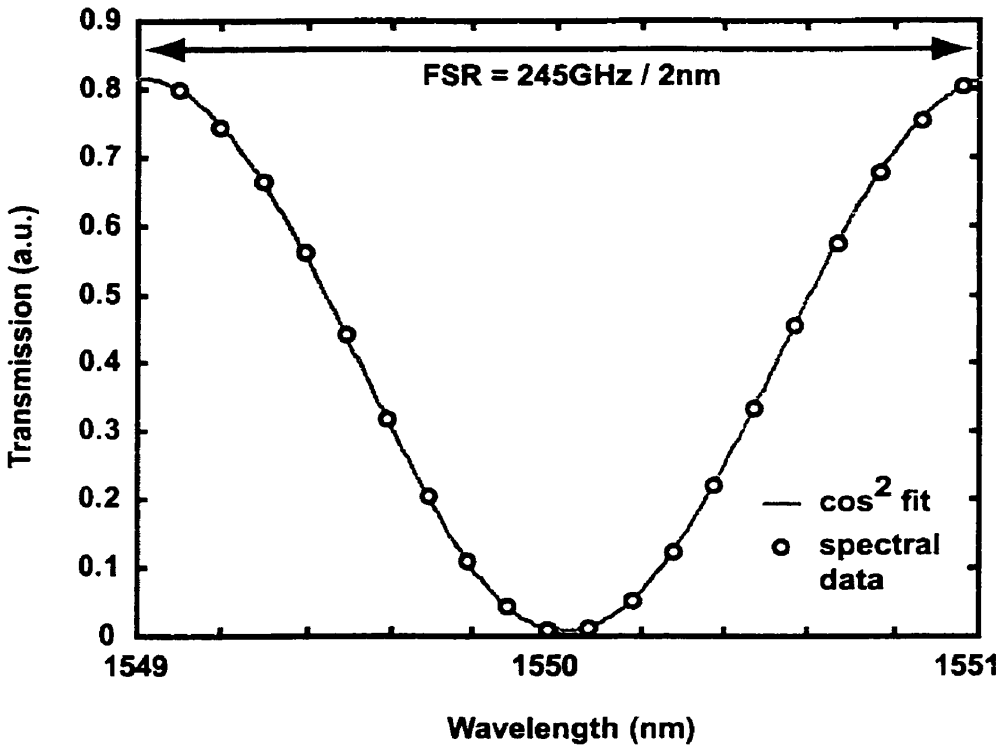

Figure 2-4: Measurement of the free spectral range of the FDM using a broadband optical source.

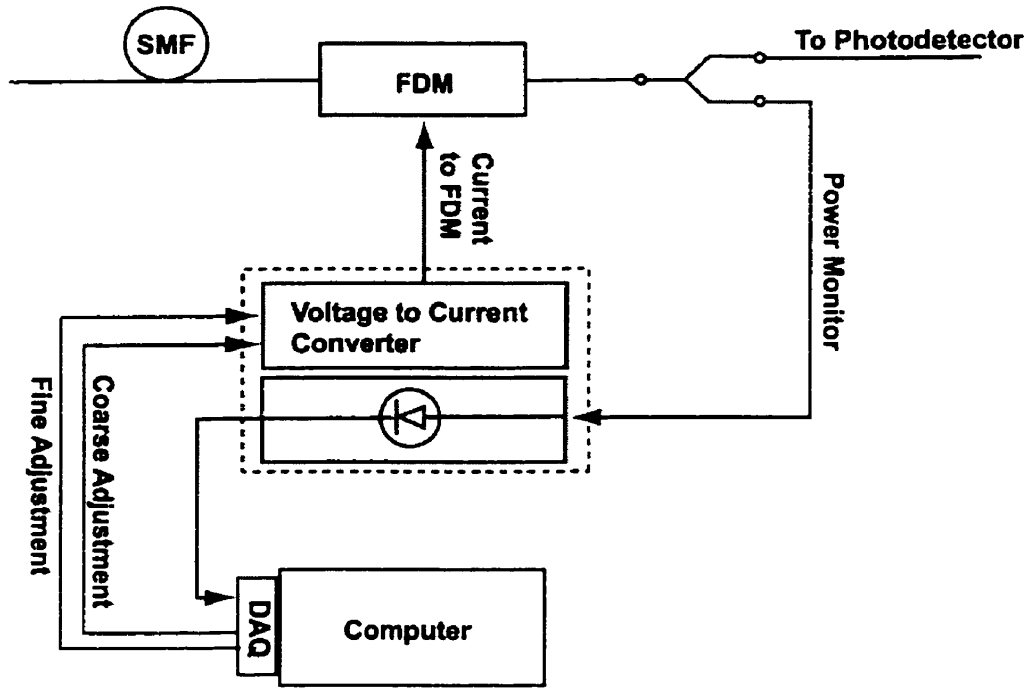

Figure 2-5: Chirp measurement control system. A small percentage of the power out of the FDM is used as a feedback element to adjust the control points to 50% transmission. The variable current source linearly translates voltage output from the computer data acquisition card to current that is used to drive the thin-film heater on the FDM.

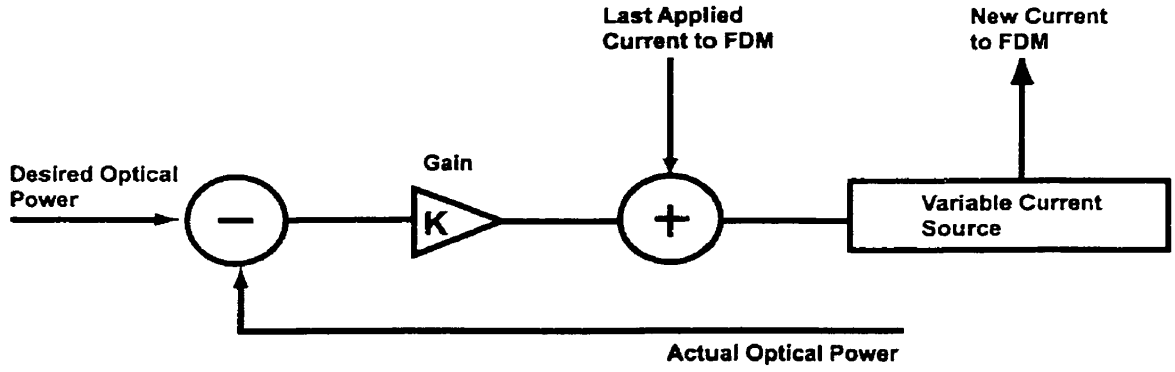

Figure 2-6: The control algorithm used to accurately maintain the 50% transmission points of the FDM while averaging and recording the waveforms. It is a simple integrator with a multiplication factor that accounts for the response of the thin-film heater. The time constant of this integrator is approximately 250ms.

2.2.4 Sampling Oscilloscope and Photodetector

An Opto Speed PDMH25B 25GHz high-output current InGaAs/InP photodiode is used to detect the optical signal. This photodiode is directly connected to a Tektronix 11801B digital sampling oscilloscope with an SD32 50GHz sampling head. On-board smoothing and averaging are used in the sampling head to minimize noise, mostly generated by the sampling head which has an RMS noise value of 1.8mV for a single acquisition. The effectiveness of averaging is shown in Figure 2-7 for a test configuration consisting of a 50Ω termination on the sampling head input. Each waveform is averaged 1024 times by the oscilloscope before being recorded, bringing the RMS noise below $100\mu V$. Use of on-board averaging and readout of the averaged data by the computer for further averaging provides good throughput, as the GPIB bus is too slow to support averaging only within the computer.

The first version of the chirp measurement system used a 45GHz New Focus InGaAs Schottky photodiode as the photodetector. This photodetector has a CW saturation power of only 1mW, limiting output voltages to less than 10mV and providing an unacceptable signal-to-noise ratio (SNR). A low-noise amplifier was inserted between the photodiode and sampling head to try and improve the SNR, but only AC coupled amplifiers are available at the bandwidths required, which meant the DC component had to be added back in later with the appropriate amount of gain. Substantial difficulty was encountered in trying to match the AC and DC gains. The gain of these amplifiers changes not only due to temperature effects but also from inconsistencies in the performance of the RF connectors each time they are connected and disconnected. After considerable work, it became apparent that this approach was impractical. Midway through the thesis work a new high-power high-current photodiode became available. The Opto Speed PDMH25B is a DC coupled device that generates output voltages in excess of 100mV into 50Ω. The cost of this device is half that of the New Focus version and significantly improves the SNR of the measurements.

One of the limitations of the chirp measurement system is the inability to accurately measure waveforms from directly modulated lasers that have a high extinction ratio. Figure 2-8 shows a waveform measured with the detection system for an over-modulated 1550nm DFB laser: over-modulated, in this case, means a laser whose peak modulation current is so large that it goes below threshold at one part of the cycle, effectively turning the laser off. It is physically

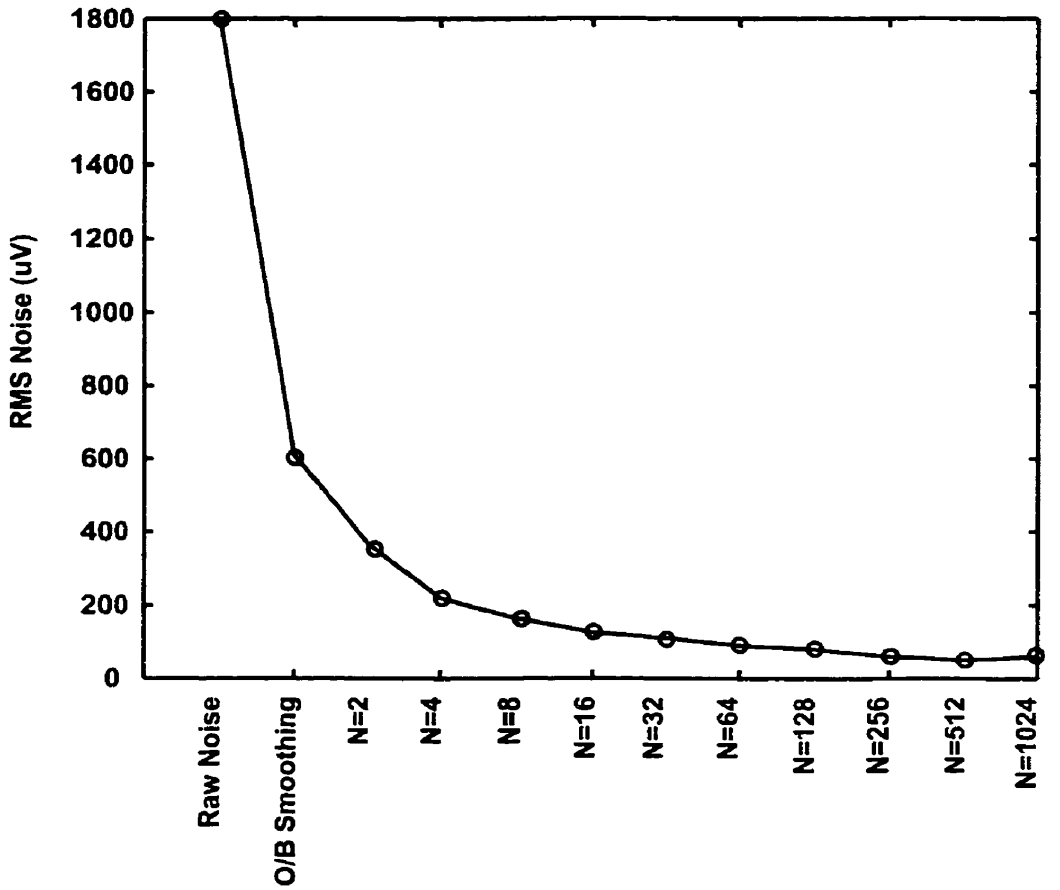

Figure 2-7: RMS noise versus the number of averages for the Tektronix 11801B sampling oscilloscope with SD32 sampling head. The first columns show the raw noise from the head and the raw noise with on-board (o/b) smoothing.

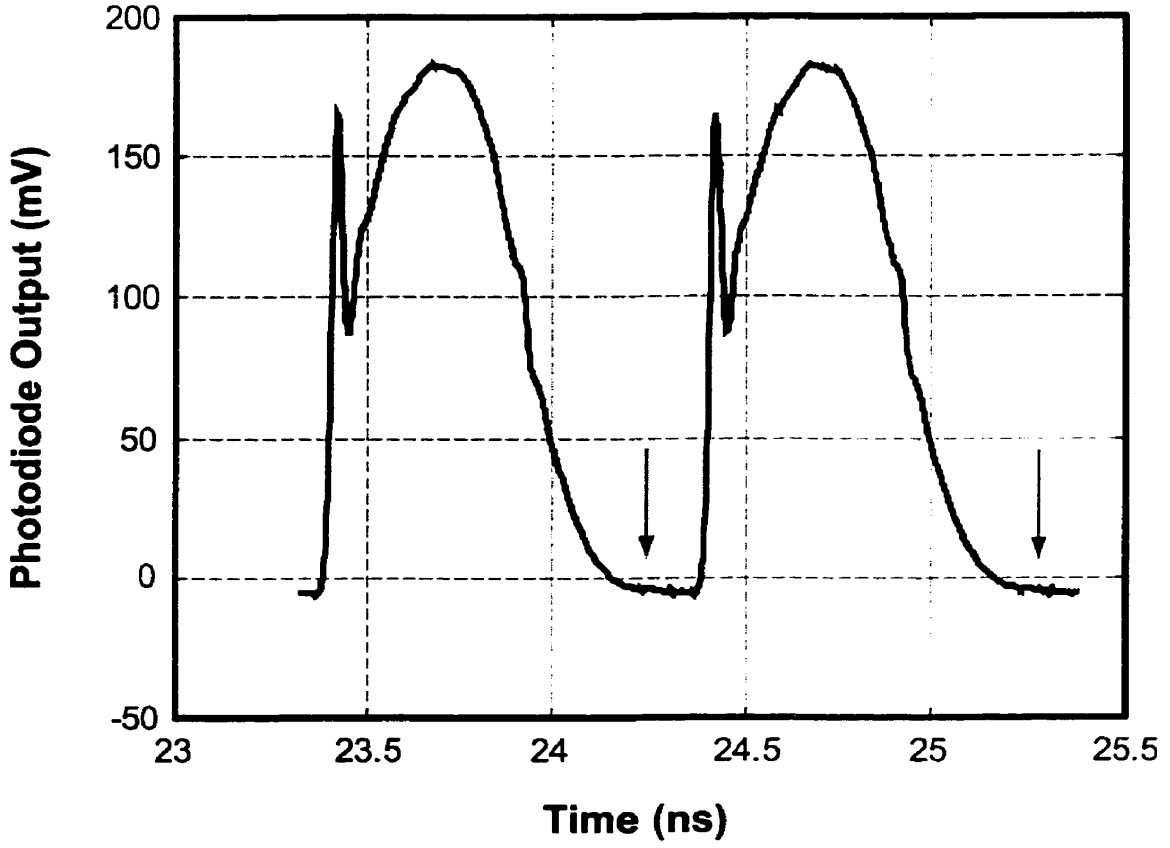

Figure 2-8: Optical power measured with the chirp measurement detection system for an over-modulated 1550nm DFB laser. The downard arrows indicate the undershooting effect due to the imperfect response of the detector.

impossible for the optical output power to go below zero, but due to the imperfect response of the detector the signal recorded by the sampling oscilloscope is negative at some times. This is illustrated in Figure 2-8, with the undershooting effect indicated by the downward arrows. It is important to emphasize that this negative signal is not due to simple offset errors within the oscilloscope or sampling head. In fact, measurements of the photoreceiver output with a 'live' optical signal are always followed by another measurement with no optical signal. Subtraction of the second waveform eliminates any offset errors in the oscilloscope, as well as possible electrical pickup. Thus, the data seen in Figure 2-8 is influenced by a real detector response which we were unable to rectify even with involvement of the manufacturer. We attempted to characterize the response of the detection system by measuring the impulse response. Unfortunately, it was difficult to make accurate measurements using this technique because of the difficulty in getting an optical pulse with minimal jitter and a narrow enough width to satisfy the bandwidth requirements. In the end, this problem was accepted as a limitation of the system.

2.2.5 Measurement Theory

Determining chirp from the two measured waveforms is based on a mathematical analysis of the frequency discriminator characteristics. Depending on the type of discriminator used and the corresponding transmission function, the final equations used to extract the chirp waveform will change. While this derivation is not new, we include it in Appendix B for completeness. The corresponding time-resolved power was originally measured directly at the detector, bypassing the other components in the chirp measurement system. The drawback of this approach is the difficulty in determining the correct phase relationship between the power and chirp waveforms. An important extension of this theory enables measurement of the time-resolved power using waveforms already used for chirp measurement. Since the two acquired waveforms have equal AM components and complementary FM components, as given by $V_+(t)$ and $V_-(t)$

$$\begin{aligned} V_A(t) &= V_{AM}(t) + V_{FM}(t) \\ V_B(t) &= V_{AM}(t) - V_{FM}(t) \end{aligned} \tag{2.1}$$

adding these two waveforms together allows one to reconstruct the time-varying power with the correct phase. This is given by

$$P(t) = 0.5 * (V_+(t) + V_-(t)) \tag{2.2}$$

So by making just one pair of measurements, both the chirp *and* power waveforms are obtained.

2.3 Experimental Results

Figure 2-9 presents time-resolved power and chirp measurements for a 1550nm DFB laser at a dithering frequency of 1GHz and modulation depths of 12% and 69%; peak frequency deviations of 1.4GHz and 7.5GHz are measured at these modulation depths, respectively. The corresponding power spectra are also shown, demonstrating the significant spectral broadening that takes place when the laser is directly modulated. The noise performance is extremely good because of the large signal output from the Opto Speed photodiode and signal averaging performed by the oscilloscope; no additional filtering or complex noise reduction algorithms are required. The minimum amount of chirp that can be measured using this system is defined by the chirp noise floor, which is related to the average signal levels, the noise levels, and the FSR of the frequency discriminator. For all the measurements made during this thesis work, 1024 averages were performed before recording each of the two waveforms. This corresponds to an RMS noise of approximately $100\mu V$. The average voltage is typically 80mV based on an input power of 5mW to the photodetector. Using these numbers, the chirp noise floor is 50MHz which is consistent with observed noise levels. The upper limit for chirp measurement is determined by the FSR of the discriminator. Frequency excursions cannot exceed the adjacent peak and trough bounding each 50% transmission point. For a discriminator with a FSR of 245GHz, the maximum measurable chirp is 61.25GHz.

By examining the $\sin^{-1}\left[\left(V_A(t) - V_B(t)\right) / \left(V_A(t) + V_B(t)\right)\right]$ function in the expression for $\Delta f(t)$, as given in Equation B.9, one can see that noise in the two acquired waveforms will be problematic when the two voltages are small and similar in amplitude. This is encountered for directly modulated transmitters operating at a high extinction ratio. Compounded with this is the imperfect response of the detector, as discussed in Section 2.2.4., which generates

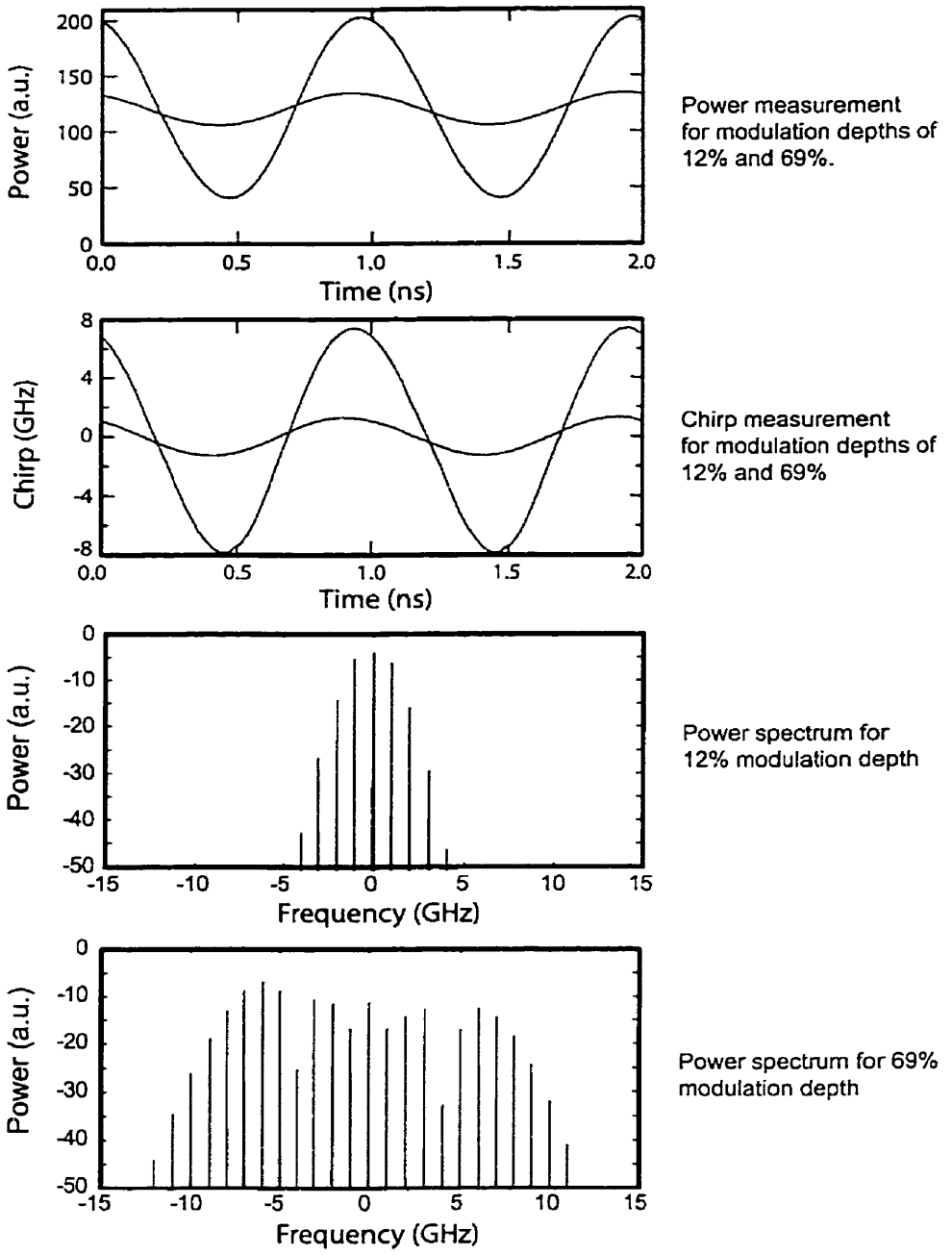

Figure 2-9: Power, chirp, and spectral measurements of a 1550nm DFB laser dithered at 1GHz and modulation depths of 12% and 69%.

additional distortion. For these reasons, it is difficult to obtain accurate chirp measurements under these conditions.

2.4 Chapter Summary

A chirp measurement system has been designed, built, and demonstrated to fully characterize the outgoing optical signal from a CATV transmitter. This system is portable, as well polarization insensitive to allow characterization of lasers and phase modulators that do not have polarization maintaining fiber at their output. A high-current photodetector provides a high SNR that enables measurement of chirp as low as 50MHz without the need for filters or complex noise reduction algorithms. To the best of the author's knowledge, the chirp measurement system described in this chapter represents the state of the art available at any laboratory in the world at present.

Chapter 3

Measuring SBS Suppression in Optical Fiber

3.1 Introduction to Chapter

In this Chapter, we show that with the appropriate analysis of the optical spectrum it is possible to accurately measure SBS suppression in optical fiber over a much wider measurement range compared to conventional techniques. Section 3.2 examines conventional suppression theory, introduced by Willems in 1994 [13]. This approach is shown to break down for the high levels of suppression that are common to analog CATV systems. A new method of spectral analysis is presented in Section 3.3. The details of this approach are described and the results are validated for two directly dithered 1550nm DFB lasers.

3.1.1 Conventional Theory

Conventional SBS suppression theory determines the level of suppression in optical fiber based on a single-peak analysis of the optical spectrum. To illustrate the details of this approach, consider a 1550nm DFB laser operated both at constant power (CW) and externally phase dithered at some arbitrary phase modulation index m. The optical spectrum in each case was given in Figure 1-14. When the laser is at a constant power, the spectrum consists of one peak. When the laser is dithered, the spectrum broadens and distributes the optical power over a

number of subcarriers separated by the dithering frequency. Conventional theory estimates the SBS suppression from the difference between the original CW power of the laser and the peak power of the broadened spectrum. To analyze this approach for a specific case, consider an externally phase modulated signal over a range of modulation indices. Assuming a normalized electric field, the power in each k^{th} order sideband is given by $J_k^2(m)$ where J_k is the kth order Bessel function. Using conventional theory, the SBS suppression can be written as [13]

$$SBS_{\text{supp}} = 10\log_{10}\left[\max_k\left(J_k^2(m)\right)\right] \tag{3.1}$$

To illustrate this, Figure 3-1 shows the spectral evolution of an optical signal for a number of harmonics as a function of the phase modulation index m; the plot has been inverted to give the trend in SBS suppression. The solid dark line strictly follows the maximum peak spectral power, illustrating the expected suppression based on conventional theory.

To examine the accuracy of this approach, we compare suppression results using conventional theory with experimental backscattering data for a directly dithered 1550nm DFB laser. Backscattering measurements are made using two inexpensive optical splitters and photodiodes that monitor the average optical power injected into and reflected from the optical fiber link. This is an appendage to the existing chirp measurement system, as shown in Figure 3-2, where an optical switch directs the transmitter output to the backscattering setup rather than the chirp measurement system. Figure 1-15, from Chapter 1, compares backscattering results with those obtained using conventional theory for a 1550nm DFB laser. Conventional theory underestimates the level of suppression beyond the first local maximum of the suppression curve. This maximum is the transition point from low-level dithering, where the spectrum is dominated by a single frequency component, to high-level dithering where two or more components share a similar power. Although the discrepancy between measurement and conventional theory might be attributed to experimental error, a very detailed examination of this data showed that not be the case. Rather, because conventional theory is based on a single-peak analysis of the broadened spectrum, it underestimates the expected suppression beyond the transition point. To improve the accuracy of this approach, a new technique for spectral analysis has been developed.

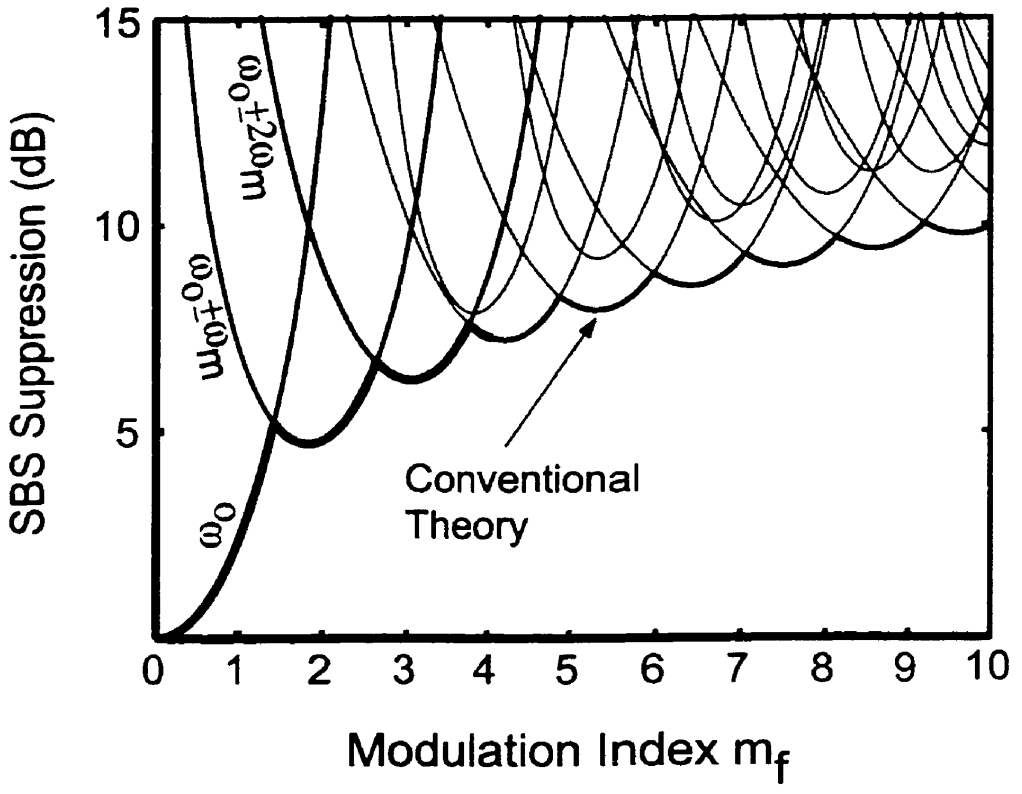

Figure 3-1: Spectral evolution of a phase modulated lightwave and the corresponding suppression based on conventional theory.

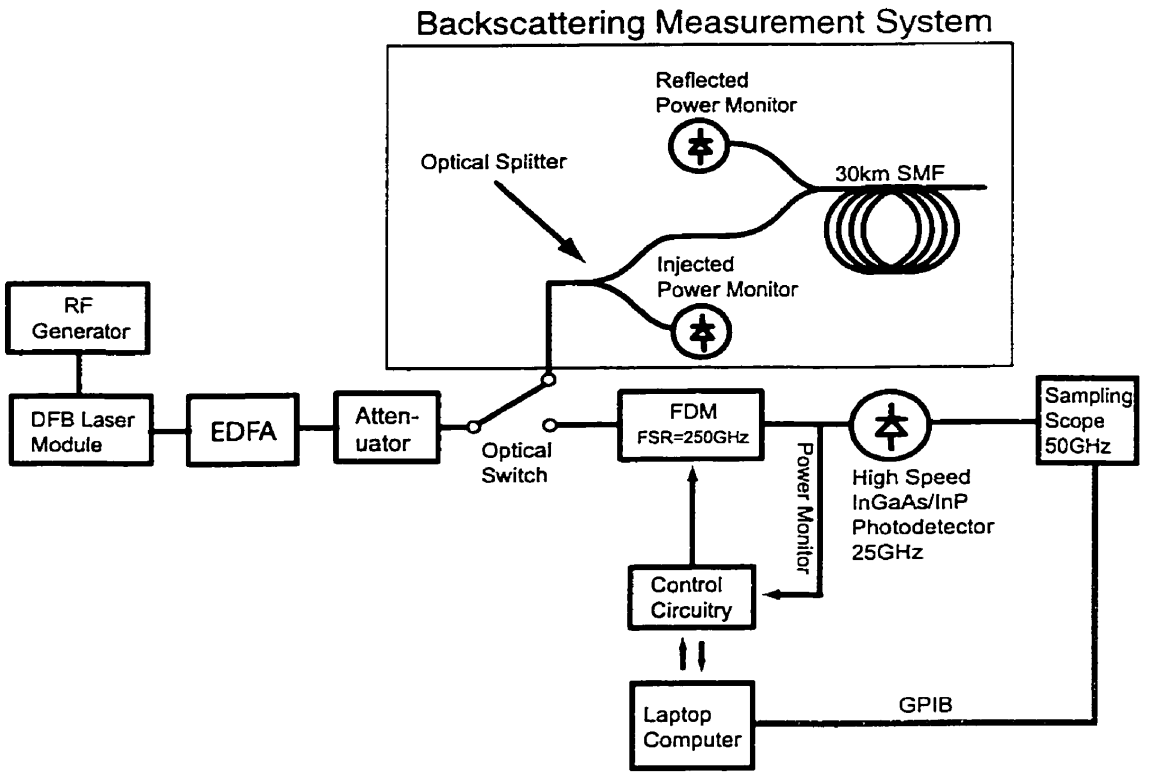

Figure 3-2: Chirp measurement system with the addition of the backscattering setup. Two inexpensive optical splitters and photodiodes are used to monitor the optical power injected into and reflected from the optical fiber link.

3.1.2 Enhanced Spectral Analysis Technique

The limitation of conventional theory is due to the single-peak analysis of the spectrum. To accurately determine the level SBS suppression in optical fiber, the backscattering contribution from each spectral component must be accounted for. Here we make the hypothesis that each spectral component can be related as an independent constant power continuous-wave (CW) laser source. Each of these hypothetical sources contributes a certain amount of backscattering due to SBS. The process of extracting the SBS suppression level involves several steps. First, consider the optical source at CW; the optical power spectrum can be written as

$$S(\omega) = P_L \delta(\omega - \omega_0) \tag{3.2}$$

where ω_0 is the optical carrier frequency, δ is a delta function, and P_L is the launched power. The broadened spectrum can be written as

$$S(\omega) = \sum_{n=-\infty}^{\infty} a_n \delta(\omega - \omega_0 - n\omega_d) \tag{3.3}$$

where a_n is the power in the n^{th} spectral component, or hypothetical laser source, and ω_d is the dithering frequency. Each of these optical sources contributes a certain amount of backscattering due to SBS. The total reflected power, P_{tot}, is the sum of these contributions and can be written as

$$P_{tot} = \sum_{n=-\infty}^{\infty} f_{CW}(a_n) \tag{3.4}$$

where f_{CW} is the backscattering function. The backscattering function defines the relationship between injected and SBS backscattered power for the laser operating at constant power. To reduce the effects of noise in this data, an analytical function is used to approximate the SBS backscattering curve, defined by the Rayleigh baseline, slope, and intercept; this is shown in Figure 3-3. The saturation of the backscattering curve at high injection powers is neglected and does not affect the results, as the function is fitted only to data around or below the threshold. The corresponding launch power is given by

$$P_L = \sum_{n=-\infty}^{\infty} a_n \tag{3.5}$$

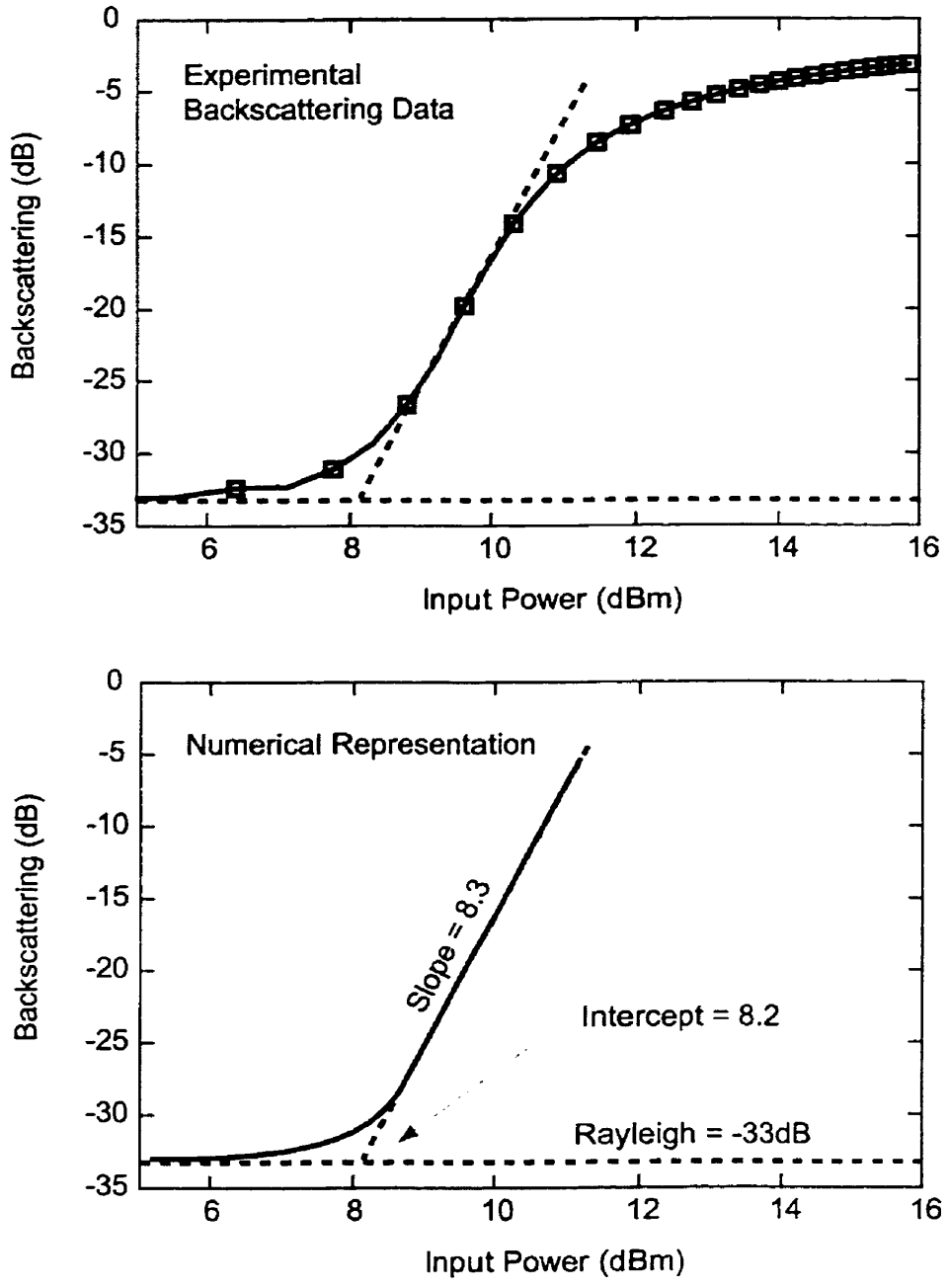

Figure 3-3: Experimental backscattering data and the analytical representation using the slope, intercept, and Rayleigh baseline.

Using P_{tot} and P_L one can calculate the backscattering in the fiber

$$\text{Backscattering [dB]} = 10\log_{10}\left(\frac{P_{tot}}{P_L}\right) \tag{3.6}$$

Substituting this backscattering level into the inverse representation of the backscattering function, one can determine the corresponding injection power required to get that amount of backscattering. The difference between this power level and the initial launch power is the SBS suppression for that particular dithering level.

In Figure 3-4, SBS suppression results using this approach are compared with backscattering measurements for two directly dithered 1550nm DFB lasers obtained from different manufacturers. The modulation frequency in both cases is 1GHz and the optical fiber link is 30km of SMF. The amount of laser dithering is quantified by the modulation depth. There is excellent agreement between the new spectral analysis results and those obtained using experimental SBS backscattering data. This validates the approach and shows a proper understanding of the relationship between SBS suppression and transmitter characteristics for CATV systems. Laser #1 demonstrates a higher level of suppression versus modulation depth compared to laser #2, suggesting that the characteristics of the laser can influence the effectiveness of single-tone suppression. This is one of the topics examined in Chapter 4.

3.2 Chapter Summary

Using the chirp measurement system, the relationship between SBS suppression and the optical power spectrum of the transmitter is investigated, showing that conventional single-peak theory breaks down for the high levels of suppression commonly used in CATV systems. A more suitable approach based on transmitter power and chirp measurement and enhanced spectral analysis is demonstrated for two 1550nm distributed feedback (DFB) lasers. This technique provides a significantly wider measurement range compared to existing techniques, enabling the development of SBS suppression schemes without requiring high power amplification. In Chapter 4, this measurement system is used to develop and characterize new SBS suppression schemes using two-tone dithering.

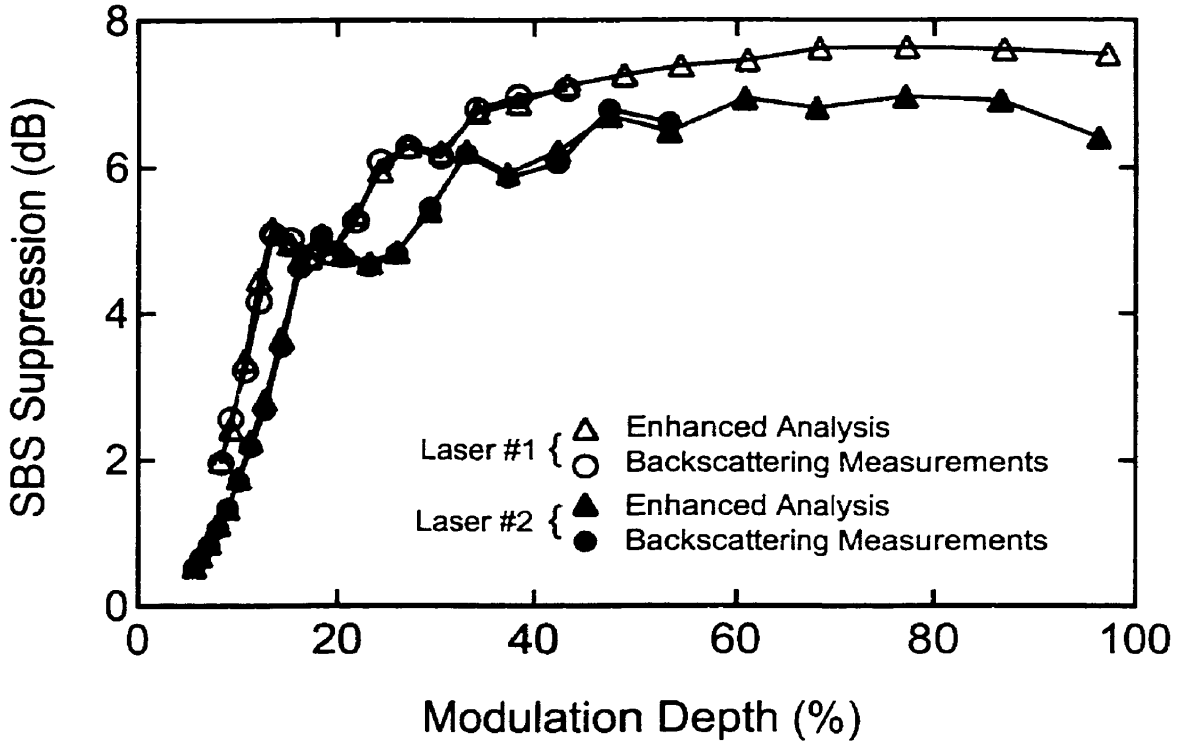

Figure 3-4: SBS suppression results for two directly dithered 1550nm DFB lasers comparing backscattering results with the enhanced spectral analysis technique. The dithering frequency is 1GHz and the fiber is 30km of SMF.

Chapter 4

Two-Tone Suppression

In this chapter, two-tone dithering techniques are investigated as a means of improving SBS suppression in optical fiber. In Section 4.1, the limitations of single-tone suppression are examined as it applies to direct laser and external phase dithering. Section 4.2 examines two-tone suppression using different combinations of these devices. It is shown that two-tone dithering is substantially better than single-tone dithering at suppressing SBS. Two-tone external phase dithering is shown to be the most effective means that is presently feasible, capable of generating a threshold of 21.4dBm. In Section 4.3, this new suppression scheme is applied to an 80-channel CATV system and its performance is characterized at high injection powers.

4.1 Single-Tone Suppression

In this section, amplitude modulation (AM) and phase modulation (PM) theory is discussed. While these terms are taken from communications, in the present case AM actually refers to modulation of the optical power, or intensity, and might better be called intensity modulation. However, as many readers will have intuition for AM, we continue to use that term.

4.1.1 The General Case: AM & PM

The general expression for the electric field of an optical signal undergoing both sinusoidal power dithering and phase dithering is given by

$$E(t) = E_0 [1 + a \sin(\omega_d t)]^{1/2} e^{i(\omega_0 t + m \sin(\omega_d t) + \theta_0)} + c.c \tag{4.1}$$

where ω_d is the dithering frequency, ω_0 is the carrier frequency, a and m are the amplitudes of the AM and PM components, θ_0 is the phase difference between the amplitude and phase dithered signals, and c.c. is the complex conjugate. The square root of the amplitude function accounts for the fact that we are in the electric field domain instead of the power domain. In general, the complex optical spectrum can be written as

$$E(\omega) = \sum_{k=-\infty}^{\infty} c_k \delta(\omega - \omega_0 - n\omega_d) \tag{4.2}$$

where c_k is a complicated function of a, m, θ_0, and ω_0. There are two simplified cases that can be considered; pure PM dithering ($a = 0$) and pure AM dithering ($m = 0$).

For pure AM dithering, Equation 4.1 can be written as

$$E(t) = E_0 [1 + a \sin(\omega_d t)]^{1/2} e^{i(\omega_0 t + \theta_0)} + c.c \tag{4.3}$$

The resulting optical spectrum broadens symmetrically introducing sideband frequencies on either side of the carrier. These sidebands have frequencies of $\pm n\omega_d$, relative to the carrier, where n denotes the order. Each pair of frequencies of order n have the same amplitude and phase. The amount of spectral broadening is determined by the modulation index a.

For pure PM dithering, Equation 4.1 can be written as

$$E(t) = E_0 e^{i(\omega_0 t + m \sin(\omega_d t) + \theta_0)} + c.c \tag{4.4}$$

and broadens into harmonics of frequency $\pm n\omega_d$, relative to the carrier. In this case, each pair of frequencies of order n have the same amplitude but the odd order sidebands are 180° out of phase with one another. Hence, PM broadening is asymmetric. The amount of spectral

broadening is determined by the phase modulation index m.

For the work done in this thesis, it is common to have both AM and PM components present in the optical signal. While the analytical details are beyond the scope of this thesis, combined AM and PM dithering results in asymmetric broadening of the optical *power* spectrum. This comes from combining symmetric (AM) and asymmetric (PM) spectra together. Figure2-9, from Chapter 2, illustrates this for a directly modulated laser. To avoid the complexity of an analytical solution, this thesis work determines the optical spectrum numerically using the details outlined in Appendix B. In the following Section, we discuss the effects of AM and PM modulation as it applies to directly modulated lasers and external phase modulators.

4.1.2 External Phase Dithering

The phase of a DFB laser output can be modulated by placing an external phase modulator at the output of the laser source. Most commercial phase modulators use $LiNbO_3$ technology with electrodes across the waveguide channel to create a strong electric field that varies the refractive index of the medium via the electro-optic effect. For sinusoidal dithering, the maximum phase modulation index depends on the V_π of the device and the allowable RF input power. The V_π is the voltage required to produce an electro-optic phase shift of 180°, and is a common figure of merit for these devices. The lower the V_π of the device, the more phase shift that can be obtained given a certain RF input power. From examination of a number of commercially available devices capable of phase modulation in the GHz range, it was found that the phase modulation index is limited to 5 radians. This corresponds to an SBS suppression level of 10dB for single-tone suppression.

4.1.3 Direct Laser Dithering

As mentioned earlier, modulation of the injection current of a DFB laser causes corresponding modulation of the optical emission frequency, known as chirp. For sinusoidal dithering, the instantaneous frequency of the optical signal can be written as

$$\omega_i(t) = \omega_0 + \Delta\omega_{\max} \sin(\omega_d t) \tag{4.5}$$

where $\Delta\omega_{max}$ is the peak amplitude of the chirp and ω_d is the dithering frequency. To get this equation in terms of phase we use the relation

$$\theta(t) = \int_{-\infty}^{t} \omega(t')\, dt' \tag{4.6}$$

to obtain

$$\theta(t) = \omega_0 t - \frac{\Delta\omega_{max}}{\omega_d} \cos(\omega_d t) + \phi \tag{4.7}$$

Equation 4.7 illustrates that sinusoidal dithering results in sinusoidal phase modulation of the optical signal. Hence, if the degree of amplitude modulation is small, the output is similar to that of a phase modulator. The phase modulation index, however, is inversely proportional to the dithering frequency indicating that SBS suppression will improve at lower dithering frequencies. To illustrate this, suppression measurements were made for a 1550nm DFB laser at a number of dithering frequencies between 250MHz and 2300MHz. The results of this investigation are given in Figure 4-1, and show the improved suppression capabilities of the laser at low dithering frequencies. Unfortunately, CATV systems require the dithering frequency to be at least twice the highest CATV frequency to ensure no distortion of the information signal, as discussed earlier. For an 80-channel system, the dithering frequency must be at least 1.1GHz. From Figure 4-1, 7dB of suppression is realistic at this frequency. These results will change depending on the FM response of the laser. This particular laser has an FM response of 88MHz / % modulation depth, that is, for every percentage in modulation depth the laser will produce 88MHz of chirp. From experimental measurements of different lasers from different manufacturers, the FM response of a 1550nm DFB laser is found to range between approximately 60 and 120MHz / %. This corresponds to a suppression limit of approximately 8dB at a laser modulation depth of 90%. The laser can be modulated beyond 90%, but the large-signal modulation response of this device makes the suppression performance unpredictable.

An important difference between direct and external phase dithering is that direct laser dithering generates significant amplitude modulation (AM), while an ideal phase modulator does not affect the signal intensity. AM can degrade the symmetry of the PM broadening process, resulting in lower levels of suppression. To illustrate this, SBS suppression is measured

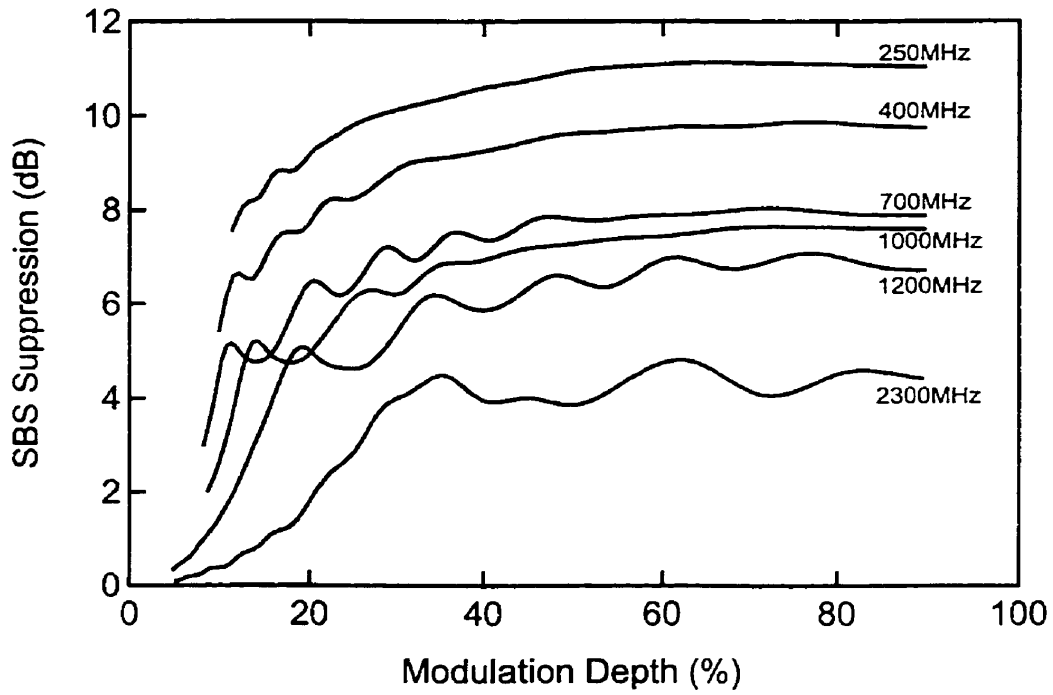

Figure 4-1: SBS suppression versus dithering frequency for a 1550nm DFB laser.

over a range of modulation depths for a directly dithered 1550nm DFB laser using the chirp measurement system. In one case, estimation of suppression was performed as normal, and in the other case AM is neglected in the suppression calculation. The results are given in Figure 4-2, showing how SBS suppression is significantly higher for a purely phase modulated optical output. At a modulation depth of 90%, there is a 3dB difference between the two results. So while SBS suppression obtained with directly modulated lasers is due mainly to their chirping, amplitude modulation plays a secondary role. Hence, a laser is not as effective at suppressing SBS as pure phase modulation of a CW source.

In both the directly dithered and externally dithered suppression schemes, SBS suppression was shown to be limited to less than 10dB. To exceed this level one needs to find ways of more effectively broadening the optical spectrum.

4.2 Two-Tone Suppression

In this section, two-tone SBS suppression is examined which is the next logical step in complexity beyond the single-tone scheme described above; it is also the most practical to implement because of the low bandwidth requirements. As discussed in Chapter 1, for a single-tone suppression scheme $f_D > 2f_U$ to avoid distorting the CATV signal. For a two-tone suppression scheme, each tone must satisfy this rule. In addition, the corresponding beat frequencies between the two dithering tones must also be greater than $2f_U$. The beat frequencies generated by two-tone dithering are

$$N * f_1 \pm M * f_2 \tag{4.8}$$

where f_1 and f_2 are the dithering frequencies and N and M are integer values. In the presence of fiber dispersion in a long distance transmission system, phase modulation is converted to amplitude modulation and these beat frequencies are detected by the optical receiver. With an appropriate choice of f_1 and f_2, however, no distortion products are generated in the CATV signal band. This occurs for dithering frequencies that satisfy the two relations

$$N * f_1 = M * f_2 \tag{4.9}$$

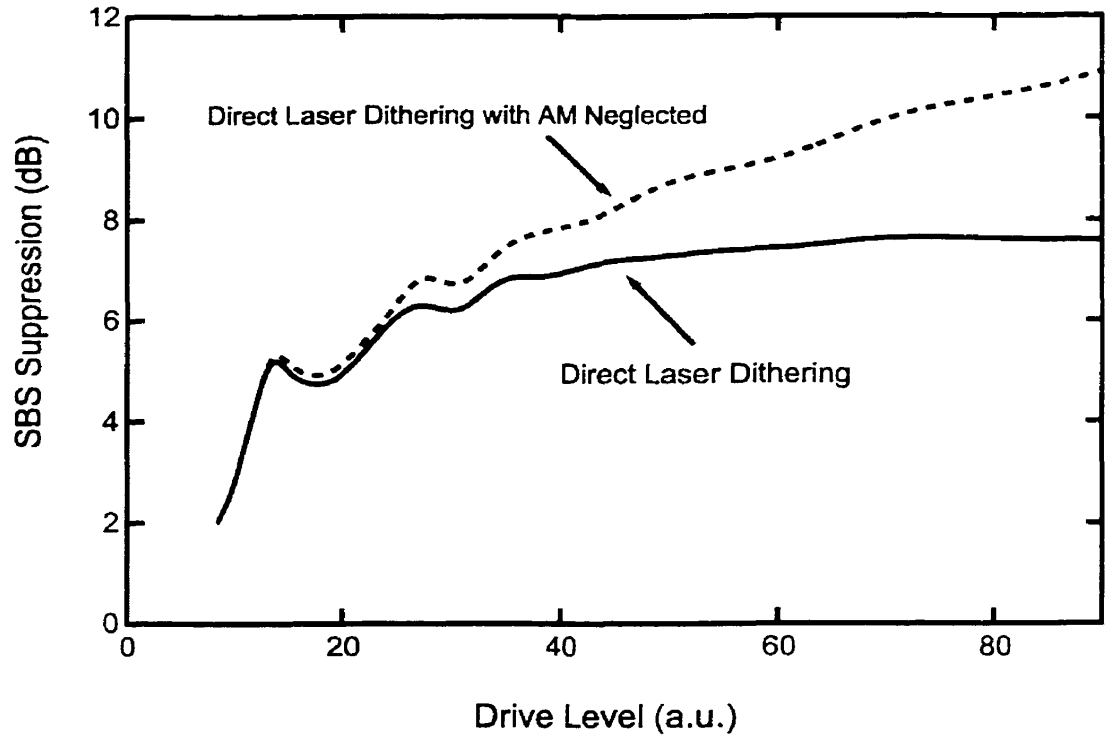

Figure 4-2: SBS suppression for a directly dithered 1550nm DFB laser with and without AM included. The solid line is the experimental results using the chirp measurement system. The dashed line is suppression results with the AM component of the optical lightwave neglected before the suppression calculation.

Ratio	Dithering Tone 1	Dithering Tone 2
3:2	1550nm DFB laser @ 3.9GHz	1550nm DFB laser @ 2.6GHz
2:1	1550nm DFB laser @ 2.6GHz	1550nm DFB laser @ 1.3GHz
3:1	1550nm DFB laser @ 3.9GHz	1550nm DFB laser @ 1.3GHz
3:2	1550nm DFB laser @ 3.9GHz	External Phase Modulator @ 2.6GHz
3:2	1550nm DFB laser @ 2.6GHz	External Phase Modulator @ 3.9GHz
2:1	1550nm DFB laser @ 2.6GHz	External Phase Modulator @ 1.3GHz
2:1	1550nm DFB laser @ 1.3GHz	External Phase Modulator @ 2.6GHz
3:1	1550nm DFB laser @ 3.9GHz	External Phase Modulator @ 1.3GHz
3:1	1550nm DFB laser @ 1.3GHz	External Phase Modulator @ 3.9GHz
3:2	External Phase Modulator @ 3.9GHz	External Phase Modulator @ 2.6GHz
2:1	External Phase Modulator @ 2.6GHz	External Phase Modulator @ 1.3GHz
3:1	External Phase Modulator @ 3.9GHz	External Phase Modulator @ 1.3GHz

Table 4.1: The twelve possible combinations of two-tone suppression and the corresponding dithering frequencies.

$$|Nf_1 \pm Mf_2| > 2f_U \tag{4.10}$$

where f_U is the upper CATV frequency.

A numerical model was written in Matlab to examine the capabilities of two-tone suppression. The model uses the enhanced spectral analysis technique, described in Chapter 3, to determine the level of SBS suppression in each case. The fundamental dithering frequency is 1.3GHz, which is just higher than twice the upper CATV frequency for an 80-channel system. All other dithering frequencies are an integer multiple of this base frequency, accommodating the distortion requirements outlined earlier. The approprtiate choice of frequencies ensures that the separation of optical subcarriers is much greater than the SBS linewidth $\Delta\nu_B$: this approach won't work for situations where the beat frequencies are separated by less than $\Delta\nu_B$. Table 4.1 lists all the possible combinations of direct laser dithering and external phase dithering for this system. For combined laser and external phase dithering there are two combinations for each ratio, because of the frequency dependence of the phase modulation index when using the laser. In other words, the suppression capability of the laser depends on the dithering frequency chosen. For two-tone laser dithering and two-tone phase dithering only one combination exists. In total, twelve dithering combinations are possible using a two-tone suppression scheme. The model assumes a laser with an FM response of 83 MHz / %, based on an average of several lasers characterized from different manufacturers. The laser model also assumes

that the power and chirp are in phase. This is true for dithering frequencies well below the relaxation oscillation frequency Ω_R of the laser. To ensure this requirement is satisfied, the laser is operated at a high bias current which increases Ω_R to a value well beyond the 3dB bandwidth [28].

This model is used to calculate SBS suppression as a function of the two dithering amplitudes from zero to a maximum value related to practically attainable limits as discussed below. The amount of laser dithering is quantified by the modulation depth, which ranges from 0 to 90%. Predictions of SBS suppression for direct laser dithering greater than 90% modulation depth are not considered reliable and are therefore excluded. The amount of phase dithering is quantified by the phase modulation index and ranges from 0 to 12 radians. As mentioned earlier, commercially available phase modulators are presently only capable of a phase modulation index of 5 radians. This range is extended in the numerical model to see if there is a significant improvement in SBS suppression at higher dithering levels. This will enable us to determine if there is an advantage in trying to design a new phase modulator with a larger maximum phase modulation index. A similar analysis for DFB lasers will be examined later in this Section.

For a complete examination of two-tone suppression, one must also look at how the phase difference between the two RF dithering tones affects the SBS suppression results. For example, Figure 4-3 shows the variation of suppression with phase difference for a 3:2 ratio scheme using just pure phase modulation. The dithering frequencies are 3.9GHz and 2.6GHz, and the phase modulation indices are 1.4 and 5. A maximum SBS suppression of 13.5dB is achieved when the two RF tones are in phase; phase difference is with respect to the 2.6GHz tone. In some cases, optimal suppression does not always occur when the two RF dithering tones are in phase. Consider two-tone phase modulation at a frequency ratio of 3:2, but with each tone at a phase modulation index of 4. The change in suppression as a function of RF phase difference is given in Figure 4-4, showing that maximum suppression occurs when the RF phase difference is approximately 10 degrees. To ensure that our numerical model calculates the maximum suppression, the RF phase difference is swept over a full period and the maximum suppression level is recorded. For this particular example, the maximum suppression is approximately 11.2dB.

Appendix A presents the full suppression results for all of the schemes listed in Table 4.1.

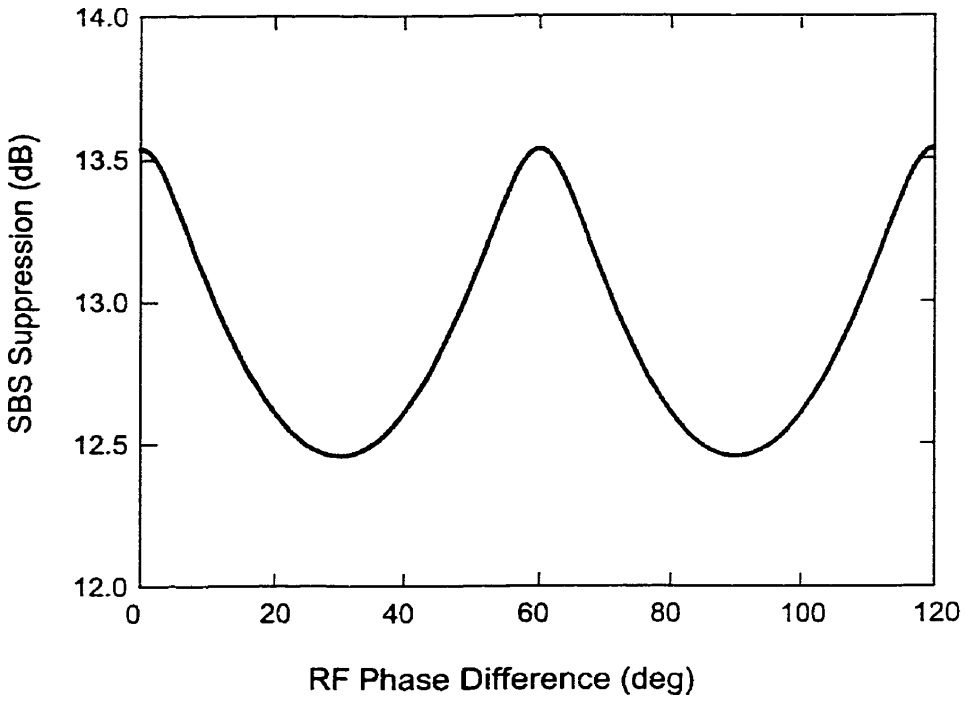

Figure 4-3: SBS suppression as a function of phase difference between the two RF dithering tones. This was generated using the numerical model and 13.5dB suppression scheme.

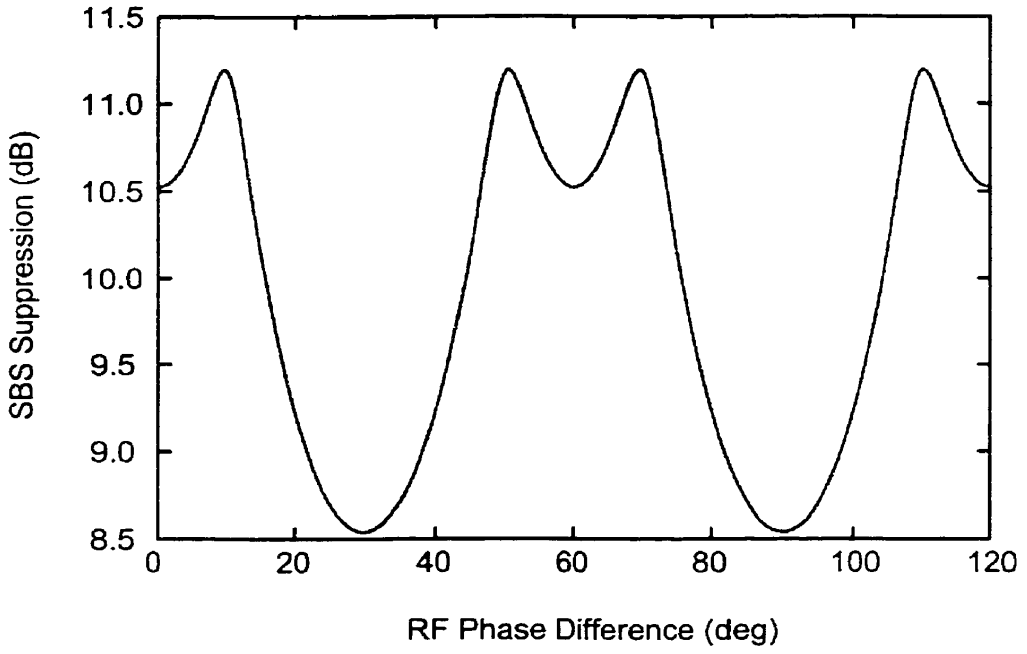

Figure 4-4: SBS suppression as a function of phase difference between the two RF dithering tones. The frequency ratio is 3:2 and the phase modulation index is 4 for each tone.

Ratio	Dithering Tone 1	Dithering Tone 2	SBS Suppression[dB]
3:2	Laser (3.9GHz)	Laser (2.6GHz)	9.1
2:1	Laser (2.6GHz)	Laser (1.3GHz)	10.1
3:1	Laser (3.9GHz)	Laser (1.3GHz)	10.0

	Laser @ 90% mod.		PM (m=0 to 5)	PM (m=0 to 12)
3:2	Laser (3.9GHz)	PM (2.6GHz)	12.4	15.3
3:2	Laser (2.6GHz)	PM (3.9GHz)	13.1	15.2
2:1	Laser (2.6GHz)	PM (1.3GHz)	10.1	12.2
2:1	Laser (1.3GHz)	PM (2.6GHz)	12.6	14.8
3:1	Laser (3.9GHz)	PM (1.3GHz)	10.2	12.5
3:1	Laser (1.3GHz)	PM (3.9GHz)	13.4	16.0
3:2	PM (3.9GHz)	PM (2.6GHz)	13.5	17.0
2:1	PM (2.6GHz)	PM (1.3GHz)	12.3	15.2
3:1	PM (3.9GHz)	PM (1.3GHz)	13.5	16.8

Table 4.2: Maximum SBS suppression for twelve possible combinations of two-tone suppression using a range of phase modulation indices.

The maximum SBS suppression for each of the twelve suppression schemes is given in Table 4.2. There are two columns of suppression results. The first column is the maximum obtainable suppression for a phase modulator who ranges from 0 to 5 radians. The second column gives the maximum obtainable suppression for the widened range, in this case from 0 to 12 radians. The data shows that the best SBS suppression scheme is for two-tone phase modulation at a frequency ratio of 3:2, as this provides the high level of suppression for the lowest bandwidth. For m between 0 and 5, SBS suppression of 13.5dB is possible. For m between 0 and 12, SBS suppression of 17.0dB is possible, indicating that a device with a higher maximum phase modulation index would be advantageous, as expected. Figure 4-5 shows the full results of this suppression technique.

The two-dimensional mesh exhibits a number of ridges across the dithering plane, illustrating the complexity of the two-tone system. SBS suppression generally increases when the dithering tones extend to higher values but within this trend are peaks and troughs that significantly improve or degrade the level of suppression. Ideally, one wants to find a point of maximum suppression that is easy to find and relatively insensitive to errors or drift in the settings of the two phase modulators. This puts less demand on the internal transmitter circuitry necessary for finding and maintaining this suppression point.

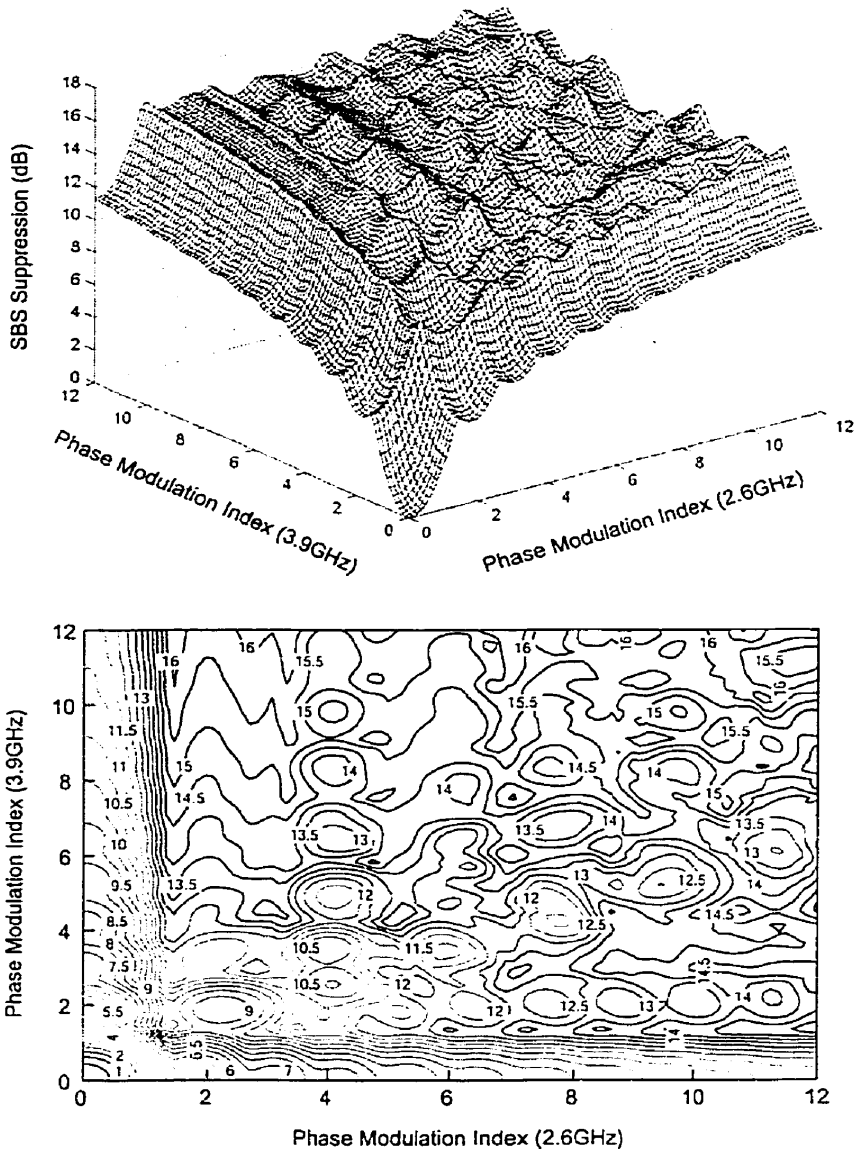

Figure 4-5: Theoretical SBS suppression results for two-tone phase modulation at frequencies fo 3.9GHz and 2.6GHz. The upper Figure is a three-dimensional mesh of the suppression results across the dithering plane, the lower Figure is the corresponding contour plot. A maximum SBS suppression of 13.5dB is demonstrated when the phase modulation index is limited to 5 radians.

As mentioned earlier, the maximum SBS suppression for the 3:2 ratio scheme is 13.5 dB. This is achieved when the 2.6GHz tone is set to a phase modulation index of 1.4 and the 3.9GHz tone is set to the maximum phase modulation index of 5. Experimentally, this operating point is easy to find. With the 3.9GHz tone initially turned off, increase the phase modulation index of the 2.6GHz tone until you reach the first peak of the single-tone suppression curve. Then turn on the 3.9GHz tone and increase m to its maximum value of 5. This line of travel will go along the first ridge that runs parallel to the 3.9GHz axis. If one were to follow this line of travel by increasing the index of the 3.9GHz tone to 12, an SBS suppression level of 16.5dB would be obtained.

To validate this suppression technique, an experimental dual-tone suppression system was constructed, as shown in Figure 4-6. The output of a 1550nm DFB laser is launched into a series of two external phase modulators. The model PM150 is a JDS Uniphase 10GHz modulator that can generate a modulation index of 5. The model CA150 is a combined phase and intensity modulator, also produced by JDS Uniphase. The intensity modulator portion of the CA150 is a non-linearized Mach-Zehnder and the phase modulation portion has a bandwidth of 2GHz and a maximum modulation index of 2. The output of the second modulator is sent to the chirp measurement system. While chirp measurement was described for the single-tone scheme presented in Chapter 3, there is a new challenge in multi-tone schemes in order to trigger the oscilloscope to yield a repetitive waveform. To trigger this dual-tone waveform, the output from each signal generator is split and input to a ZFM-4212 Mini Circuits RF mixer. The difference frequency is isolated using a band-pass filter and sent to the trigger input of the sampling oscilloscope. The measured power, chirp and optical spectrum are shown in Figure 4-7.

As is evident from Figure 4-7, the present SBS suppression scheme has resulted in the optical spectrum being equalized over a $\pm$20GHz bandwidth containing over thirty frequency components. This was accomplished using only two tones with a maximum dithering frequency of 3.9GHz. To achieve a similar level of suppression and spectral equalization using Korotky's approach, as discussed in Chapter 1, one would need three tones and a bandwidth greater than 10GHz. This new technique requires fewer dithering tones and is more bandwidth efficient.

A more detailed examination of the power waveform in Figure 4-7 shows that there is approx-

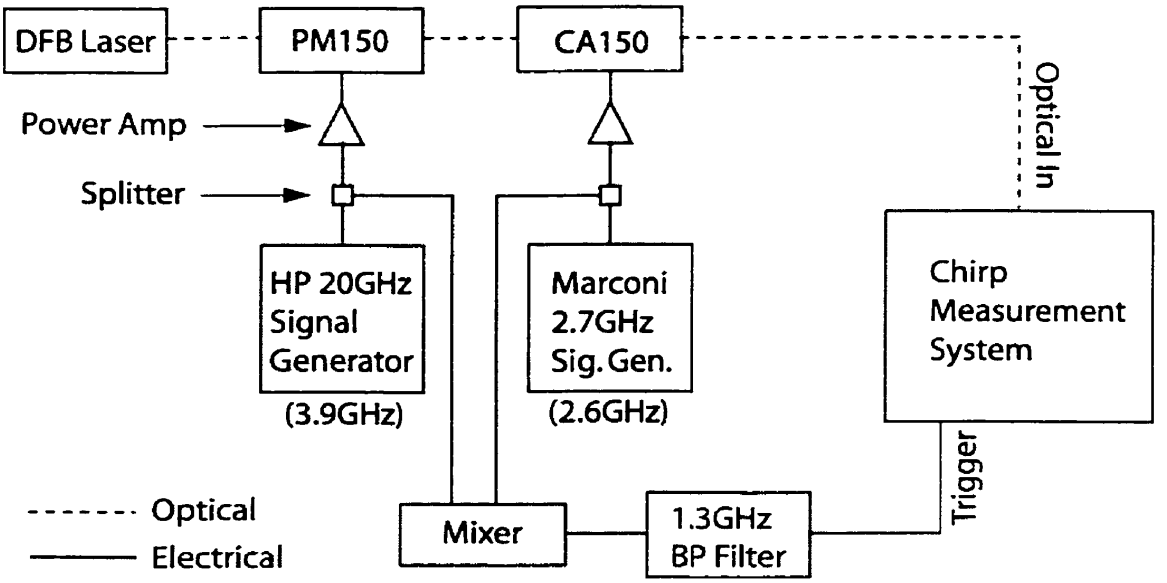

Figure 4-6: Experimental layout of the dual-tone SBS suppression system. Two signal generators are used to impose phase dithering on the optical lightwave.

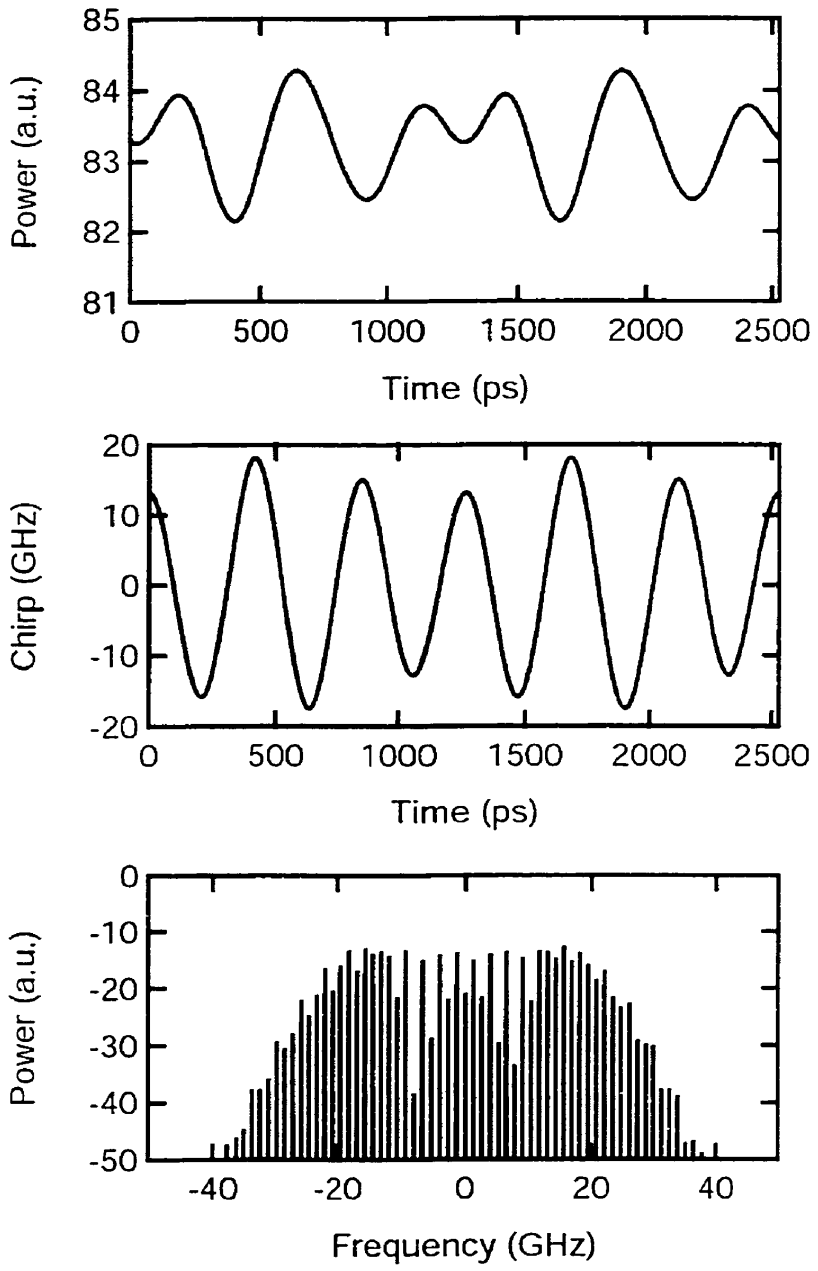

Figure 4-7: Power, chirp, and optical spectrum for a 1550nm DFB laser with two-tone dithering applied using phase modulators at a frequency ratio of 3:2.

imately 1% residual amplitude modulation (RAM) generated by this external phase dithering scheme. RAM not only generates components at the dithering frequencies but at higher-order frequencies as well. Experimental observations show that high-order components drift in amplitude and phase and adversely affect the results obtained using the chirp measurement system. Conversely, RAM is so small that is has little affect on the optical spectrum compared to phase modulation, and does not influence the SBS suppression results. Therefore, a numerical low-pass filter was included in the chirp measurement code to eliminate this problem: RAM without the filtering is shown in Figure 4-8.

The chirp measurement results were verified by taking corresponding backscattering data using a high-powered EDFA. This EDFA is a unit produced by JDS Uniphase and has a maximum output power of 24.5dBm. The backscattering results for the two-tone suppression scheme are shown in Figure 4-9. When the laser is operating at CW the SBS threshold is 8.1dBm. For two tone dithering at the settings described above there is a lateral shift in the backscattering curve of 13.4dB. This agrees with the numerical model and chirp measurement results to within an error of $\pm$0.1dB. The new SBS threshold for this particular laser is 21.4dBm.

Earlier, the SBS suppression was shown to vary with the phase difference between the two dithering frequencies. To confirm the experimental behaviour is consistent with the model, a phase shifter was inserted at the output port of the signal generator producing the 2.6GHz tone. The phase was varied and the SBS suppression measured using the chirp measurement system. The phase difference between the two RF tones was measured by processing the chirp waveform through two numerical band-pass filters centered at the two dithering frequencies to isolate the individual sinusoidal signals. From this, the phase difference between the two tones in the experiment is determined. The results of this investigation are shown in Figure 4-10. Experimental and theoretical results agree with slight discrepancies due to measurement error. These results confirm that SBS suppression is dependent on the phase difference between the two RF signals. In order to achieve maximum SBS suppression, one must not only properly set the modulation index of the two dithering tones but also make sure the phase difference between phase modulation achieved by the two RF signals is an integral multiple of 60 degrees.

None of the nine configurations that use laser dithering are capable of exceeding the 13.5dB

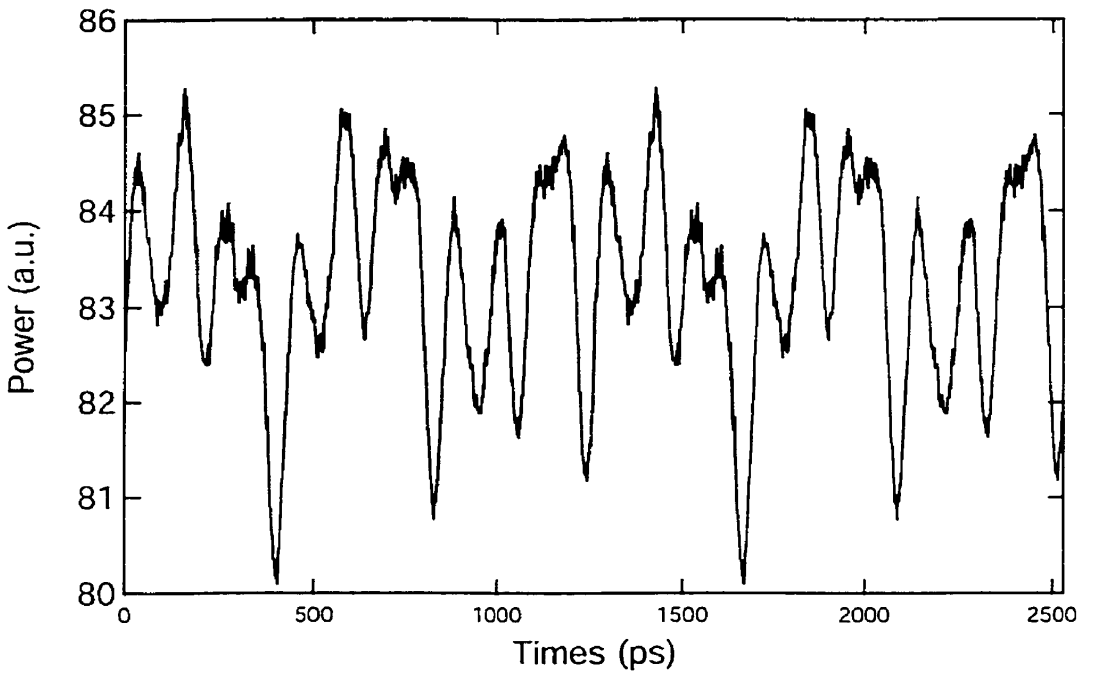

Figure 4-8: Residual amplitude modulation generated by external phase dithering.

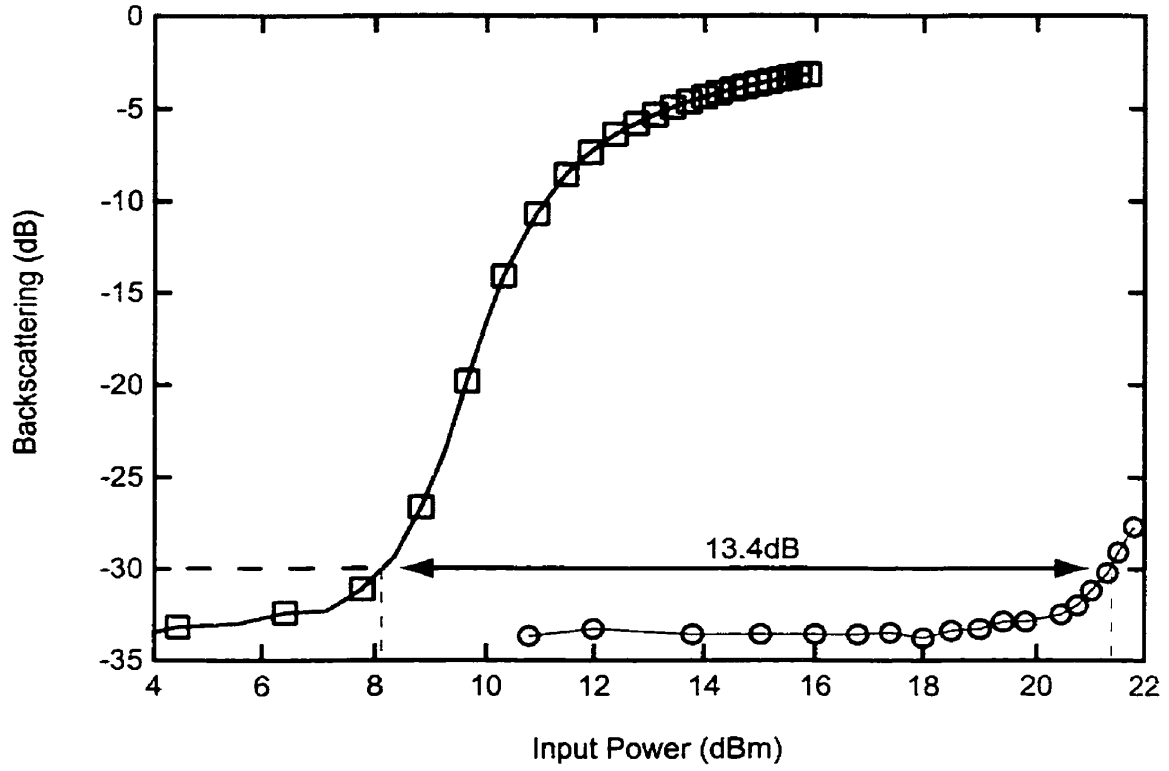

Figure 4-9: Experimental backscattering data for a 1550nm DFB laser using two-tone phase dithering at a frequency ratio of 3:2. An SBS suppression of 13.4dB is achieved.

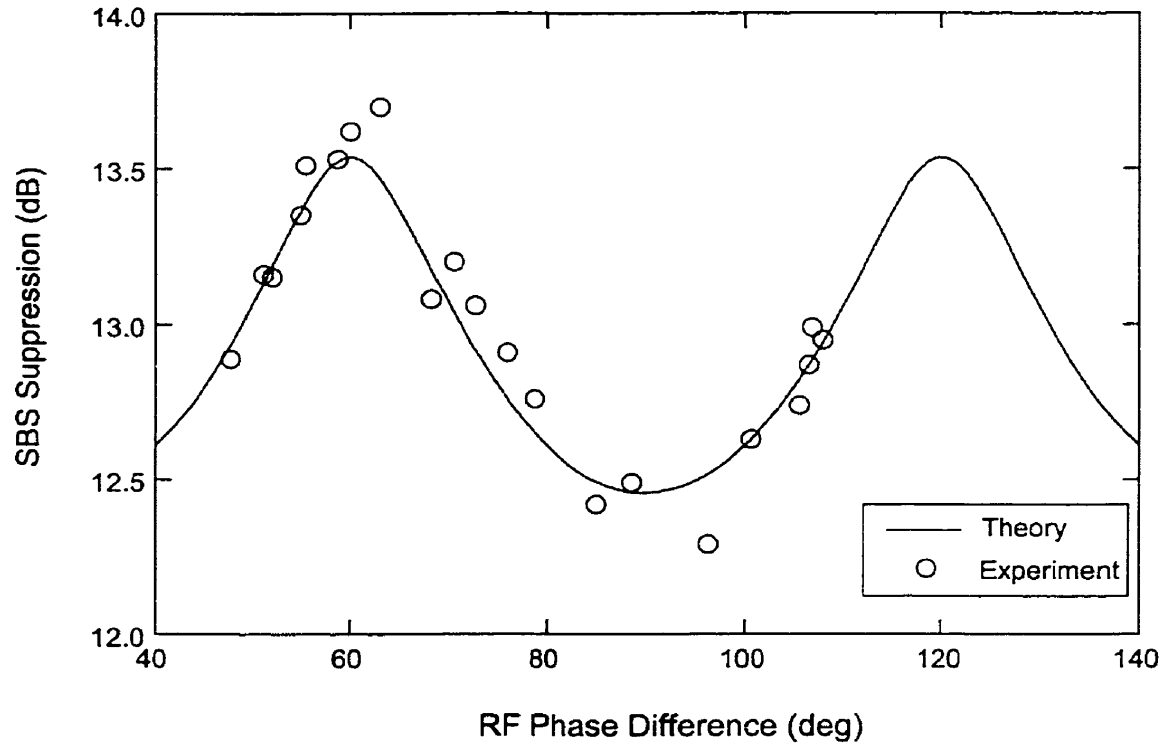

Figure 4-10: Theoretical and experimental results verifying the dependence of SBS suppression on the phase difference between the two dithering tones.

Ratio	Dithering Tone 1	Dithering Tone 2	SBS Suppression[dB]
3:2	Laser (3.9GHz)	Laser (2.6GHz)	14.2
2:1	Laser (2.6GHz)	Laser (1.3GHz)	14.9
3:1	Laser (3.9GHz)	Laser (1.3GHz)	14.5

	Laser @ 90% mod.		PM (m=0 to 5)	PM (m=0 to 12)
3:2	Laser (3.9GHz)	PM (2.6GHz)	14.1	15.5
3:2	Laser (2.6GHz)	PM (3.9GHz)	14.0	16.4
2:1	Laser (2.6GHz)	PM (1.3GHz)	12.6	14.4
2:1	Laser (1.3GHz)	PM (2.6GHz)	13.7	15.8
3:1	Laser (3.9GHz)	PM (1.3GHz)	12.7	14.0
3:1	Laser (1.3GHz)	PM (3.9GHz)	14.5	16.9

Table 4.3: Maximum SBS suppression, assuming enhanced FM laser response as described in the text, for combinations of two-tone suppression that involve direct laser dithering.

suppression level obtained with pure phase modulation. Of course, these results depend on the FM response of the laser. As mentioned earlier, the numerical model assumes an FM response of 83MHz / %, which is an average obtained by characterizing the response of a number of 1550nm DFB lasers from different manufacturers. To complete the investigation of two-tone suppression, we examine the effect that changing the FM response of the laser will have on the SBS suppression results. Specifically, the FM response of the laser is increased by a factor of four in the numerical model giving a new FM response of 332 MHz/%. The suppression results for this case are given in Table 4.3. The maximum suppression is 14.5dB using two-tone laser dithering at a frequency ratio of 2:1. This is greater than the level of suppression that was obtained using pure phase dithering. The important distinction is that an external phase modulator is not required, which significantly reduces the cost of the CATV transmitter. Therefore, if the DFB laser design was changed to increase the FM response, SBS suppression would improve considerably for the same dithering levels.

4.3 CSO Performance

Having established in the previous section that SBS may be suppressed to record levels of launched power, we now turn to a study of the performance of such systems in the transmission of CATV signals. Specifically, in this section the performance of an 80-channel CATV system is

examined using two-tone SBS suppression. The schematic of this system is shown in Figure 4-11. The output of a 1550nm DFB laser is sent to the first in a series of two modulation devices. The PM150 is a pure phase modulator and is dithered at 3.9GHz and a phase modulation index of 5, and the CA150 is a combination phase modulator and intensity modulator: these are the same devices used in previous measurements. The second dithering tone is applied to the phase modulator portion of this device with a dithering frequency of 2.6GHz and a phase modulation index of 1.4. This will generate an SBS threshold of 21.4 dBm, as discussed earlier. The CATV signal is applied using the intensity modulator portion of the CA150. This intensity modulator is a single-stage Mach-Zehnder that is operated at quadrature to ensure minimal composite second-order (CSO) distortion. The quadrature point was maintained by using the electrical output monitor on the EDFA to measure and minimize CSO at a specific channel: these adjustments were made by varying a DC bias voltage applied to the modulator. Since a linearized intensity modulator[29] is not being used, we accept that composite triple-beat (CTB) distortion will be high and focus attention on CSO performance. After the CA150, the optical signal is sent to a high-powered EDFA and then to a CATV characterization system owned and operated by Scientific-Atlanta Canada Inc.. Using this system, CSO is measured before and after the optical fiber link for a variety of launch powers.

To characterize the performance of the CATV system, the CSO distortion as a function of injection power was measured for fiber lengths of 32, 48, and 64km. The results of this experiment are shown in Figure 4-12. The dotted line corresponds to a level of -65dBc, which is a commercially accepted limit for CSO. At a propagation distance of 32km one can launch 21dBm of power into the fiber while still maintaining an acceptable level of distortion. At 48km, injection power is limited to 17dBm. At 64km, there is no injection power that is capable of maintaining an acceptable level of CSO distortion.

The reason for the degradation is the interaction of fiber dispersion with self-phase modulation in the fiber [30][31] [32]. SPM is caused by the fact that the index of refraction, n, is slightly modified as a function of the transmitted light intensity. Thus, as discussed in Chapter 1, at the peak swings of instantaneous light intensity, n varies from what it is at the unmodulated case. A varying phase component implies that the instantaneous optical frequency is also changing. This SPM-induced chirp will continuously generate new frequency components

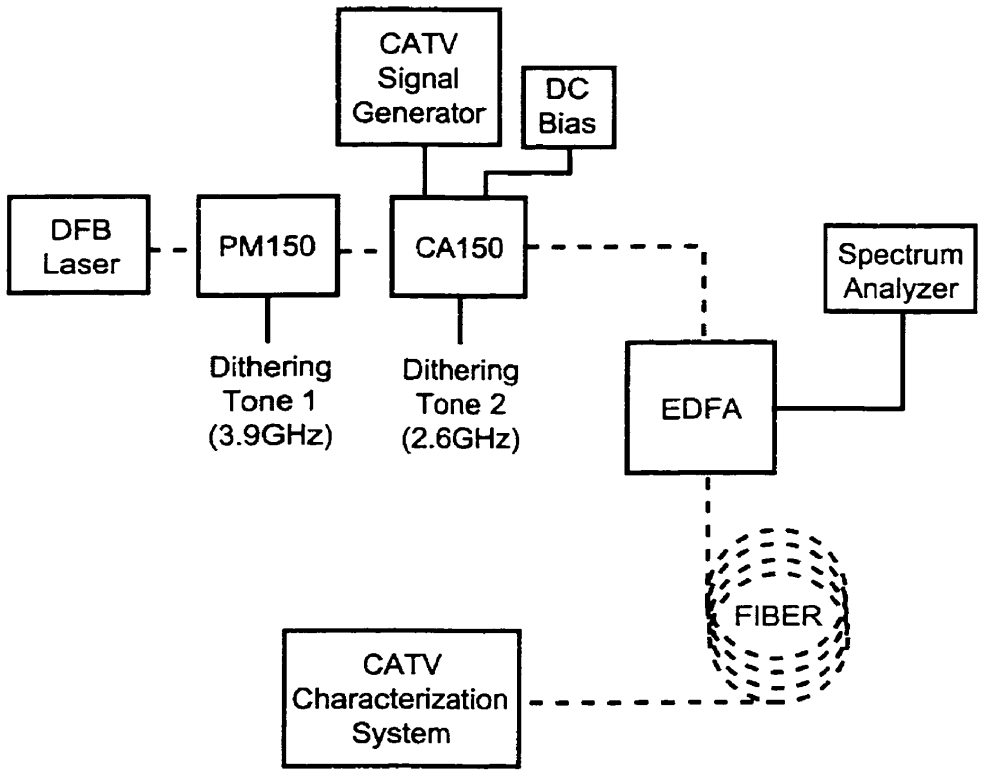

Figure 4-11: Experimental setup for measuring CSO in an 80-channel CATV system.

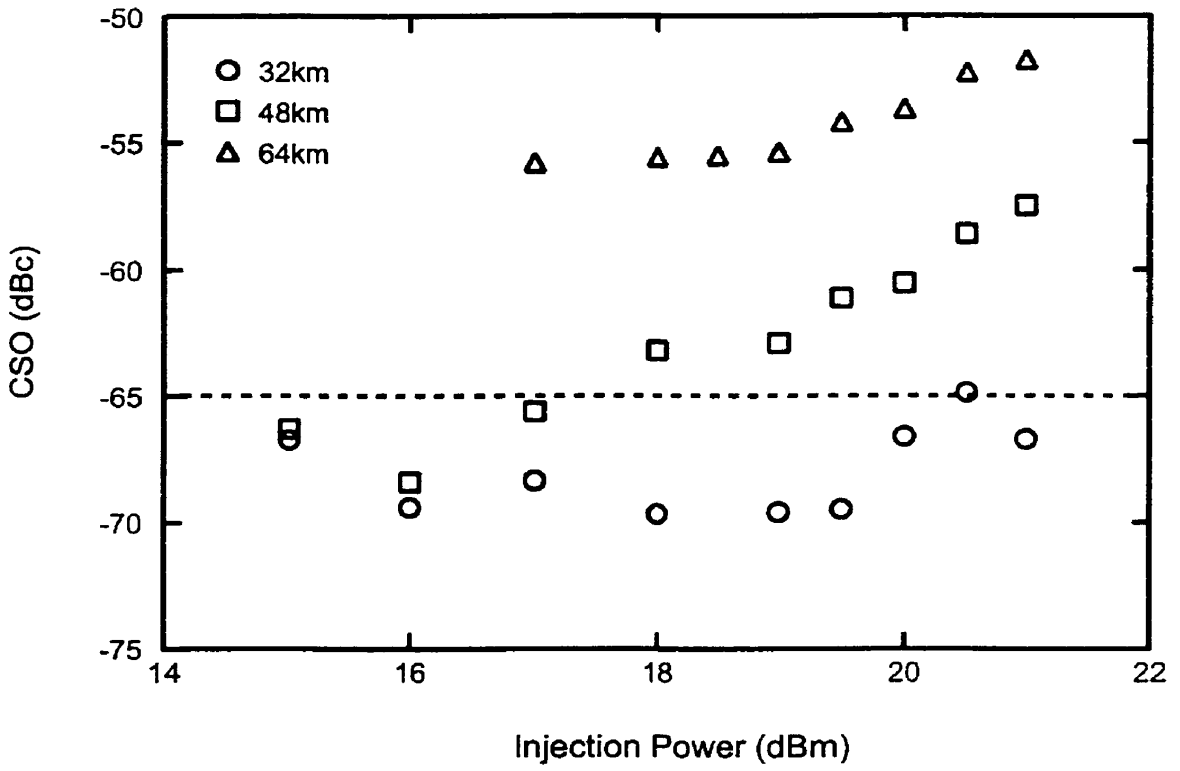

Figure 4-12: CSO as a function of injection power for an 80 channel CATV system at fiber lengths of 32, 48, and 64km. Two-tone phase dithering is used to suppress SBS to 21.4dBm.

as the optical signal propagates down the fiber, adding new CSO beats that are detected at the receiver. Therefore, with SBS suppressed, SPM is the dominant nonlinearity. In Chapter 5, ways of overcoming this limitation are discussed.

4.4 Chapter Summary

It has been shown that two-tone dithering of the optical signal is substantially more effective than single-tone dithering at suppressing SBS. For realistic response of the laser and external phase modulator one can generate 13.4dB of suppression, which is 3.4dB higher than what has been previously reported. If the FM response of the laser is increased by a modest amount, this same level of suppression would be possible by dithering the DFB laser alone. This would eliminate the need for an external phase modulator and significantly decrease the cost of the CATV transmitter. When SBS has been suppressed in optical fiber, SPM becomes the dominant linearity. The interaction of SPM with fiber dispersion degrades the CSO distortion of the CATV signal, limiting the injection power.

Chapter 5

Conclusions and Future Work

5.1 Conclusions

The author has presented a study of SBS suppression in analog optical CATV transmission systems. A time-resolved chirp measurement system has been designed, built, and tested to examine the relationship between SBS suppression and transmitter characteristics. Chirp as low as 50MHz can be measured using this technique, and the complex average electric field and corresponding optical spectrum can be obtained. This approach was used to examine the relationship between SBS suppression and CATV transmitter characteristics, with the aim of developing enhanced suppression techniques.

A number of broad conclusions can be made from this work:

- Using measured chirp and power waveforms generated by the CATV transmitter and enhanced analysis of the corresponding optical spectrum, one can accurately determine SBS suppression levels in optical fiber over a wider measurement range. This approach enables development of SBS suppression schemes without requiring high power amplification. It has important implications in that it separates amplifier and transmitter development, allowing the two to proceed independently.

- DFB lasers and externally phase-modulated CW lasers both show similar SBS suppression, dominated by phase modulation of the optical output. Sinusoidal dithering results in sinusoidal phase modulation of the optical signal, broadening the spectrum and sup-

pressing SBS. For the laser, however, the maximum phase modulation index is inversely proportional to the dithering frequency. Due to the low FM response of these devices and the high dithering frequencies required to avoid distorting the CATV signal, direct laser dithering is impractical for generating high levels of suppression. In fact, the maximum suppression using two-tone laser dithering is shown to be only 9.5dB. Suppression results improve if one combines laser dithering with external phase dithering. However, once an external phase modulator has been inserted into the CATV transmitter it is more effective to just apply both dithering tones to the external device since this approach offers the highest level of suppression.

- Two-tone dithering is more effective at suppressing SBS than single-tone dithering. The most effective suppression scheme is pure two-tone phase dithering at a frequency ratio of 3:2, generating an SBS threshold of 21.4dBm and requiring an RF bandwidth of only 3.9GHz. Higher levels of suppression are possible if one increases the PM response of these devices. For the laser this means increasing the FM response, for the phase modulator this means increasing the V_π of the device and the allowable modulation power.

- With SBS suppressed, self-phase modulation (SPM) is the dominant nonlinearity in the optical fiber. For an 80-channel CATV system, the interaction of SPM with fiber dispersion degrades the CSO distortion to unacceptable levels.

5.2 Future Work

The next step in complexity from two-tone dithering is three-tone dithering. In this case, all three frequencies must satisfy the relations

$$A * f_1 = B * f_2 = C * f_3 \tag{5.1}$$

$$|Af_1 \pm Bf_2 \pm Cf_3| > 2f_U \tag{5.2}$$

where A,B, and C are integers and f_U is the upper CATV frequency. This suppression scheme is difficult to implement because of the increase in the number of degrees of freedom. One not only has to find and maintain the appropriate RF levels for three dithering tones but also

their relative phase. This is six degrees of freedom instead of three compared to the two-tone system. Because of the complexity of this scheme we have not examined it in this thesis. Nevertheless, three-tone dithering is capable of exceeding the 13.5dB suppression limit. To demonstrate this, a modified numerical model was written where a third dithering tone is added to the three combinations of two-tone external phase dithering discussed in Section 4.2.1. The initial two-tone system is set to its maximum suppression value and then a third tone is added with a phase modulation index varying from 0 to 5 radians. All three RF frequencies are assumed to be in phase. The results for this three-tone suppression scheme are shown in Figure 5-1. An SBS suppression of 13.9dB is demonstrated for the original two-tone system at a frequency ratio of 3:1 and the additional third tone with a phase modulation index of 4.6; The required bandwidth increases from 4.5GHz to 7.5GHz which in some cases may make it difficult to implement. These results only represent a small fraction of the possible combinations of operating parameters when using a three-tone suppression scheme. While implementation of this scheme is difficult, it would offer a higher level of suppression.

One way of overcoming SPM-induced CSO distortion is to use a differential detection system. This technique was first introduced by Nazarathy [33] in 1993. A schematic of the system is shown in Figure 5-2. Two complementary optical signals are generated from the transmitter using the same optical laser source. This is typically accomplished using an appropriately designed directional coupler integrated with the Mach-Zehnder modulator output. For successful operation, the two channels are balanced in gain and matched in delay. That is, the complementary optically modulated signals which are generated with opposite polarity and with equal amplitude at the transmitter must maintain opposite polarity and equal amplitude at the receiver. In recombining, the RF carriers add coherently, random noise adds incoherently, and commode mode noise and distortion are cancelled. As a result, the effects of fiber-induced CSO are minimized [34]. For implementation of differential detection, the total distance in each arm must be matched to better than $(c/n)/\nu$ where ν is the frequency of the highest CATV channel (in this case 550MHz) and c/n is the velocity of the light in fiber [35]. For standard SMF this corresponds to a length of 0.36m; equalization is typically performed by coarsely trimming the fiber lengths and using a proprietary electrical length equalization scheme. While this is a proven method for minimizing CSO distortion in analog CATV systems, the requirement and

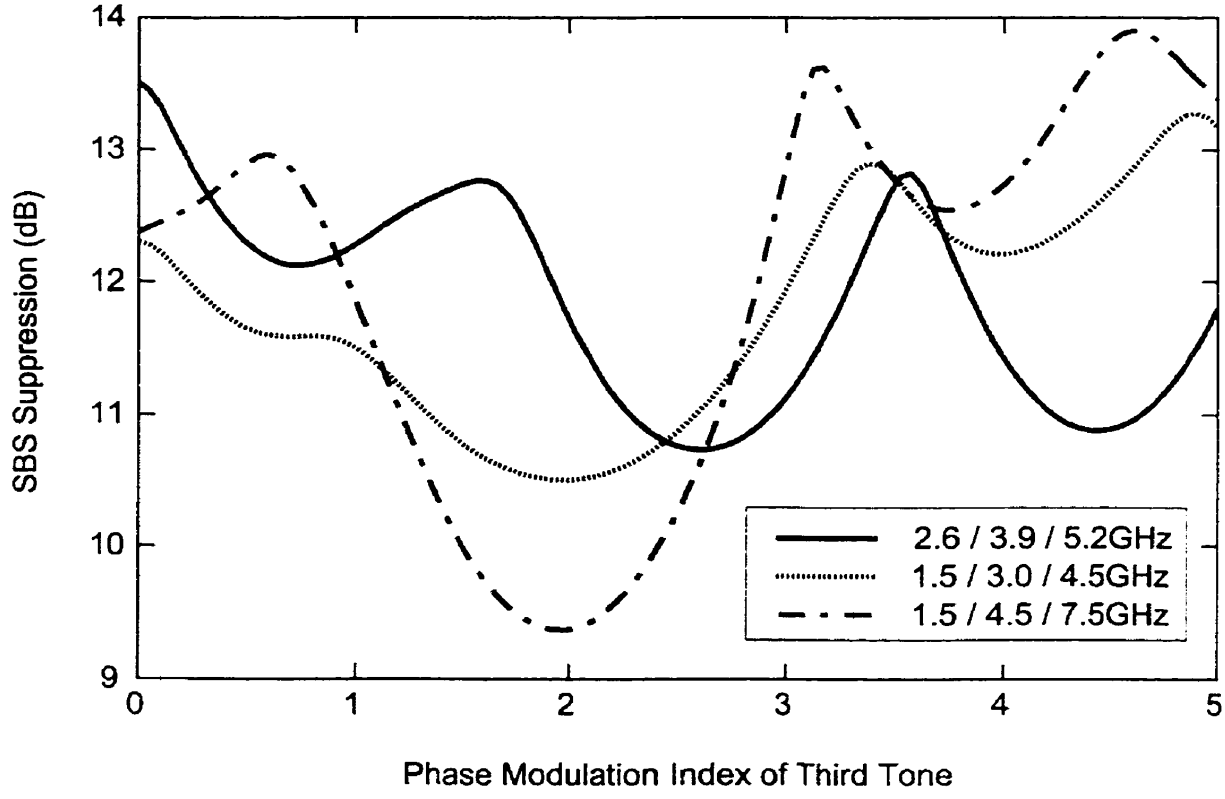

Figure 5-1: SBS suppression vs phase modulation index of a third tone using pure external phase dithering. The initial two-tone system is set to its maximum suppression level and all RF frequencies are assumed to be in phase.

cost of an additional fiber link and balanced receiver makes it a less than ideal solution.

A more desirable approach is introduced by Desem and Piehler [31] [34], where it is shown that phase dithering applied at the transmitter can influence the level of CSO distortion. In this work, a single phase dithering tone is applied to the CATV transmitter and CSO is reduced to acceptable levels for a specific fiber length. This same technique may be useful for reducing CSO in the presence of two-tone phase dithering. It may prove possible to detune the two dithering tones from their optimal point in exchange for an improvement in CSO distortion. In this way, one could find the best trade-off between SBS suppression and CSO and perhaps increase the allowable injection power. We tried to simulate this for an 80-channel CATV system using the split-step Fourier transform method[2], but due to the significant spectral broadening induced by the two-tone suppression scheme, the required frequency window and corresponding number of points make the program extremely computationally intensive. Nevertheless, if the appropriate resources were to become available this technique could represent a practical solution to the problem. In its absence, a considerable amount of empirical investigation would likely be required.

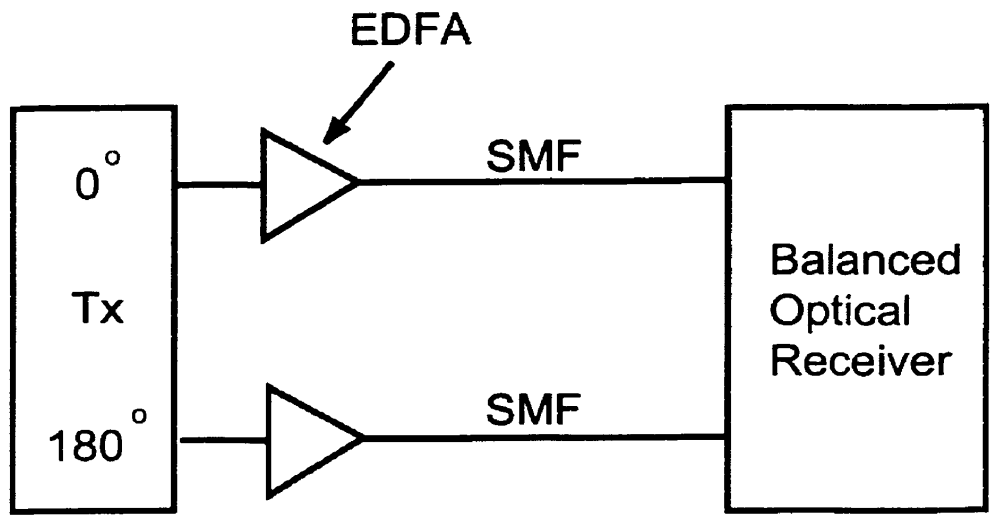

Figure 5-2: Differential detection system used for cancelling CSO distortion in analog CATV systems.

Bibliography

[1] Ciciora, W., Farmer, J., and Large, D. *Modern Cable Television Technology.* Morgan Kaufmann, San Francisco, (1999).

[2] Agrawal, G. P. *Nonlinear Fiber Optics.* Academic Press, San Diego, (1989).

[3] Schiess, M. and Carlden, H. *Electronics Letters* **30**, 1524–1525 (1994).

[4] Koyama, F. and Iga, K. *Journal of Lightwave Technology* **6**, 87–93 (1988).

[5] Childs, R. B. and O'Byrne, V. A. *IEEE Journal of Selected Areas in Communications* **8**, 1369–1376 (1990).

[6] Trisno, Y. S. and Huber, D. R. *IEEE Photonics Technology Letters* **3**, 666–668 (1991).

[7] Jackson, M. K., Smith, V., and Maycock, J. *OSA Technical Digest Series* **2**, 279–280 (1996).

[8] Mao, X. P., Bodeep, G. E., Tkach, R. W., Chraplyvy, A. R., Darcie, T. E., and Derosier, R. M. *IEEE Photonics Technology Letters* **4**, 287–289 (1992).

[9] Takushima, Y. and Okoshi, T. *Electronics Letters* **28**, 1155–1157 (1992).

[10] Tsujikawa, K., Nakajima, K., and Ohashi, M. *IEEE Photonics Letters* **10**, 1139–1141 (1998).

[11] Nilsson, A. C., Kuo, C. Y., Kleefeld, J., Gall, C. H., Riddle, A. N., and Chou, H. *United States Patent* **5828477** (1995).

[12] Mao, X. P., Bodeep, G. E., Tkach, R. W., Chraplyvy, A. R., Darcie, T. E., and Derosier, R. M. *OSA Technical Digest* , 141–143 (1993).

[13] Willems, F. W., van der Plaats, J. C., and Muys, W. *Electronics Letters* **30**, 343–345 (1994).

[14] Tremblay, G., Maurer, G., Leilabady, P. A., Vendetta, S. W., and Pier, T. J. *Raynet Corporation, Menlo Park, California 94025, USA* .

[15] Yariv, A. *Optical Electronics*. Saunders College, Orlando, (1991).

[16] Pedrotti, F. L. and Pedrotti, L. S. *Introduction to Optics*. Prentice-Hall, New Jersey, (1987).

[17] Devaux, F., Sorel, Y., and Kerdile, J. F. *Journal of Lightwave Technology* **11**, 1937–1940 (1993).

[18] Linke, R. A. *Journal of Quantum Electronics* **21**, 593–597 (1985).

[19] Jeong, J. and Park, Y. K. *Electronics Letters* **1** (1997).

[20] Vodhanel, R. S. *Electronics Letters* **24**, 1359–1361 (1988).

[21] Saunders, R. A., King, J. P., and Hardcastle, I. *Electronics Letters* **30**, 1336–1338 (1994).

[22] Korotky, S. K. *United States Patent* **5566381** (1995).

[23] Atlas, D. *United States Patent* **5930024** (1997).

[24] Desem, C. *Electronics Letters* **30**, 2055–2056 (1994).

[25] Tammela, S., Ludvigsen, H., Kajava, T., and Kaivola, M. *IEEE Photonics Technology Letters* **9**, 475–477 (1997).

[26] Olsen, C. M. and Olesen, H. *Journal of Lightwave Technology* **9**, 436–441 (1991).

[27] Kotaki, Y. and Soda, H. *OFC Technical Digest* , 310–311 (1995).

[28] Tucker, R. S. *Journal of Lightwave Technology* **3**, 1180–1192 (1985).

[29] Jackson, M., Smith, V. M., Hallam, W. J., and Maycock, J. C. *Journal of Lightwave Technology* **15**, 1538–1545 (1997).

[30] Piehler, D., Kuo, C., Kleefeld, J., and Gall, C. *22nd European Conference on Optical Communication - ECOC'96* (1996).

[31] Desem, C. *Electronics Letters* **30**, 2055–2056 (1994).

[32] Phillips, M. R., Darcie, T., Marcuse, D., Bodeep, G., and Frigo, N. *IEEE Photonics Letters* **3**, 481–483 (1991).

[33] Nazarathy, M. and Berger, J. *United States Patent* **5253309** (1993).

[34] Piehler, D., Kuo, C., Kleefeld, J., Gall, C., Nilsson, A., and Zou, X. *In Optical Amplifier and Their Applications, 1996 Technical Digest* , 246–249 (1996).

[35] Piehler, D., Zou, X., Kuo, C., Kleefeld, J., Garcia, G., Ralston, J., and Mathur, A. *Electronics Letters* **8** (1996).

Appendix A

Full Two-Tone SBS Suppression Results

There are twelve possible combinations of direct laser and external phase dithering using a two-tone suppression scheme. The following pages present the full suppression results.

Ratio	Figure	Dithering Tone 1	Dithering Tone 2
3:2	A-1	DFB laser @ 3.9GHz	DFB laser @ 2.6GHz
2:1	A-2	DFB laser @ 2.6GHz	DFB laser @ 1.3GHz
3:1	A-3	DFB laser @ 3.9GHz	DFB laser @ 1.3GHz
3:2	A-4	DFB laser @ 3.9GHz	Phase Modulator @ 2.6GHz
3:2	A-5	DFB laser @ 2.6GHz	Phase Modulator @ 3.9GHz
2:1	A-6	DFB laser @ 2.6GHz	Phase Modulator @ 1.3GHz
2:1	A-7	DFB laser @ 1.3GHz	Phase Modulator @ 2.6GHz
3:1	A-8	DFB laser @ 3.9GHz	Phase Modulator @ 1.3GHz
3:1	A-9	DFB laser @ 1.3GHz	Phase Modulator @ 3.9GHz
3:2	A-10	Phase Modulator @ 3.9GHz	Phase Modulator @ 2.6GHz
2:1	A-11	Phase Modulator @ 2.6GHz	Phase Modulator @ 1.3GHz
3:1	A-12	Phase Modulator @ 3.9GHz	Phase Modulator @ 1.3GHz

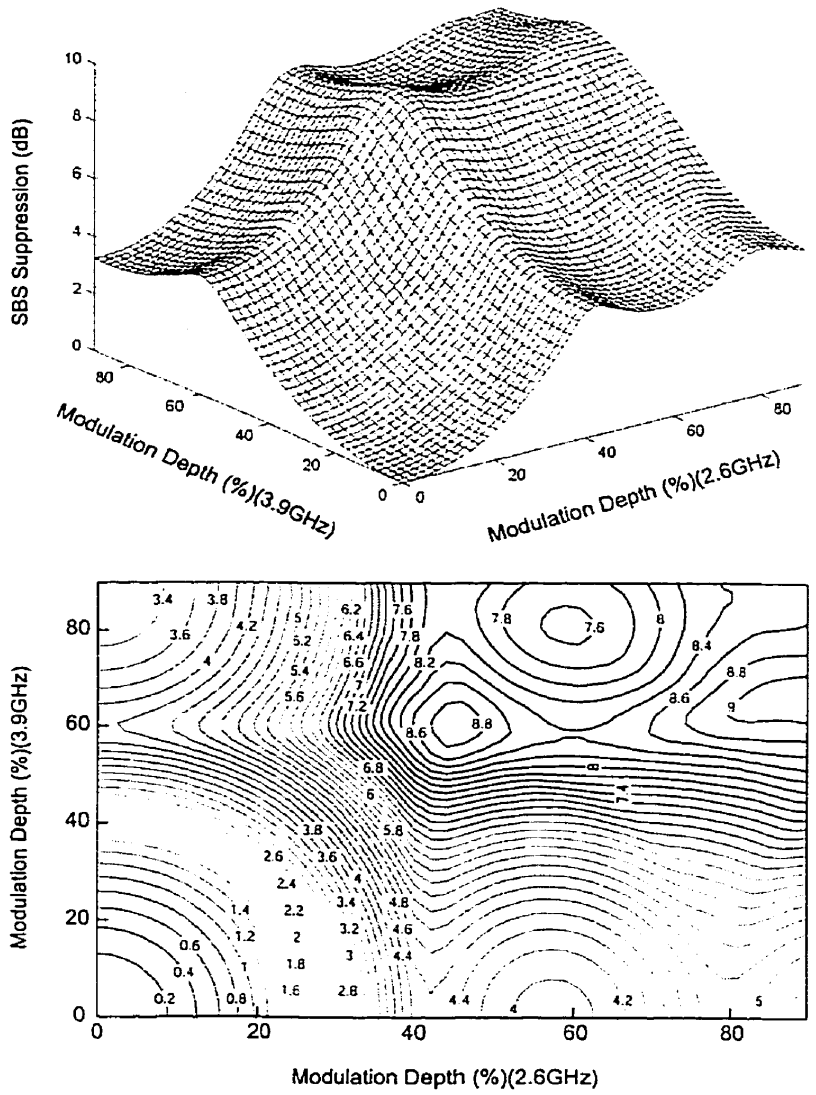

Figure A-1: Theoretical SBS suppression results for two-tone laser dithering at frequencies of 2.6GHz and 3.9GHz. Maximum SBS suppression is 9.1dB.

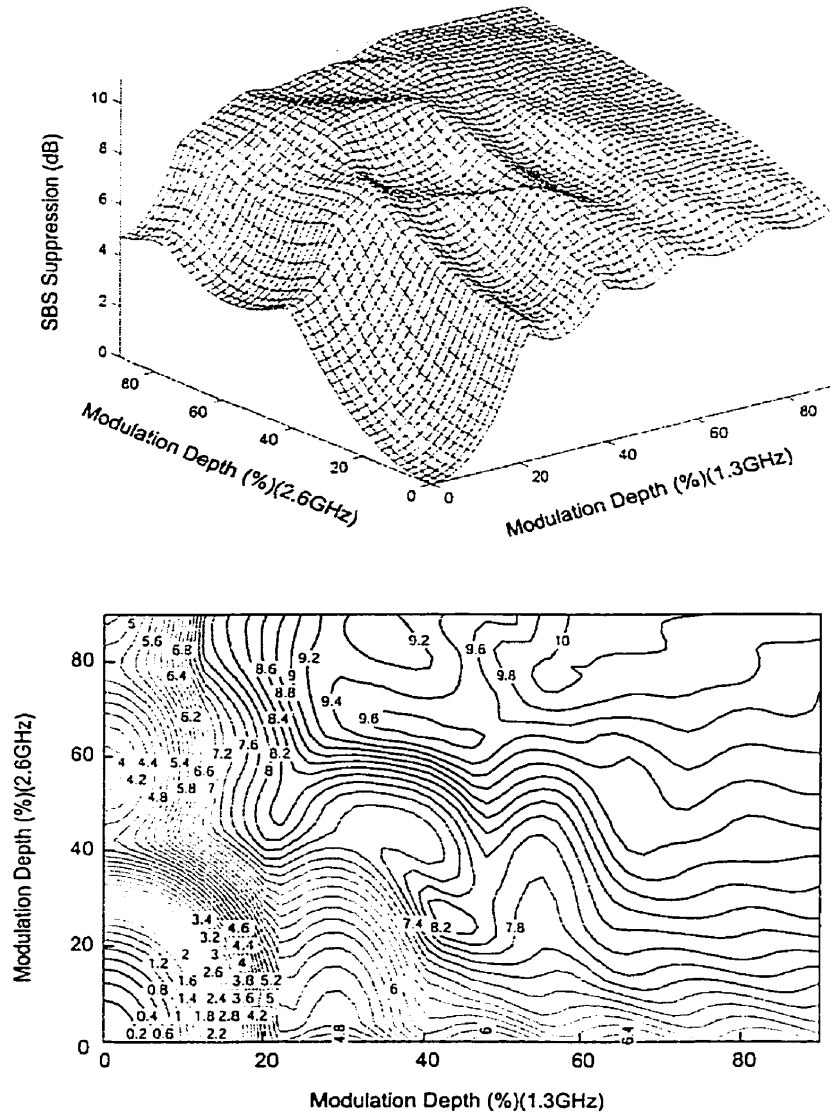

Figure A-2: Theoretical SBS suppression results for two-tone laser dithering at frequencies of 2.6GHz and 1.3GHz. Maximum SBS suppression is 10.1dB.

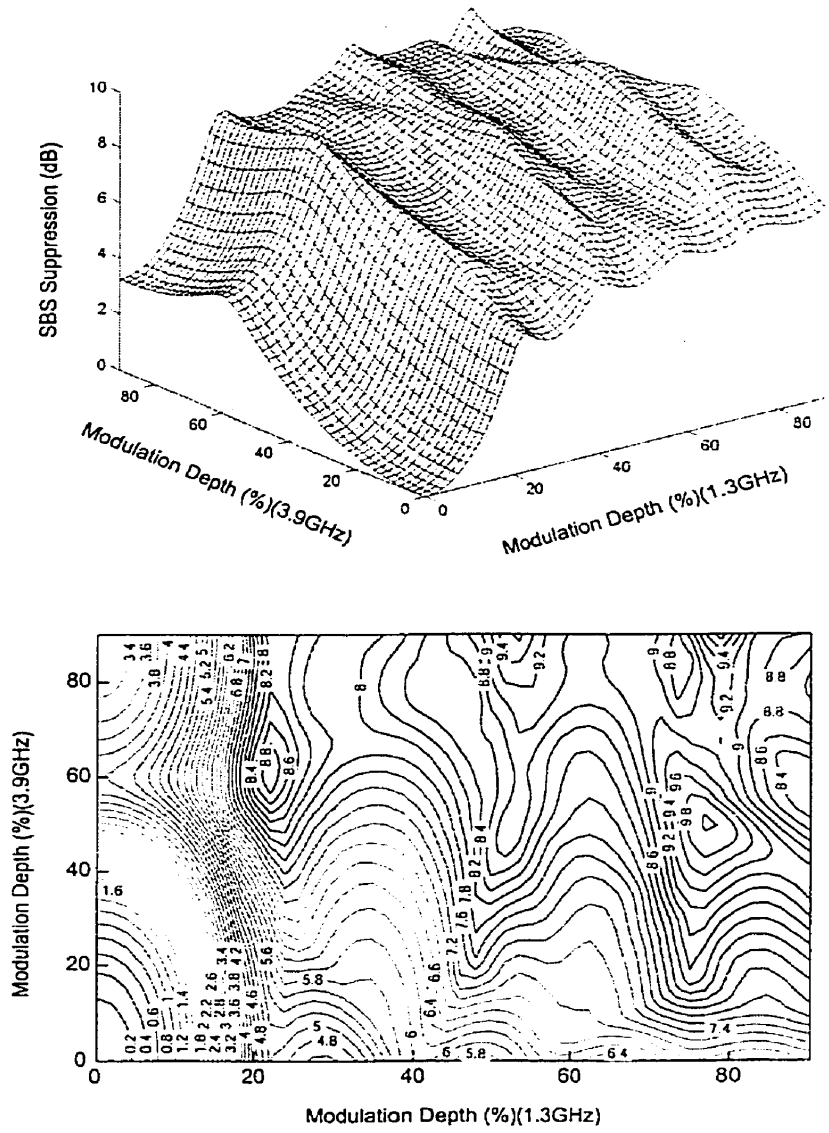

Figure A-3: Theoretical SBS suppression results for two-tone laser dithering at frequencies of 1.3GHz and 3.9GHz. Maximum SBS suppression is 10.0dB.

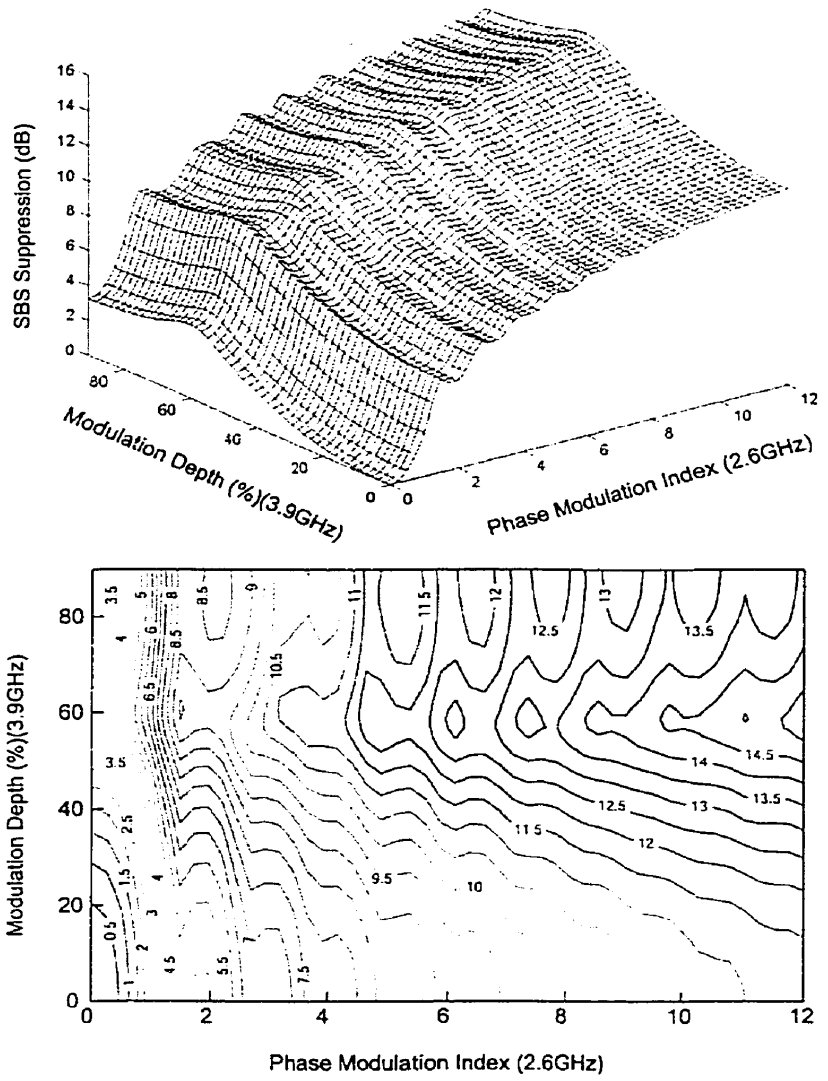

Figure A-4: Theoretical SBS suppression results for combined laser and external phase dithering at frequencies of 3.9GHz and 2.6GHz, respectively. Maximum SBS suppression is 12.4dB for m between 0 and 5 radians.

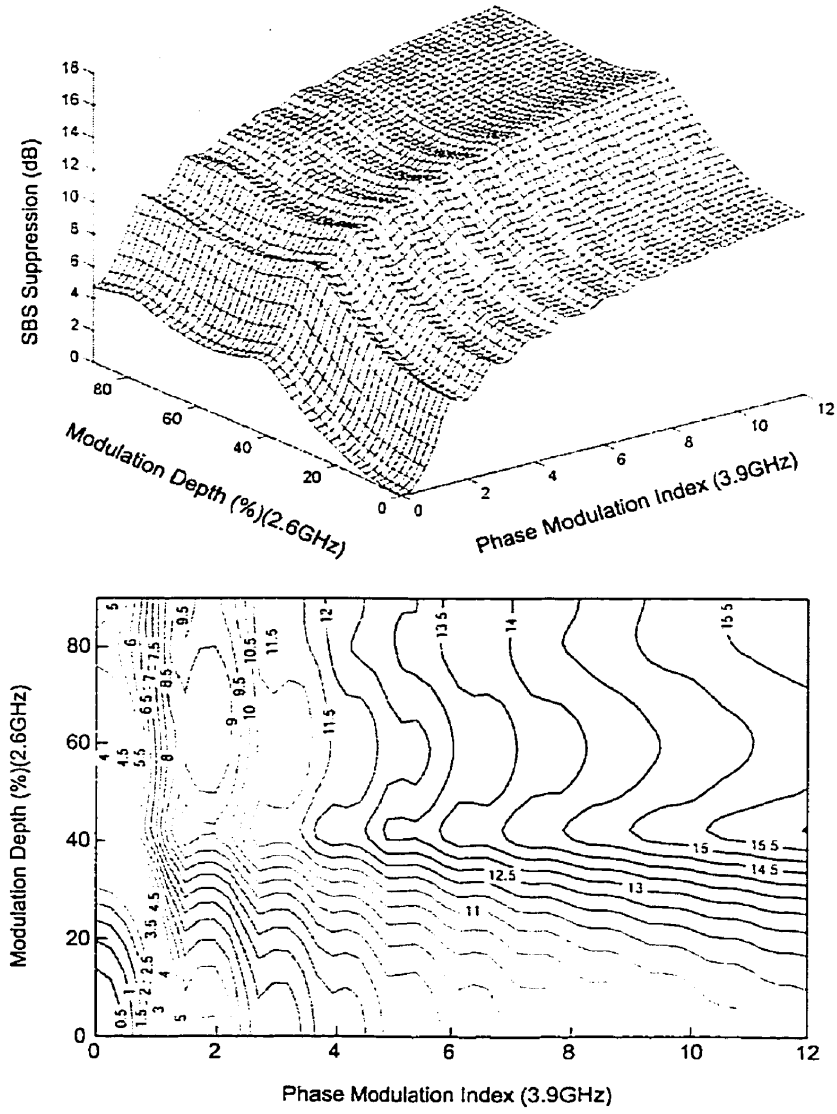

Figure A-5: Theoretical SBS suppression results for combined laser and external phase dithering at frequencies of 2.6GHz and 3.9GHz, respectively. Maximum SBS suppression is 13.1dB for m between 0 and 5 radians.

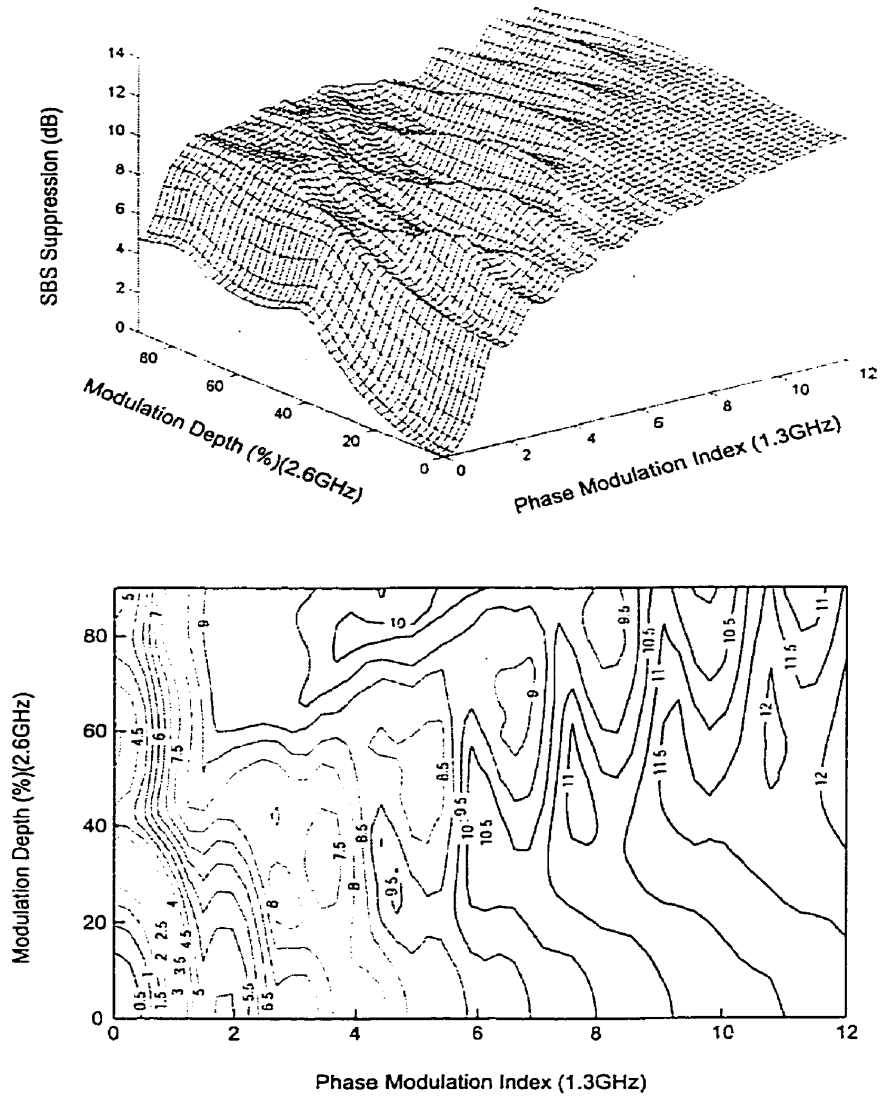

Figure A-6: Theoretical SBS suppression results for combined laser and external phase dithering at frequencies of 2.6GHz and 1.3GHz, respectively. Maximum SBS suppression is 10.1dB for m between 0 and 5 radians.

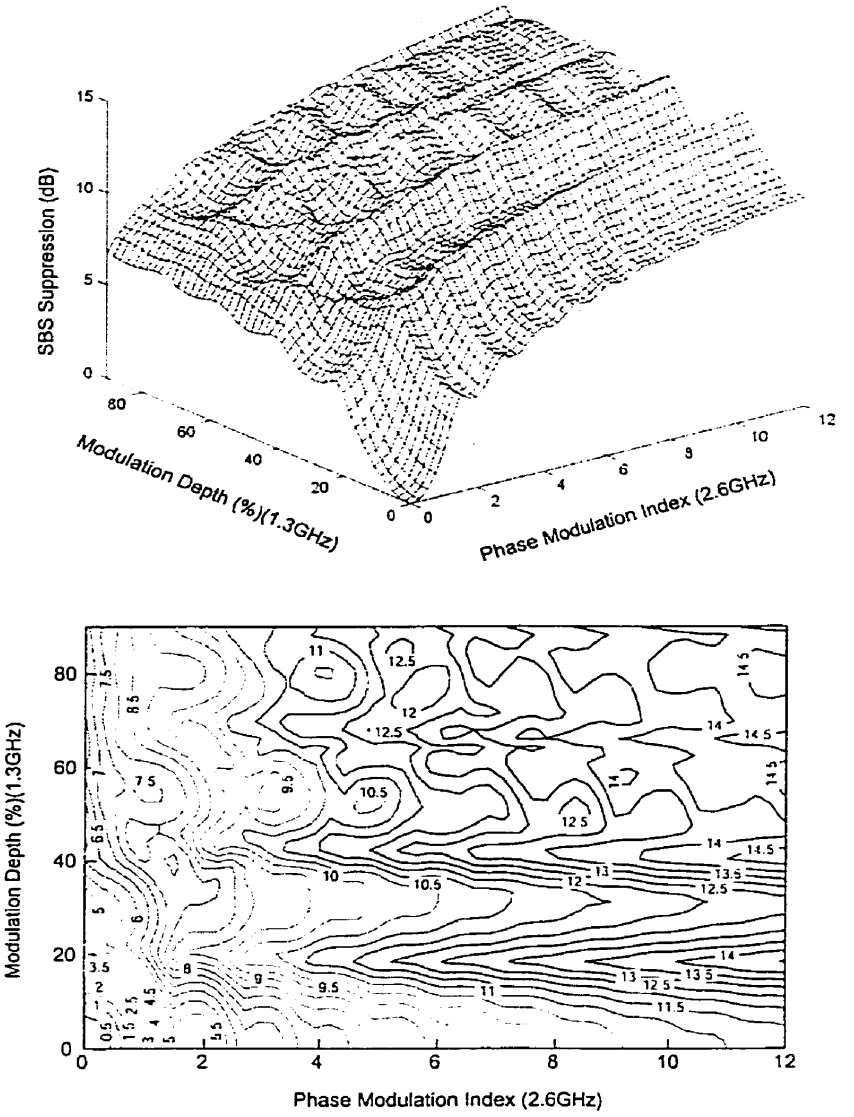

Figure A-7: Theoretical SBS suppression results for combined laser and external phase dithering at frequencies of 1.3GHz and 2.6GHz, respectively. Maximum SBS suppression is 12.6dB for m between 0 and 5 radians.

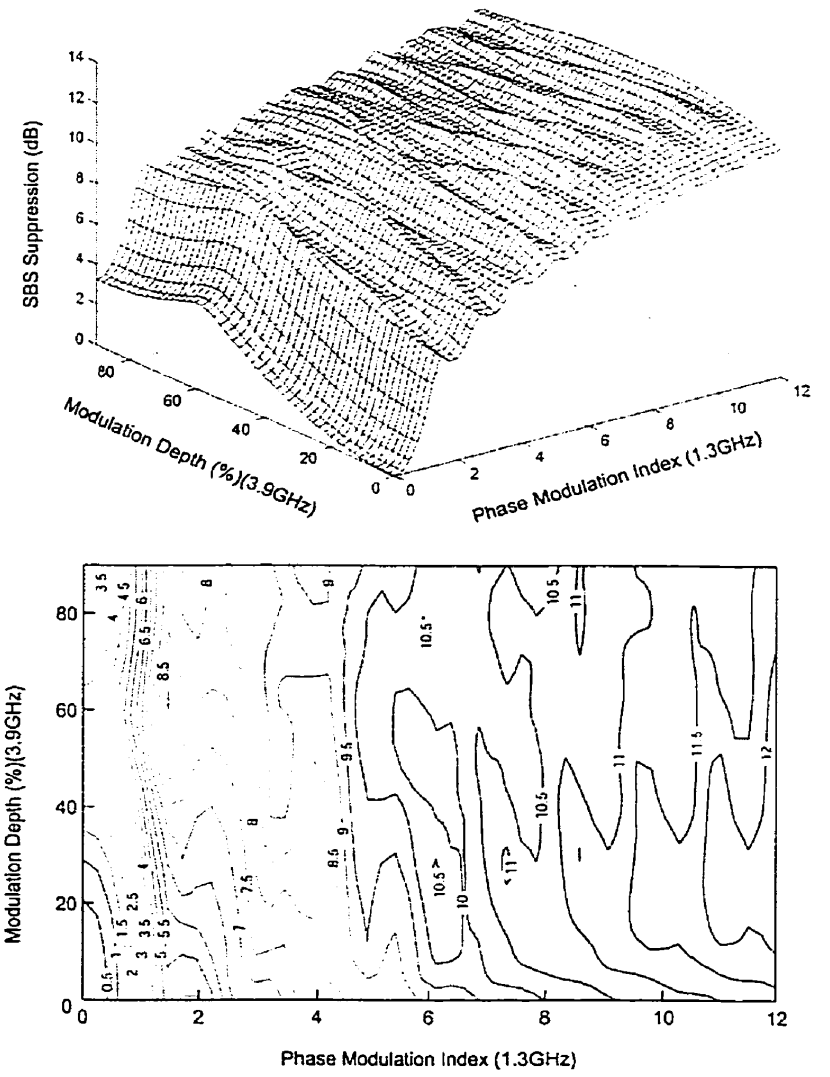

Figure A-8: Theoretical SBS suppression results for combined laser and external phase dithering at frequencies of 3.9GHz and 1.3GHz, respectively. Maximum SBS suppression is 10.2dB for m between 0 and 5 radians.

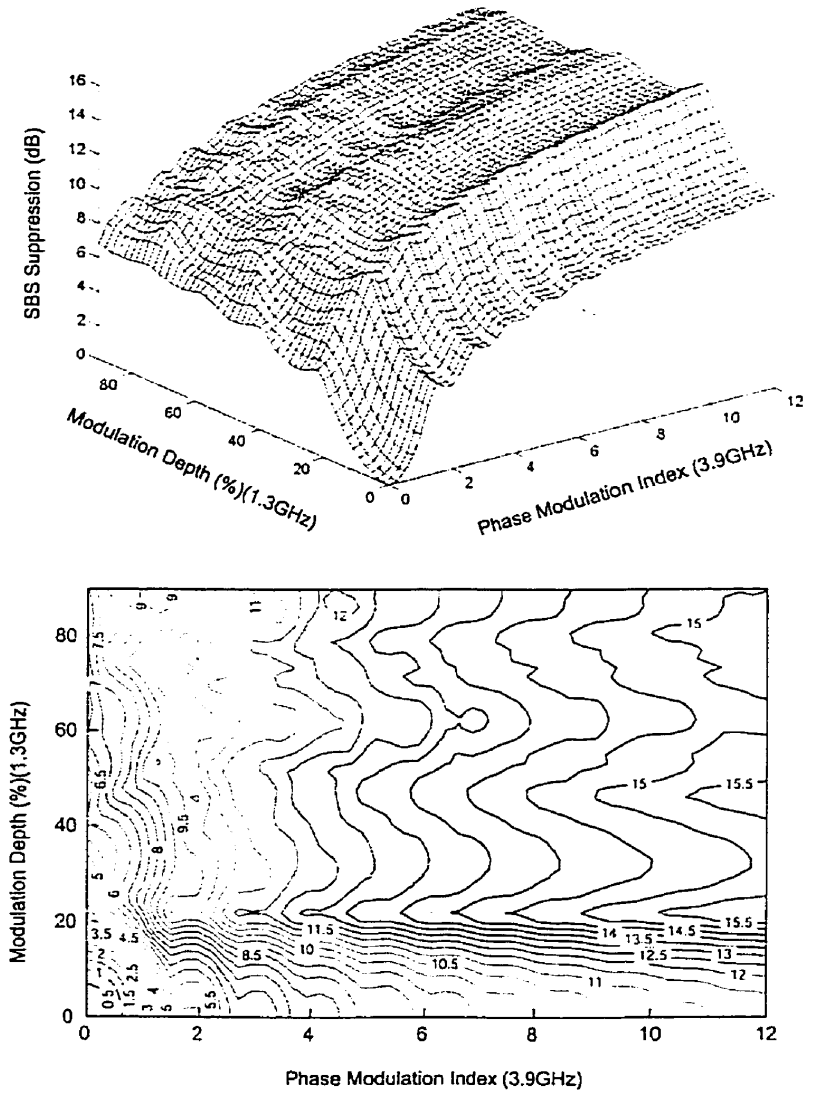

Figure A-9: Theoretical SBS suppression results for combined laser and external phase dithering at frequencies of 1.3GHz and 3.9GHz, respectively. Maximum SBS suppression is 13.4dB for m between 0 and 5 radians.

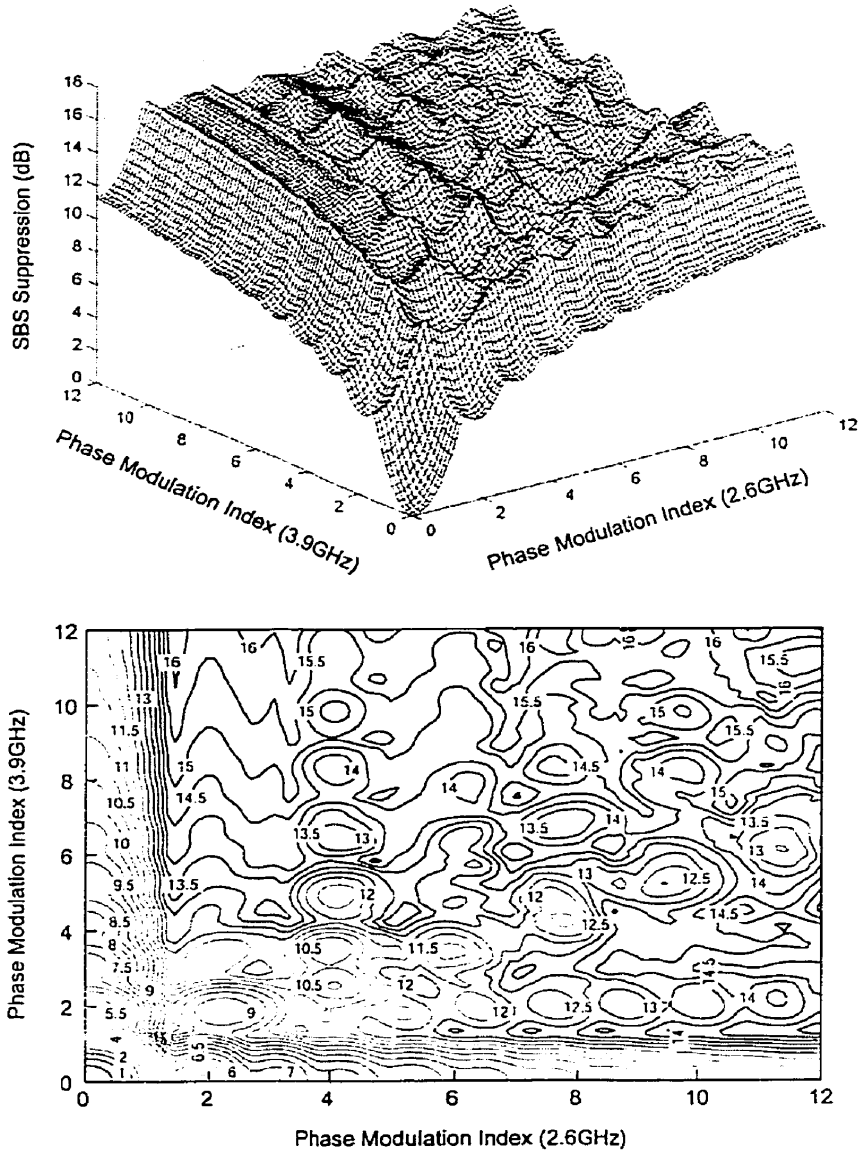

Figure A-10: Theoretical SBS suppression results for two-tone phase dithering at frequencies of 3.9GHz and 2.6GHz. Maximum SBS suppression is 13.5dB for m between 0 and 5 radians.

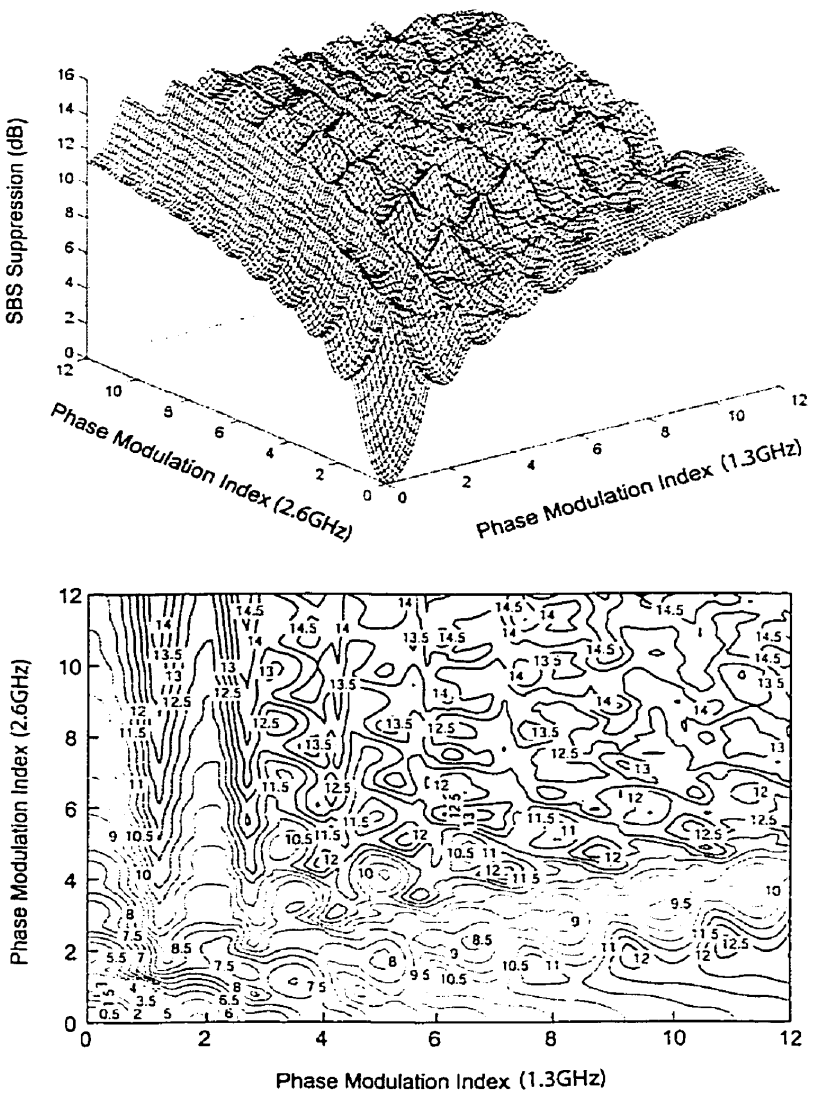

Figure A-11: Theoretical SBS suppression results for two-tone phase dithering at frequencies of 1.3GHz and 2.6GHz. Maximum SBS suppression is 12.3dB for m between 0 and 5 radians.

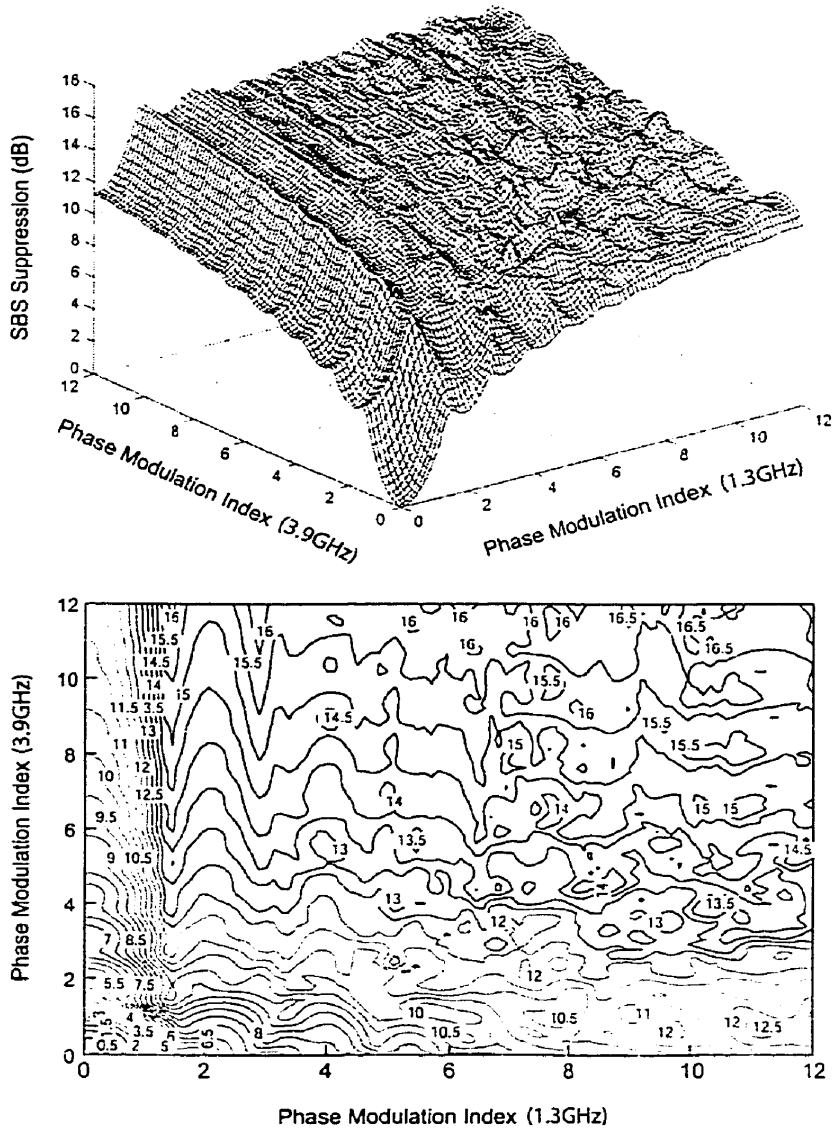

Figure A-12: Theoretical SBS suppression results for two-tone phase dithering at frequencies of 1.3GHz and 3.9GHz. Maximum SBS suppression is 13.5dB for m between 0 and 5 radians.

Appendix B

Chirp Measurement Theory

For a Mach-Zehnder interferometer with unequal path lengths, the static transmission function is given by

$$T(f) = \cos^2\left(\frac{\pi}{FSR}f + \phi\right) \tag{B.1}$$

where ϕ accounts for temperature tuning of the FDM. Letting $\phi = 0$ be the peak of the transmission curve, we define $\phi = \frac{\pi}{4}$ and $\phi = \frac{3\pi}{4}$ as the 50% points A and B, respectively. When $\phi = \frac{\pi}{4}$ the control point is on the positive slope of the transmission function, whereas the $\phi = \frac{3\pi}{4}$ control point is on the negative slope. The slope determines if the chirp to intensity conversion is positive or negative. The waveforms corresponding to the two control points can be written as

$$V_A(t) = P_{IN}(t)\left(\cos^2\left(\frac{\pi}{FSR}\Delta f(t) + \frac{\pi}{4}\right)\right) \tag{B.2}$$

$$V_B(t) = P_{IN}(t)\left(\cos^2\left(\frac{\pi}{FSR}\Delta f(t) + \frac{3\pi}{4}\right)\right) \tag{B.3}$$

We extract Δf from waveforms $V_A(t)$ and $V_B(t)$. Using the trigonometric identities

$$\cos^2(x) = \frac{\cos(2x) + 1}{2} \tag{B.4}$$

$$\cos(a + b) = \cos(a)\cos(b) - \sin(a)\sin(b) \tag{B.5}$$

we can rewrite the equations for $V_A(t)$ and $V_B(t)$ as

$$V_A(t) = P_{IN}(t)\left[\frac{-\sin\left(\frac{2\pi}{FSR}\Delta f(t)\right)+1}{2}\right] \tag{B.6}$$

$$V_B(t) = P_{IN}(t)\left[\frac{+\sin\left(\frac{2\pi}{FSR}\Delta f(t)\right)+1}{2}\right] \tag{B.7}$$

Introducing the relation

$$\frac{V_A(t)-V_B(t)}{V_A(t)+V_B(t)} = \sin\left(\frac{2\pi}{FSR}\Delta f(t)\right) \tag{B.8}$$

we can solve for $\Delta f(t)$

$$\Delta f(t) = \frac{FSR}{2\pi}\sin^{-1}\left(\frac{V_A(t)-V_B(t)}{V_A(t)+V_B(t)}\right) \tag{B.9}$$

and P(t)

$$P(t) = 0.5\cdot(V_A(t)+V_B(t)) \tag{B.10}$$

Equations B.9 and B.10 allow reconstruction of the full complex average electric field of the measured electric field, given by

$$E(t) = \sqrt{P(t)}e^{i\theta(t)} \tag{B.11}$$

where E(t) is the electric field envelope function [2], and the phase is directly related to chirp by the expression

$$\phi(t) = -2\pi\int_{-\infty}^{t}\Delta f(t')\,dt' \tag{B.12}$$

The full complex electric field yields all the information about the average transmitted characteristics. It does not, of course, contain information related to the amplitude or phase fluctuations, as it was obtained from time-average measurements. With the complex electric field waveform, it is straightforward to evaluate the optical power spectrum by Fourier transform, which is used extensively in this thesis

$$E(\omega) = \Im\{E(t)\} \tag{B.13}$$

The optical spectrum of the full electric field is centered at ω_0. However, in this thesis the electric field envelope function is sometimes used, which has the optical carrier suppressed. This envelope function is useful in describing optical signals with spectral width around the carrier, $\Delta\omega$, much less than the carrier frequency. A full derivation of the envelope function approach is given by Agrawal [2].